Mikroniek

PROFESSIONAL JOURNAL ON PRECISION ENGINEERING VOLUME 49 – ISSUE 3

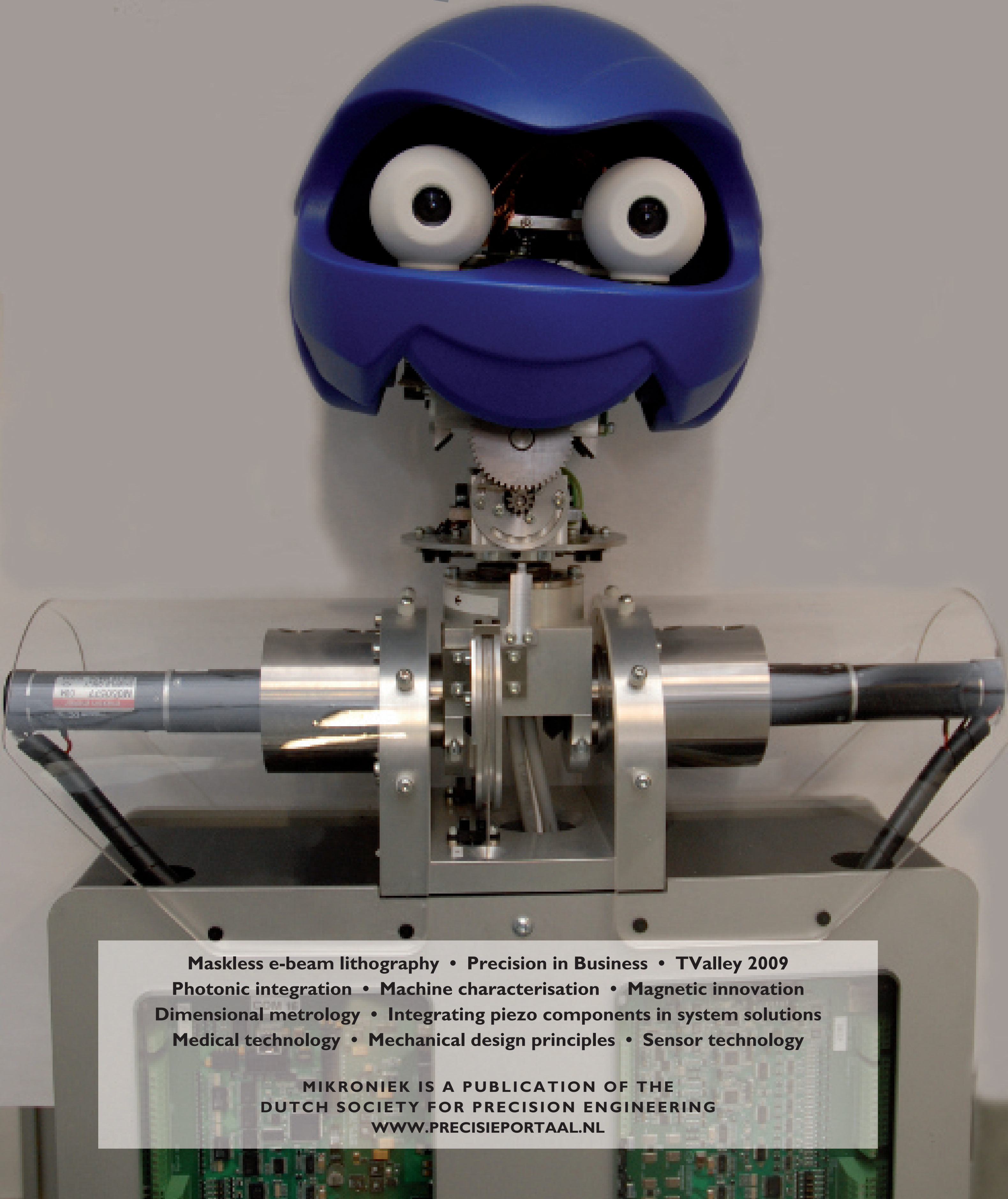

Maskless e-beam lithography • Precision in Business • TValley 2009
Photonic integration • Machine characterisation • Magnetic innovation
Dimensional metrology • Integrating piezo components in system solutions
Medical technology • Mechanical design principles • Sensor technology

MIKRONIEK IS A PUBLICATION OF THE
DUTCH SOCIETY FOR PRECISION ENGINEERING
WWW.PRECISIEPORTAAL.NL

3

Mikroniek - 2009

In this issue

Publication information

Objective
Professional journal on precision engineering and the official organ of the DSPE, the Dutch Society for Precision Engineering. Mikroniek provides current information about scientific, technical and business developments in the fields of precision engineering, mechatronics and optics.
The journal is read by researchers and professionals in charge of the development and realisation of advanced precision machinery.

Publisher
DSPE
PO Box 359
5600 AJ Eindhoven, The Netherlands
Telefoon +31 (0)40 – 296 99 11
Telefax +31 (0)40 – 296 99 10
E-mail info@dspe.nl

Subscription costs
The Netherlands
€ 70.00 (excl. VAT) per year
Abroad
€ 80.00 (excl. VAT) per year

Editor
Hans van Eerden
E-mail hans.vaneerden@dspe.nl

Advertising canvasser
Sales & Services
PO Box 2317
1620 EH Hoorn, The Netherlands
Telephone +31 (0)229 – 211 211
E-mail sns@wxs.nl

Design and realisation
Twin Media bv
PO Box 317
4100 AH Culemborg, The Netherlands
Telephone +31 (0)345 – 470 500
Fax +31 (0)345 – 470 570
E-mail info@twinmediabv.nl

Mikroniek appears six times a year.

ISSN 0026-3699

The cover photo (the Twente Humanoid) is courtesy Demcon.

editorial

What makes Dutch industry different

As a newcomer, I am often asked what I think of the Netherlands. At last count I've lived in six countries, so I have become oblivious to trivial differences and focus on the 'real' ones.
What I'm struck at is how strongly the Dutch technical community adopts a multi-disciplinary approach to development. Examples include a strong culture of mechanical/software/hardware co-design and first-principles based analysis techniques in systems development, and a very modular approach to subsystem interface design. Coupled with Dutch pragmatism, the end result is that development usually proceeds quite quickly and that there is an excellent basis for multidisciplinary teams to work together on solving the (inevitable) problems.
Now of course my experience at MAPPER may not be representative. Our team is by far the most impressive in terms of analytical and problem-solving skills that I've ever had the privilege of working with. But at many of our supplier and partner companies I see very much the same mix of cultural elements mentioned above.
This probably explains why there are so many world-class Dutch companies successful in highly demanding markets. In semicon alone for example, ASMI, ASML, BESI, Assembleon, OTB, FEI, etc. What's also amazing is that many of our suppliers also work with these companies – there is indeed a very strong, Silicon Valley calibre network effect.
Are emerging countries potentially threatening the success of this 'Dutch innovation model'? Regarding the semicon market globally, I think it is inevitable that the bulk of the equipment industry will ultimately migrate to Asia, if only for being physically close to its customers. However, the Dutch history as a trading nation gives the country an advantage here – the Dutch, unlike many other people, know that an 'arms-length' approach to working with customers doesn't work.
There are many examples of countries defending strong positions in the face of emerging competitors – think of the German car or Swiss watch industry. Our industry is somewhat different in that a solid understanding of evolving semiconductor manufacturing technology is essential in order to develop the right product, but at least we have the advantage of having a technology roadmap in the ITRS.
I'm very confident that – provided the very strong network of knowledgeable suppliers and partners continues to prosper – the Netherlands will continue to have a major presence in the semiconductor equipment business.

Christopher Hegarty
Chief Executive Officer MAPPER Lithography

How to save over $ 100 mln per year on lithography cost?

Maskless electron beam lithography has emerged as one of the contenders for IC manufacturing. MAPPER's high-throughput solution provides 10 wafers-per-hour exposure units on 1 m² for 22 nm and beyond. This article will explain how such an approach will save IC manufacturers over $ 100 mln per year on lithography cost.

• *Bert Jan Kampherbeek and Marco Wieland* •

Optical lithography today is the leading technology for semiconductor manufacturing. Many technologies have been proposed in the past to replace optical lithography under the assumption that scaling was no longer possible. To date, optical lithography has managed to find solutions to extend the scaling limit – recent examples include low-k1 imaging and double patterning. These innovations however have one major implication: cost. Both lithography tool cost as well as mask (set) cost have risen exponentially to the point that the most advanced optical scanner today costs about € 40 mln and advanced mask set costs of € 2 mln are no rarity. Therefore, if optical lithography is to be replaced with another technology, it will not be so much for performance reasons, but mainly for cost reasons.

High-throughput e-beam solution

Maskless electron beam lithography, or electron beam direct write, has been around for a long time in the semiconductor industry. Mostly this technique has been used for mask writing applications as well as device engineering and in some cases chip manufacturing, thanks to its high resolution and flexibility in changing designs.

However, because of its relatively low throughput compared to optical lithography, electron beam lithography has never been the mainstream lithography technology. MAPPER offers a massively parallel electron beam approach; see Figure 1. This approach eliminates the fundamental throughput limitations of a single-electron beam system by arranging 13,000 parallel electron beams in an optical column no larger than a pack of milk. This

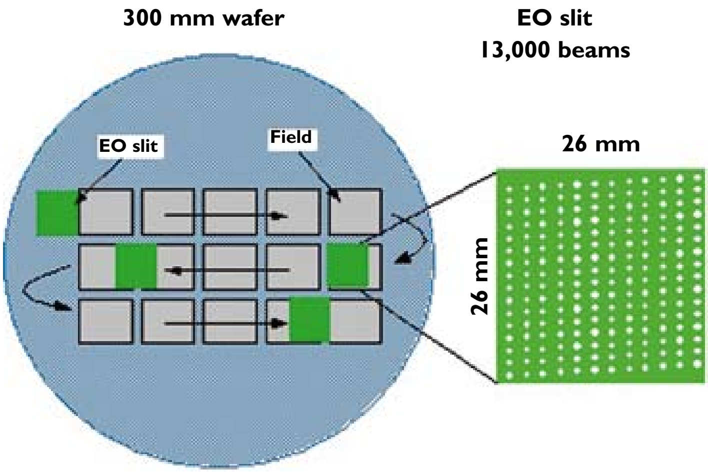

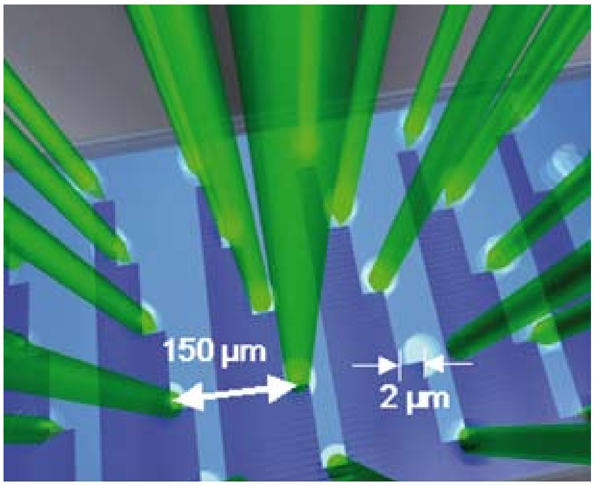

Figure 1. MAPPER's massively parallel electron beam approach.
(a) Arrangement of electron beams and writing strategy.
(b) Zoom of (top view of) beam positions in Electron Optics (EO) slit.

number of beams allows for a 10 wph (wafers per hour) throughput.

The 13,000 electron beams are arranged in an Electron Optics (EO) slit. The beams are on a pitch of 150 µm in such a way that if one looks at the beams from the direction perpendicular to where the slit has a width of 26 mm, the beams are effectively 2 µm apart. The writing strategy is such that complete fields are exposed within one stage scan. The wafer is moved underneath the EO slit from one end of the wafer to the other end; this is done by a wafer stage. Simultaneously to the stage movement, all electron beams are deflected over 2 µm by means of an electrostatic deflector array and the beams are individually switched on and off. In this way a full field can be exposed with only one stage scan, enabling 10 wafers per hour.

The optics that is required to create the array of focused spots is shown in Figure 2. It consists of a single high-brightness cathode run in space-charge limit. An electrostatic collimator lens is used to create a collimated beam. After passing the collimator, the single beam is split up into 13,000 beams by the aperture array. After the aperture array the beamlets are focused by the condenser lens array in the intermediate focus plane. In this plane the beam blanker array is placed that can deflect each individual beam away from a clear aperture on the beam stop array to stop the electrons and switch off the beam at the wafer. After the beam stop array the beams are demagnified by the projection lens array and focused in the wafer plane. A deflector array is positioned between the beam stop array and the projection lens array to scan the beams over a range of 2 µm perpendicular to the wafer stage movement.

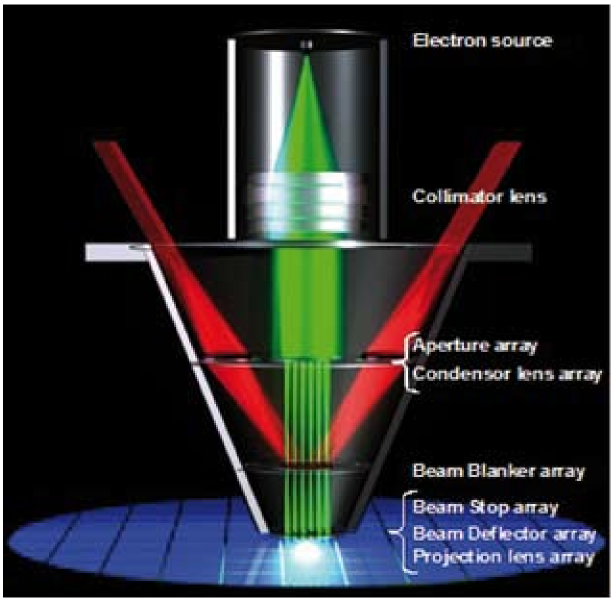

Figure 2. Schematic of MAPPER's massively parallel e-beam column.

System overview and roadmap

MAPPER's machine is capable of 10 wph. This is of course a low productivity compared with an optical scanner. However, throughput is not the only aspect that counts; footprint and tool cost are the two remaining parameters for enabling a competitive cost of ownership. Therefore MAPPER has made a design that enables a footprint of only 1 x 1 m^2 at a selling price of roughly € 5 mln. This creates the opportunity to cluster for example 10 units together to end up with a cluster machine capable of doing 100 wph on a footprint of approximately 15 m^2 or 23 m^2 including service area, which is comparable to today's optical scanners in terms of footprint and cost. Figure 3 shows the current machine with a non-optimized footprint of 1.3 x 1.3 m^2 and how these machines can be grouped in a 100 wph cluster.

Currently, this machine has 110 electron beams capable of exposing 32 nm node patterns [1]. To extend this capability to 10 wafers per hour at the 22 nm node, MAPPER is currently working on a high-speed data path architecture and an upgrade of the optics to 13,000 beams delivering a 150 μA current on the wafer.

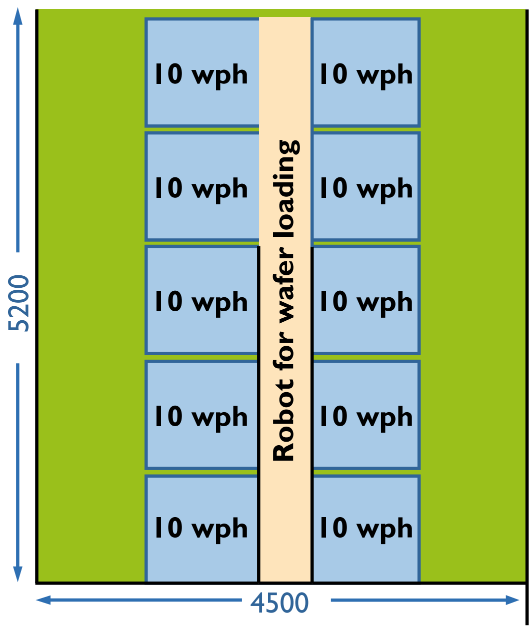

Figure 3. A 100 wph cluster tool.
(a) Schematic.
(b) The current footprint of a single 300 mm tool.

Comparing lithography technologies on cost

In most discussions about cost different technologies are compared by their cost of ownership (CoO), given by the following equation:

$$\text{CoO [\$ / wafer]} = \frac{\text{tool price [\$]}}{\text{TPT * 24 * 365 * 5 [hours]}} + \frac{\text{mask cost [\$]}}{\text{\# wafers /design}} + \text{process cost}$$

where TPT = throughput rate (wph), and assuming 100% yield and usage, and 5 years of operation.

The difficult thing about this CoO calculation is that the numbers are different for different products, especially if the mask costs are not to be neglected. Therefore it is a very difficult task for a chip manufacturer to estimate how many wafers are going to be made on average per design, and to be able to judge whether a maskless machine is more favorable or not than a machine needing a mask.

A different look at lithography cost

In the following example, EUV, Double Patterning and MAPPER are compared. The objective is to estimate the total lithography cost for these technologies *per* fab *per* year.

Assume for the purpose of the discussion that all lithography technologies have identical performance, uptime and yield. Let us take a 300 mm wafer fab for 22 nm products with 30,000 wafer starts per month and 15 critical layers to be patterned with one of the three solutions.

Assuming a 100% uptime and yield, this means that seven EUV machines at 100 wph are required, seven Double Patterning machines at 200 wph are required and 64 MAPPER machines at 10 wph are required. Following the above mentioned MAPPER tool price and using an estimated price of EUV and Double Patterning machines of € 40-45 mln and taking into account that the throughput for Double Patterning machines has to be cut in half, this straightforward calculation shows that the capital expenditures for the three technologies are comparable and are roughly € 56-64 mln per year assuming a 5-year depreciation period.

Now what about mask cost?

How many mask sets are required for this 30,000 wafer starts per month per fab? Let us take the example of a best-selling product like Nvidia's GeForce 8800GT / 8800GTS512 / 9800GTX / 9800GX2 family.

In Q3 2008, 111 million GPUs (Graphics Processing Units) were sold [2] and Nvidia had a market share of 27.8% [3]. This means Nvidia made about 31 million GPUs. Assume that about 10% of these GPUs were their most advanced, like the one mentioned previously, this results in 3.1 million GPUs. With a die size of 330 mm^2 [2] and a yield of 90% this comes down to 16,000 wafers per quarter or roughly 5,000 wafers per month.

Therefore, to fill a 30,000 wafer starts per month fab with the world's best-selling products you need about 72 chip designs per year. Taking into account that you need at least two mask sets per design, you end up with 140 mask sets. This represents € 140-280 mln per year for mask sets between € 1-2 mln each. Of course, in reality you need more mask sets than in this example, because there are numerous examples of products that do not end up being a bestseller.

Comparing the € 140 mln number to the amount spent on capital expenditures per year, it is obvious that mask costs are far more important for a Logic IC manufacturer than the cost of hardware.
This comparison will not hold for memory and microprocessors since the number of mask sets required per year will be lower. However, even for these IC manufacturers the mask set cost will be at least comparable to the capital expenditures, and thus maskless lithography will result in a cost reduction of at least 50%.

Conclusions

MAPPER is developing a massively parallel electron beam direct write system. Even at relatively low throughputs of 10 wph per machine this solution is cost effective for semiconductor manufacturing, because of:

- small footprint of ~1 m^2 per exposure unit;
- low system price;
- possibility of clustering several exposure units together;
- no mask cost, saving the IC manufacturers hundreds of millions per year.

Authors' note

Bert Jan Kampherbeek received his Masters degree in Applied Physics in 1999 at Delft University of Technology in the field of Electron Optics. He is one of the three founders of MAPPER Lithography and currently holds the position of VP Market Development.
Marco Wieland received his Masters degree in Applied Physics in 1999 at Delft University of Technology in the field of Electron Optics. He is one of the three founders of MAPPER Lithography and currently holds the position of VP Research & Development. Marco holds over thirty patents.

References

[1] M. J. Wieland, G. de Boer, G. F. ten Berge, et al., MAPPER: High Throughput Maskless Lithography, SPIE Proceedings 2009.
[2] www.tgdaily.com/content/view/37554/135
[3] www.tomshardware.com/news/GPU-videocard-Nvidia-AMD,6533.html

Information

www.mapperlithography.com

Philips Applied Technologies

The Dutch Society for Precision Engineering used to organize Precision-in-Business (PiB) days, where member companies could present their precision technologies to colleague DSPE members. This spring, the tradition was taken up again, and the first PiB-day took place on 23 April at Philips Applied Technologies on the High Tech Campus Eindhoven. Over thirty people attended the interesting presentations by 'Apptech', one of the Netherlands' largest high-tech contract innovation companies.

Philips Applied Technologies, part of Royal Philips Electronics, is a contract Research and Development organization that supports the development of products, applications and technical solutions. Customers include Fortune-500 market leaders and fast-growing companies as well as start-ups. For decades, Philips Applied Technologies (Apptech, in short) has been a dedicated 'Philips customers only' company; nowadays, half of the turnover is generated by external customers.

From concept to ramp-up

Apptech offers integral solutions (concept development, design and engineering to product industrialization, testing small series production in preparation for mass production), consultancy (industrial engineering, product innovation and business engineering) and specialist services (quality and reliability engineering, including EMC testing, industrialization and manufacturing, and integral packaging design and development).

The over 800 Apptech employees are amongst others experts in the fields of mechatronics, system-in-package, digital systems & technologies, industry consulting, environment & safety, and new product introduction. Their competences include software, electronics, robotics, precision motion and sensors. Apptech's application domains range from high-tech systems, robotics, and medical devices and implants, to multimedia experience, energy and home automation.

Next generation lithography

Rob Wendrich, director of Customer Relations Management, kicked off the PiB-day with a general introduction of Philips Applied Technologies. Next, systems architect Marcel Renkens presented the case of mechatronics for the next generation lithography, in particular Extreme UltraViolet Lithography (EUVL). Following Moore's law concerning the continuous miniaturization of features in integrated circuits, the roadmap pointed at extreme ultra-violet (λ = 13.5 nm) as radiation source for the lithography process at the so-called 22 nm node. This small critical dimension allows an overlay error between consecutive lithographic patternings of a mere 4.5 nm. As this overlay error is made up of many contributions, each individual contribution to the overlay error may not exceed 1 nm. Renkens discussed the consequences for mirror orientations (in EUVL lens optics are replaced by mirror optics, as lens materials absorb EUV

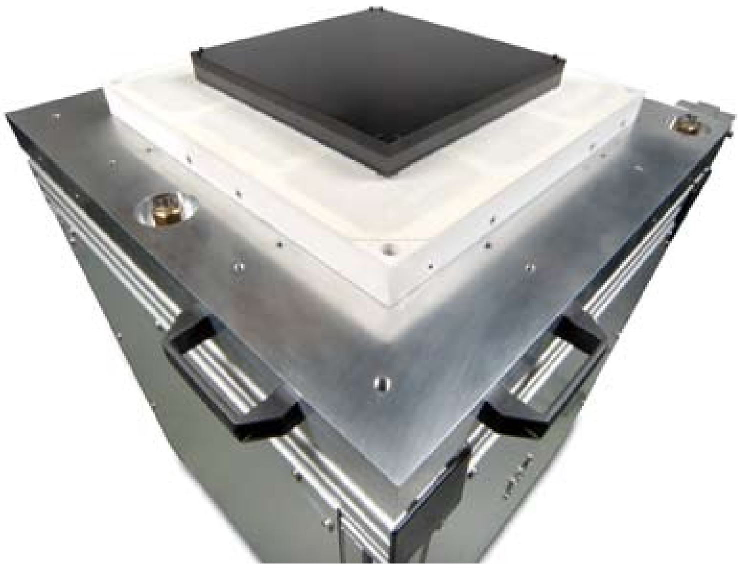

Figure 1. The Planar MagLev Stage was developed for high-precision X/Y motion in various environments, such as high-vacuum.

radiation too strongly). He showed that the optical path is much more sensitive to errors in mirror orientation than in lens orientation. From calculations it followed that the mirror orientation error should be as low as 1 nrad, which poses extreme demands on vibration isolation. And this is only one of the many challenges in EUVL machine construction.

Vacuum operation

Renkens continued to discuss the consequences of vacuum operation (in a EUVL machine and in general), ranging from the use of low-outgasing components to design-for-cleaning. Finally, he presented various vacuum-compatible stage technologies. For example, the so-called differential scale drive (featuring a conduit coupling with multi-stage air suction) has as its advantage that the drive (as a potential contamination source) remains outside the vacuum.
In 2007, Apptech presented its NForcer technology, based on a conventional linear motor that has been modified to allow for movements in two directions (i.e. in the horizontal as well as the vertical direction). Because of the contactless operation, magnetic induction motors are particularly suited for vacuum applications. The NForcer technology can be used to achieve magnetic levitation.

The magnetic levitation principle was further elaborated in Apptech's Planar MagLev Stage; see Figure 1. This new motor concept comprises cable-less magnetic hover plates that provide six degrees of freedom (DOFs) for precision X/Y motion above stationary coils. According to the Lorentz principle, the interaction between the electric coils and the magnetic plates can induce large horizontal displacements and small displacements in the remaining four DOFs (z, R_x, R_y and R_z). Due to the absence of mechanical contact between the hover plates and the coil plate, the system requires no lubricants. This offers benefits in comparison to roller bearing stages: accurate 6-DOF corrective positioning, no contamination due to wear or lubricants, no mechanical lifetime problems, and no intrinsic disturbance of motion.

Smart tool

Electromechanical engineer Jos Versleegers talked about the development of a simple, yet smart tool, the so-called Cleave Test Tool, for connecting telecommunications glass fibres. The challenge was to construct an all-mechanical, high-accuracy tool. Glass fibres have a 125 µm diameter, containing an 8 µm optical core. Before mechanically connecting two fibres, each fibre end has to be cleaved obliquely – when the end plane is oblique, optical reflections will be directed away from the optical core and hence not interfere with incoming signals. The optimum cleavage angle was determined to be 8 degrees.
Versleegers showed the construction that was designed to achieve this cleavage angle with a tolerance of 0.5 degrees. Another challenge concerned the (transversal) misalignment of the two fibre end planes, which should be less than 0.5 µm. To that end, a special connection plug was designed to allow for the accurate positioning. The design was finished succesfully, and now the tool is being produced in high numbers for one of Apptech's customers.

MEMS micro-mirror

Following the presentations, a number of demos were given in the Apptech labs. A high-frequency scanning micro-mirror for projection displays demonstrated Apptech's combined expertise in semicon fabrication technologies and mechatronics; see Figure 2. The mirror is fabricated using MEMS technology (Micro Electro-Mechanical Systems), MEMS offering a high-volume, low-cost solution for mechanical precision and integration. The projection principle is well-known, resting on laser beam deflection using one or more tilting mirrors. The design challenges were found in mirror flatness, dynamic performance (18.5 kHz operation frequency) and miniaturization of the required mechanics (leaf springs instead of the conventional cantilever torsion beams) into a format small enough to be used in a handheld laser

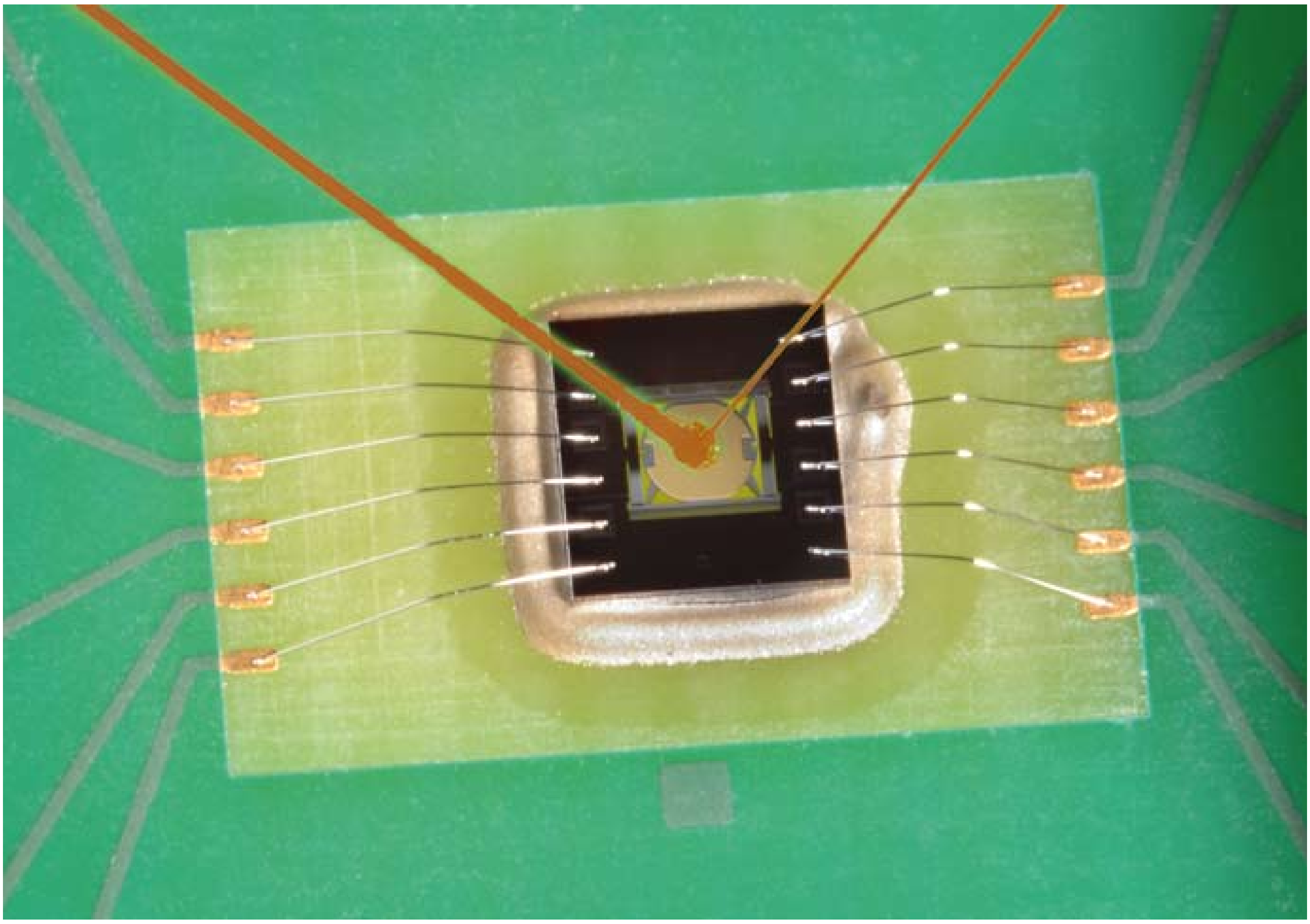

Figure 2. A micro-mirror fabricated using MEMS technology.

projection display device (integrated, for example, in a mobile phone).

Behind the curtains

Other demos included friction stepper technology for compact, robust linear displacement actuators in consumer products or low-cost industrial applications (see Figure 3), a compact real-time motion control USB card, a robotic arm exhibiting human-like, compliant behavior, as well as robotic eyes that exactly match the speed and movement of the human eye. All in all, the PiB-day offered the participating DSPE members a few interesting insights 'behind the curtains' of Philips Applied Technologies.

Information

www.apptech.philips.com

Figure 3. A friction stepper actuator designed to provide focus and optical zoom functions for mobile phone cameras.

A breakthrough

Photonic Integrated Circuits, also called optical chips or PICs, are considered as the way to make photonic systems or subsystems cheap and ubiquitous. However, PICs still are several orders of magnitude more expensive than their microelectronic counterparts, which has restricted their application to a few niche markets. Recently, a novel approach in photonic integration has emerged to reduce the R&D costs of PICs by more than a factor of ten. It will bring the application of PICs that integrate complex and advanced photonic functionality on a single chip within reach for a large number of small and larger companies. Europe is leading in this novel approach and the Netherlands is playing a key role.

• *Meint Smit* •

Figure 1 shows the complexity development of optical chips for application in Wavelength Division Multiplexing (WDM) in telecommunication systems, the technology that enabled worldwide high-speed internet and that is a major driver for photonic integration. The complexity is measured as the number of optical components per chip [1] [2]. Figure 2 shows an early example of such a chip. The most complex chip reported today is a WDM transmitter chip that integrates 40 wavelength channels, each of them containing a laser, a modulator, a power monitor and a channel equalizer [3].

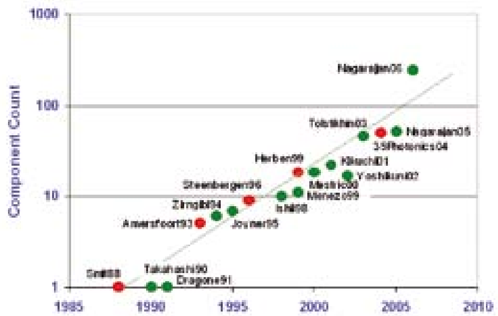

Figure 1. The complexity development of photonic ICs for WDM applications (red points reported by Dutch groups).

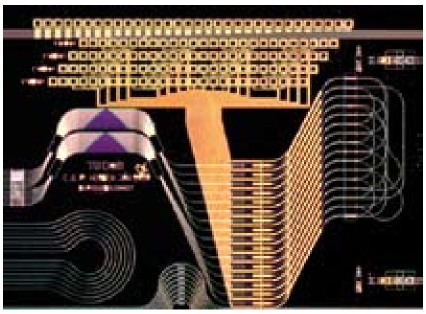

Figure 2. An optical crossconnect (OXC) chip that can switch four wavelength channels independently from two input waveguides to two output guides. It integrates two wavelength demultiplexers with 16 optical switches on a chip area of 8x12 mm^2 (the point labeled 'Herben99' in Figure 1).

in photonic integration

Moore's law

Figure 1 shows a clear exponential trend in the complexity development for photonic ICs, similar to Moore's law in electronics (which 'predicts/describes' the complexity of electronic ICs doubling each 18 months). The figure suggests that photonics is following the process-driven development of microelectronics, albeit at a slower pace and with a 30 years time shift. There is an important difference, however: the well-known Intel plot is about commercially applied devices, whereas most of the points in Figure 1 are research results which did not bring it to the market. The only chip currently applied in a commercial product is the WDM transmitter chip (10x10 Gb/s) of the US-based company Infinera (labeled Nagarajan05 in Figure 1). It is used in a 100 Gb/s WDM system that is proving to be very competitive, and it is the first demonstration that complex PICs provide a competitive edge.

What went wrong?

Why have so few of the advanced PICs reported in the literature made it to the market, despite the fact that in the last two decades several billion dollars have been invested worldwide in development of integration technologies? The main reason is that they are too expensive to compete with technologies like micro-optic or hybrid integration. The problem with current project funding models within Europe is that they tie the technology development closely to an application: no money without a clear and challenging application. Hence the technology has to be fully optimized for that application and, as a result, we have almost as many technologies as applications. Due to this huge fragmentation the market for these specific technologies is usually too small to justify their further development into the industrial volume manufacturing process that would really lead to low chip costs. The few that made it suffer from small profit margins, if any. This is quite different from the situation in microelectronics where a huge market is served by a relatively small set of integration (CMOS) technologies, and development costs of the integration process are shared by a large number of (large-volume) applications.

Generic integration technology

The solution seems obvious, following the micro-electronics approach: developing low-cost Application Specific Photonic ICs (ASPICs) in *generic integration technologies* that can serve a wide variety of applications and have much better market perspectives. In microelectronics a broad range of functionalities is realised from a rather small set of basic building blocks, like transistors, diodes, resistors, capacitors and interconnection tracks. By connecting these building blocks in different numbers and topologies we can realize a huge variety of circuits and systems, with complexities ranging from a few hundred up to over a billion transistors.

In photonics we can actually do something similar. Most optical circuits consist of a rather small set of components: lasers, optical amplifiers, modulators, detectors and passive components like couplers, filters and (de)multiplexers. By proper design these components can be reduced to an even smaller set of basic building blocks. In a generic integration technology that supports integration of the basic building blocks we can realize a variety of functionalities.

Figure 3 illustrates which functionalities can be realised in a generic Indium Phosphide technology that supports integration of three basic building blocks: passive waveguide devices (PWD), phase modulators (PHM) and semiconductor optical amplifiers (SOA). With these a variety of modulators, switches and lasers can be realised. Figure 4, for example, shows an integrated discretely tunable laser with nanosecond switching speed, useful for packet switching applications, which has recently been developed in a generic technology by the COBRA research

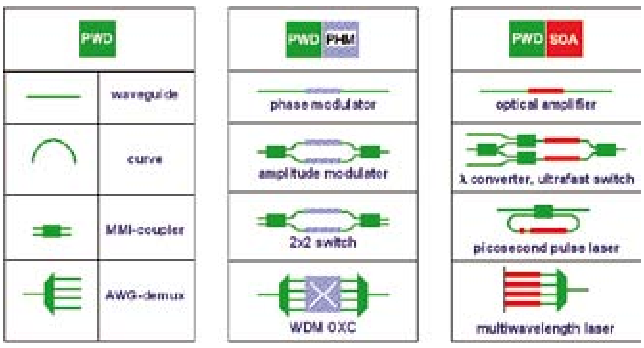

Figure 3. Examples of the functionalities that can be realised in a generic integration technology that supports three basic building blocks: passive waveguide devices (PWD), (optical) phase modulators (PHM), and semiconductor optical amplifiers (SOA).

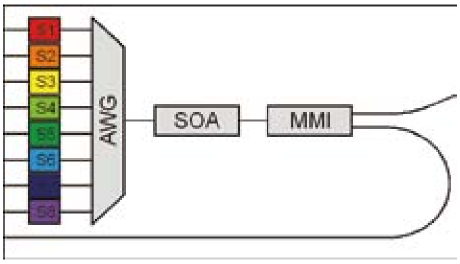

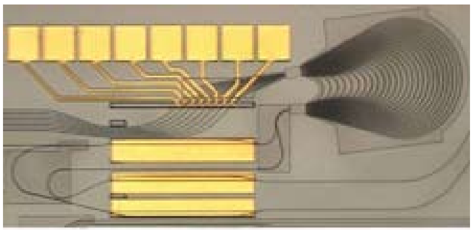

Figure 4. Circuit scheme and microscope photograph of a fast discretely tunable laser with 100 GHz channel spacing, which has recently been realised in the COBRA InP-based generic integration process. Chip dimensions are 1.5 x 3.5 mm^2.

institute in Eindhoven. The schematic on the left shows how the laser is composed of only two basic building blocks: PWDs in the MMI-coupler, the arrayed-waveguide grating (AWG) demultiplexer and the interconnections, and SOAs for amplification and switching.

An advantage of generic integration technologies is that, because they can serve a large market, they justify the investments in developing the technology for a very high performance at the level of the basic building blocks, which will make circuits realised in this technology highly competitive. This performance will not apply for every application, of course. Just like in CMOS different classes of applications need different processes, e.g. for high-voltage, high-power or low-power, high-speed etc.
In a similar way, generic photonic processes will need a few different generic technologies, optimized for different kinds of applications, to cover a major part of all applications. In a fully-fledged generic integration technology we will need a few additional building blocks, like polarisation converters for on-chip handling and control of polarisation, DBR gratings as on-chip reflectors, and fibre mode adapters for low-loss coupling to fibres. And we might also want a process with compact electro-absorption modulators instead of the longer phase modulators. But the number of basic building blocks will remain pretty small, and the number of generic technologies required is far smaller than the number of technologies which are presently in use.

Today, several companies in Europe have integration processes that are suitable as a starting point for development of a truly generic integration process. What still is missing, is the organizational and software infrastructure to provide easy and low-cost access.

A foundry approach

In September 2004, the European Network of Excellence on Photonic Integrated Components and Circuits, ePIXnet, started with a healthy mix of academic and industrial partners on an ambitious mission: to move from a model of independent research to a model of integrated research with shared use of expensive technological infrastructure, such as cleanroom facilities. The idea was to stimulate cleanroom owners to organise access to their facilities for a broader circle of non-cleanroom owning partners.

Next, ePIXnet took the step to the foundation of integration technology platforms. Two major integration technologies were identified: InP-based, supporting the highest degree of functionality, including compact lasers and amplifiers, and silicon photonics technology, offering most of the functionality offered by InP except for the compact lasers and amplifiers, but at a potentially better performance and lower cost because of its compatibility with mature CMOS technology; see Figure 5. For both technologies a platform organization was established. Later a third platform with dielectric waveguide technology was added, offering low-loss and high-quality passive optical functions and some thermo-optic active functions, through the whole wavelength range from visible to infrared. In addition to these three integration platforms, ePIXnet established four supporting platforms: for nanolithography, packaging, high-speed characterization, and massive cluster computing. Now, early 2009, we may conclude that ePIXnet activities will survive after the expiration of EU network funding by the end of 2008.

The Silicon Photonics platform is presently supported by Europe's major CMOS research institutes IMEC and LETI and coordinated by the University of Ghent (Belgium). It

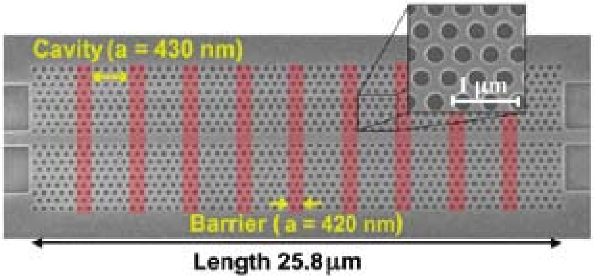

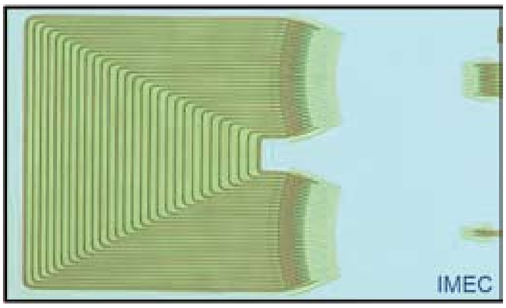

Figure 5. Examples of circuits realised in the ePIXfab silicon-on-insulator technology platform: a complex photonic crystal waveguide filter with a periodically changing lattice constant (left) and an extremely compact 8-channel AWG demultiplexer with high performance.

offers low-cost shared access to processes for high quality silicon photonic ICs to an increasing number of customers, also from outside Europe.
The InP-based technology platform is supported by a consortium containing Europe's key players in the field of InP-technology: chip manufacturers, photonic CAD companies, equipment manufacturers and research institutes. It is coordinated by Eindhoven University of Technology. Within the framework of an EU project and a Dutch national project it is working on the development of industrial generic foundry capability, including software design kits for fast and accurate chip design, and generic packaging and test facilities. Commercial photonic foundry operation is projected in 2013. Restricted access to alpha and beta versions may start as early as 2011. Until that time the COBRA research institute in Eindhoven will provide small-scale access to its generic integration process, for research purposes (proof-of-concept, example in Figure 4).
The third platform, which is supported by the Dutch company Lionix and the University of Twente, provides access to its flexible Triplex dielectric (glass) waveguide technology (SiO_2 and Si_3N_4); see Figure 6. Also the four supporting platforms are rapidly broadening their user base outside the ePIXnet network, gradually moving to full user funding.

The generic integration approach adopted by the ePIXnet platforms is expected to lead to a dramatic cost reduction in both PIC R&D and manufacturing, and a significant reduction of the number of design cycles needed to come to a satisfactory device, mainly because these platforms offer access to a well-characterized process, rather than to a cleanroom. A breakthrough is expected to happen in the next few years. And, due to cooperation that was initiated in ePIXnet, it will most probably start in Europe. Although the ideas about foundry operation have been developed in close cooperation with the organization of the US optoelectronics industry OIDA, Europe clearly has a head start in this novel approach to Photonic IC R&D and manufacturing.

Applications

Consequently, this cost reduction will lead to a large growth of PICs market share. So far, the use of PICs has been mainly restricted to some niche areas in high-end telecom applications. Now, they will also become competitive in high-volume markets like the telecom access network.
But when chip costs drop photonic chips will increasingly penetrate other applications, as in fibre sensors. A significant part of sensor costs is in the readout unit, which contains a light source, a detector and some signal


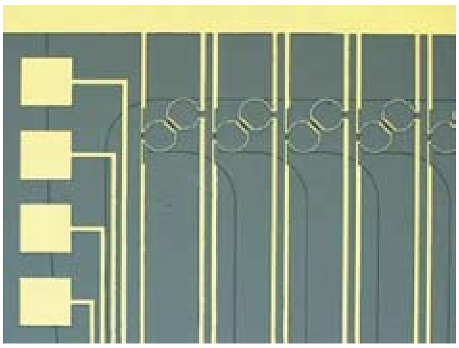

Figure 6. Two examples of ASPICs realised in the Triplex generic technology platform: a photonic true-time delay system for microwave phased arrays antennas (left) and an integrated optical add-drop multiplexer (right).

processing circuitry. Here PICs can replace a significant part of existing modules, and enable novel sensor principles (regarding for example strain, heat or chemical signals).

Another interesting class of devices are pico- or femtosecond pulse lasers. Here PICs containing mode-locked lasers, optionally combined with pulse shapers, can provide small and cheap devices that can be used in widely differing applications, such as high-speed pulse generators and clock recovery circuits, ultrafast AD converters, and multi-photon microscopy.
Once ASPICs and their development get really cheap they will enter into many advanced products. This offers ample opportunities to small and larger companies for applying ASPICs in their products.

Roadmap
The microelectronics roadmap is focused on progress along the Moore's law curve. In photonics, a different development may be expected. It will start with commercial application of ASPICs with a complexity in the range of 5-50 components in rather basic generic foundry processes. The next step will be an increase in performance and capabilities of the generic processes, e.g. with respect to speed, power consumption and number of basic building blocks supported, which may lead to some – but no dramatic – increase in the complexity of the chips. Once the foundry processes cover a wide range of applications, their steady performance improvement will allow for designing increasingly complex chips.

However, it may not be expected that the complexity supported by the generic processes as described here will exceed a component count of 1,000, for a number of reasons. Firstly, SOAs and lasers typically have a power dissipation of several 100 mW. So their number is typically restricted to several tens up to a maximum of a few hundreds, because of heat sinking limitations. Secondly, although they often carry digitally modulated signals, the basic building blocks and the circuits built from them essentially operate in an analog mode, which means that on passing a number of components the signal will accumulate noise and distortion and needs to be regenerated. Regenerators can be integrated too, but they consume space and power.

Finally, from a functionality point of view it is difficult to imagine what circuits would need more than a thousand components. In micro-electronics, the breakthrough to VLSI did not occur in analog electronics but in digital electronics, where signal regeneration inherently occurs after each processing step, so that operations can be concatenated endlessly.

Digital photonics
For photonic integration to move towards (V)LSI circuit complexity a change from analog to digital signal processing will be necessary too. Especially digital photonics based on coupled micro- or nanolasers is a promising candidate for integrating large numbers of digital circuits. It is not obvious, however, that digital photonics will become as successful as digital electronics, because it abandons a lot of the advantages of light, such as the design freedom offered by the wavelength dimension, and in all-optical signal processing the absence of electrical charge which limits operation speeds. And in digital applications it has to compete with electronics 'at its best', in digital signal processing.

Yet, the situation for digital photonics is not hopeless. The recent breakthrough in plasmonic lasers [4] [5], which are not larger than modern transistors and can operate with low switching energies at very high switching speeds, holds the promise that digital photonic circuits with more than 100,000 lasers operating at THz clock rate, will become reality. Such circuits might avoid a lot of power-hungry electro-optical conversions in high-speed internet routers. And they might bring photonic integration three decades further on the Moore's law curve. But this will take many years. The first thing to happen is the breakthrough of 'analog' generic photonic foundry technology. And in Europe this may happen pretty soon.

Author's note
Professor M.K. (Meint) Smit is leader of the Photonic Integration Technology group at the COBRA inter-university research institute in Eindhoven. This article is a slightly abridged version of a publication in Fotonica Magazine, January 2009.

References

[1] R. P. Nagarajan and M.K. Smit, “Photonic integration”, *IEEE LEOS Newsletter* Vol 21, Nr. 3, June 2007, pp. 4-10.

[2] M.K. Smit and C. Van Dam, “PHASAR-based WDM devices: principles, design and applications”, *J. of Sel. Topics in Quantum Electron.*, Vol. 2, No. 2, June 1996, pp. 236-250.

[3] R. Nagarajan et al., “Large-scale photonic integrated circuits for long haul transmission and switching”, *J. Opt. Networking*, Vol. 6, No. 2, Feb. 2007, pp. 102-111.

[4] M. T. Hill et al, “Lasing in Metallic-Coated Nanocavities”, *Nature Photonics*, Vol. 1, pp. 589-594, 2007.

[5] F. Zuurveen, “Metal-coated nano-cavity laser”, *Mikroniek*, Vol. 48, No. 3, June 2008, pp. 34-36.

Information

w3.ele.tue.nl/en/oed
www.epixnet.org

Comparison of laser-interferometric

With the rising precision of machine tools the demand for more precise and more efficient measurement systems increases. At present, several systems with different measurement procedures are available. This article describes three systems for the geometrical characterisation of machine systems: TRAC-CHECK and TRAC-CAL by ETALON AG, and MT-Check by IBS Precision Engineering. A qualitative comparison is made regarding the possibilities of compensation for measured geometrical errors as well as the measurement execution. Furthermore, a metrology frame for the characterisation of the dynamic tool path accuracy, which has been developed at Fraunhofer IPT, is presented briefly.

• ***Jakob Flore*** • [*

The machining accuracy of machine tools depends on numerous influences. By stressing the machine, thermal deformation and the static and dynamical stiffness take effect. Further inaccuracies in the fabrication and assembly of the machine parts cause geometrical and kinematic deviations, also in the unstressed state [1]. This paper deals with the characterisation and compensation of the geometrical errors. These errors refer to the movements of a unidirectional axis and describe the deviations between the nominal and actual movement.
According to [1], for a translational axis the positional deviation, the straightness deviations (in both lateral directions), rolling, yawing and pitching are the relevant errors (see Figure 1). Including the deviations for rectangularity, a conventional three-axis machine system has a total of 21 geometrical errors.

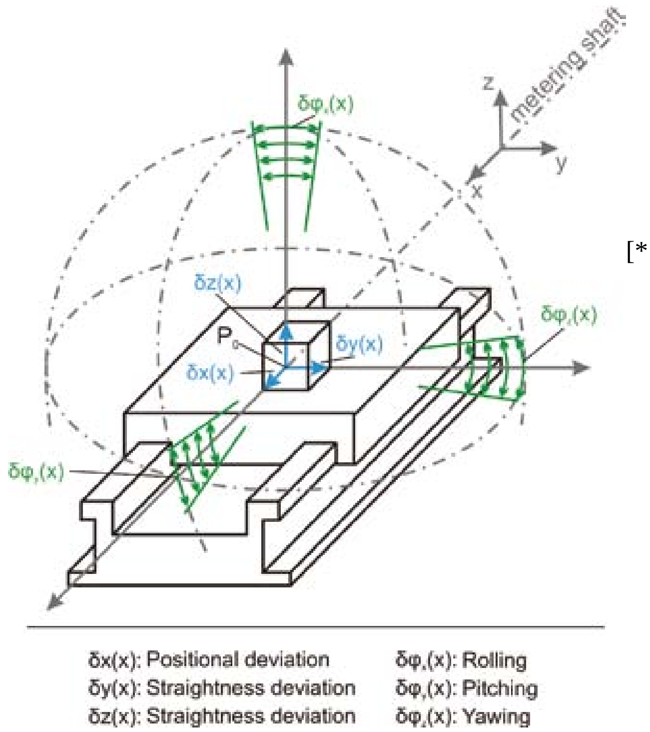

Figure 1. Geometrical deviations of a translational axis [1].

tactile and

measurement systems

Possibilities of compensation

The final target of the machine characterisation is to compensate for the measured geometrical errors. For this purpose, several compensation strategies have been developed, to be implemented in the control unit of the machine. In general, the measured data is stored in the control unit for the calculation of error motion commands. Depending on the compensation strategy, different ways of describing the errors are required. Following [2] and [3], two different examples of strategies, the space-grid compensation and the volumetric compensation, are briefly explained below.
The space-grid compensation is based on a three-dimensional grid, filling out the workspace, which is defined by the lengths of the axes. The crosses of the grid describe nominal workspace positions. For each of these positions, a three-dimensional error vector is stored in the control unit, which represents the deviation between the nominal and the actual position. The control unit uses these vectors in the generation of the motion commands.
The volumetric compensation is based on various mathematical functions, which describe the specific geometric errors of an axis (e.g. positional deviation, rolling, etc.) depending on the nominal axis position. To compensate for the geometrical errors, the control unit solves the corresponding equations and includes the specific influences into the generation of the motion commands.

Three measurement systems

In the context of recent work, the Fraunhofer Institute for Production Technology IPT examined and compared measurement systems for the characterisation of geometrical axis errors. The focus was set on the system LaserTRACER including the evaluation software TRAC-CHECK and TRAC-CAL by ETALON AG and a system by IBS Precision Engineering called MT-Check. In reference to [4], [5], [6] and [7] the functionality of these systems is briefly outlined below.

The LaserTRACER is a laser-interferometer-based measurement system for machine tools and coordinate measuring machines; see Figure 2. The laser beam follows a pentaprism reflector which has to be mounted near the tool centre point. In order to do this, two drives, controlled by using a photosensitive diode, afford the flexible and rapid tracking. On the basis of the modifications of the laser beam length the geometrical deviations are detectable.
The LaserTRACER contains a Class 2 Laser with a wavelength of about 632 nm and offers a measurement range from 0 to 6 m and an accuracy of measurement of about 0.3 µm + 0.3 µm/m.
Depending on the software used, different measurement routines can be executed whereby different deviations are quantifiable.

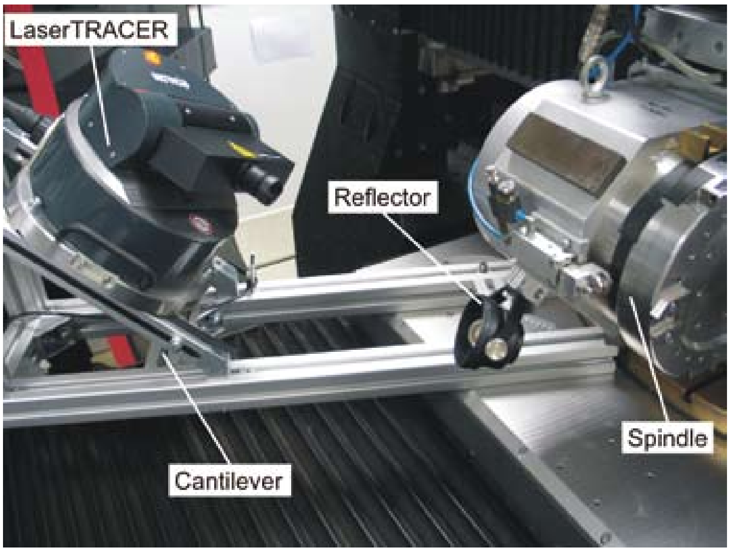

Figure 2. LaserTRACER and reflector installed on an ultra-precision machine tool.

For a three-axis system, the software TRAC-CHECK enables the determination of positional deviation of an axis and also deviations of rectangularity of a Cartesian coordinate system. In order to execute the measurement, straight lines with discrete measuring points have to be defined at which the modifications of the laser beam length are recorded. By defining a line along the axis the positional and straightness deviations are detectable,

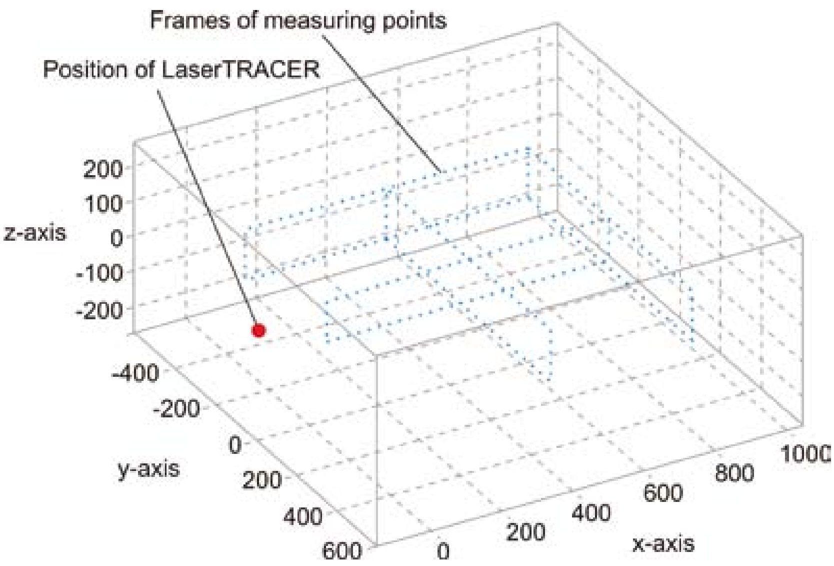

Figure 3. Frames of measuring points.

whereas by defining a diagonal line the deviation of the rectangularity can be measured.
Also for a three-axis system, the software TRAC-CAL enables the determination of positional, straightness and rectangularity deviations, and also the rolling, pitching and yawing of each axis, so all 21 geometrical errors are detectable. For this purpose, at least six positions of the LaserTRACER have to be defined. Frames of measuring points, contained in the workspace of the machine, have to be measured from each position; see Figure 3.

The system MT-Check by IBS Precision Engineering is based on an electro-mechanical probe for the data acquisition and a ball beam as an etalon; see Figure 4. Three eddy current sensors with a calibrated measurement range of 1.0 mm are included in the probe. Each of them measures against a plate which is mounted with springs. This design allows a tactile measurement. The specific arrangement of the sensors enables the acquisition of a three-dimensional signal according to a Cartesian coordinate system. The ball beam contains several ceramic balls, which have calibrated positions and diameters that are highly constant (22 mm, roundness < 0.5 µm). The system accuracy is better than 2 µm and it offers a measurement range from 0 to 0.5 m. Using larger ball beams, the measurement range can be raised up to 1.5 m. In order to execute the measurement, the probe has to be fixed in or near the tool holder. The ball beam has to be clamped along the relevant axis. Before the measurement can be conducted the coordinate systems of the machine, the probe and the ball beam have to be aligned by the control unit. During the measurement, the probe touches each of the balls. The signals of the three sensors correspond to a deviation vector in the Cartesian coordinate system. The software evaluates this data and provides the positional and straightness deviations.

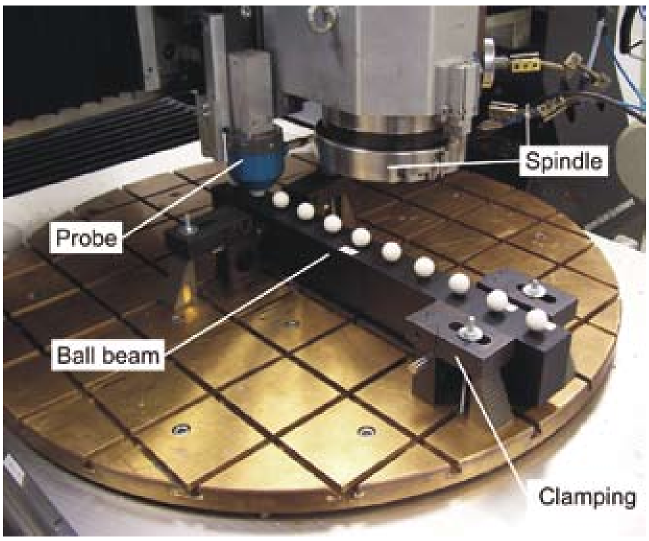

Figure 4. MT-Check installed on a machine tool.

Measurement setup and results

In order to test and compare the three measurement systems, the ultra-precision planing machine UHM (stroke of the axes: 1.800 x 900 x 200 mm³) of Fraunhofer IPT was characterised with TRAC-CHECK, TRAC-CAL and MT-Check. A discussion of all measurement results does not fit in the scope of this article. Therefore, only the positional deviation of the x-axis is considered. Furthermore, only the half-length of the x-axis was measured because of the following reasons. The UHM is a machine with a low portal (located at the centre of the x-axis) on which the y- and z-axis are mounted. The x-axis has to be moved through this portal. On the x-axis (workpiece table) the LaserTRACER is fixed. Because of its size, it is not possible to move the axis trough the portal. Therefore just half of the x-axis is measurable. Using the MT-Check, only half a meter of the x-axis is measurable because of the ball beam length (see Figure 4). Additionally, it has to be mentioned that due to the geometry of the UHM and the size of the LaserTRACER, the LaserTRACER had to be fixed with a cantilever on the x-axis to avoid collisions (see Figure 2).
The measurement results are shown in Figure 5.

Discussion

Each of the diagrams in Figure 5 shows different results for the positional deviation of the x-axis. This can be ascribed to the different measurement procedures and evaluation algorithms of the systems.
TRAC-CHECK employs a simple laser-interferometric measurement of lengths. The straightness deviation and the rolling, pitching and yawing of the x-axis influence the measured position but these influences are not separated from the positional deviation. Because of this, the positional deviation measured with TRAC-CHECK corresponds to an overall deviation of the x-axis.
The evaluation algorithms of MT-Check distinguish the influences of the positional and straightness deviations, whereas the contributions of rolling, pitching and yawing of the x-axis are incorporated in the measured positional and straightness deviation.
A separation of the 21 geometrical errors is achieved by measuring with TRAC-CAL. All the different deviations are determined independently from each other.

Thus, the measured positional deviations differ from each other according to the measurement system used. In general, the measurement systems produce different descriptions of the deviations.
A reasonable comparison of the measurement results is possible by adding the individual deviations to an overall positional deviation. This requires the knowledge of all the relevant geometrical parameters of the measurement setup, such as distances between the etalons or the LaserTRACER positions and the centres of rotation of the rotary errors.
In order to use the measurement data for compensations by the control unit, the description of the deviations has to suit the compensation method. For example, for the volumetric

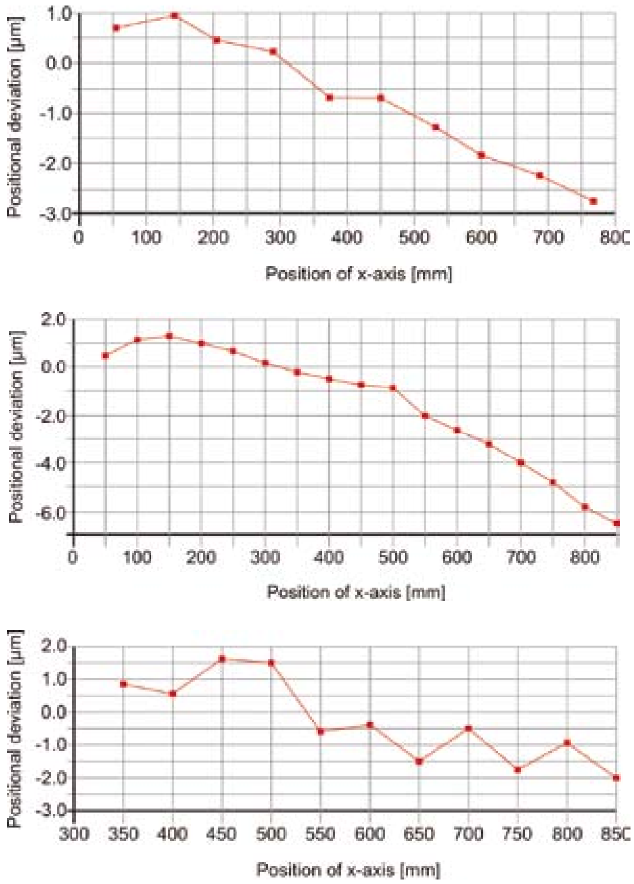

Figure 5. Positional deviation of the x-axis, averaged over five forward and backward cycles, from measurements on three systems.
(a) TRAC-CHECK.
(b) TRAC-CAL.
(c) MT-Check.

compensation each of the possible deviations has to be determined as an independent mathematical function, whereas the space-grid compensation refers to an overall positional deviation.

Comparison

During the measurements, several observations concerning the execution by each of the systems were made.
The installation of the instruments for measurements with the LaserTRACER needs just a few minutes. No precise adjustments of the instruments are required. However, generating the measurement strategy (frames of measurement points, positions of the LaserTRACER) can be very time-consuming, especially if the geometry of the axes or the machine is disadvantageous. Examples of a disadvantageous geometry are short axis length, low portals or a tight housing. In generating the strategy, the user has to avoid collisions during the measurement process and has to take into account that the quality of the measurement results depends on the strategy. The execution and evaluation of the measurement can be conducted comfortably because of automatic routines. However, it is hard to understand and reproduce the evaluation of the measurement data. The effect of possible errors in measurement is not easy to detect in the results, so that a second or third measurement is needed to confirm the results.

The installation of the instruments for measurements with MT-Check requires several time-consuming adjustments by the control unit. Moreover, the measuring length is limited by the length of the ball beam. On the other hand, this fact is favourable in case of the measurement of machines with a disadvantageous geometry (see above). No time-consuming development of measurement strategies is needed, however. Because of automatic routines, the measurement execution and evaluations also can be conducted comfortably.

In general, three conclusions can be drawn:

- For machine systems with a small workspace or a disadvantageous geometry the MT-Check system is more useful, whereas for large machine systems the LaserTRACER systems are easier to operate.
- To get a complete description of all the geometric deviations (e.g. to use for a volumetric compensation) a characterisation with the LaserTRACER or TRAC-CAL is more efficient. For a quick measurement of only one axis or for some test measurements the MT-Check system may be preferred.
- The application of the measurement systems based on the LaserTRACER is sometimes difficult and requires a skilled user, especially because of measurement strategy development, which has a strong influence on the quality of the results.

Metrology frame

Next to the geometrical deviations, several dynamic effects influence the machining accuracy. These effects depend on a lot of factors like the tool path speed respectively acceleration or the weight that is moved along the axes, and cause deviations of the tool path.
At Fraunhofer IPT, a metrology frame was designed in order to characterise the three-dimensional path accuracy of highly dynamic milling machines. It was developed for the integration on a three-axis machine. Use of this frame allows the metrological determination and optimisation of the dynamic properties, the parameters of the drive control and the adjustment of the damping system of the decoupling axes.

Figure 6 shows the design of the metrology frame. The frame is made up of slides equipped with air bearings. The possible stroke of the axes is 180 x 180 x 80 mm³. In each direction the Heidenhain high-resolution metrology system LIDA is used to measure the tool path. The lightweight construction limits the weight to be moved to a mere 4 kg. The design allows the tool path to be measured as close as possible on the tool centre point. Including an estimation of the displacement due because of the bearing stiffness, a maximum deflection of the frame of less than 2 μm can be expected.

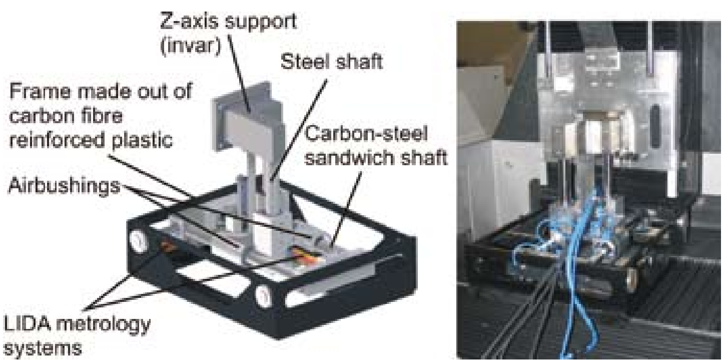

Figure 6. Design of the metrology frame.

The measurements with the metrology frame have to be executed as follows; see Figure 7. At first, the static accuracy can be characterised by measuring discrete points on the tool path. Further, the path accuracy can be determined at different path speeds and control parameters.

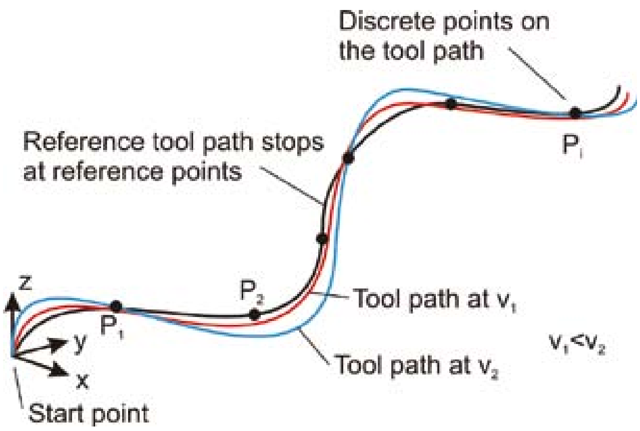

Figure 7. Approach for the characterisation of the tool path.

Analysing the measurement results, strategies for a minimisation of the deviations and an optimised setup of the decoupling systems can be derived. Moreover, it is possible to adjust NC programs for the workpiece machining in order to minimise the path deviations at high path speeds.

Summary

The axes of a machine system have geometrical deviations. In order to quantify these errors, complex measurement systems have been developed that facilitate a quick and complete characterisation. The comparison of three current systems shows that depending on the machine system (large/small) and the measurement task different systems are preferable. Furthermore, the description of the deviations differs from one system to another.
A metrology frame designed by Fraunhofer IPT allows the determination and compensation of tool path deviations caused by dynamical effects.

Acknowledgement

The research work for the metrology frame was funded by the German Federal Ministry of Economics BMWi, supported by the Arbeitsgemeinschaft industrieller Forschungsvereinigungen Otto von Guericke e.V. (AiF), AiF-FV-Nr.: 13868 N/ 237 ZN, and supported by the Network of Excellence 4M, which is funded by the European Union within the Sixth Framework Program.

Author's note

Dipl.-Ing. Jakob Flore works in the Department for Production Machines at the Fraunhofer Institute for Production Technology IPT in Aachen (Germany).

References

[1] Weck, M., “Werkzeugmaschinen, Messtechnische Untersuchung und Beurteilung”, Springer-Verlag, 2001
[2] Bretschneider, J., Geometriefehler kompensieren, *mav*, 2008 (10), pp. 68-71
[3] Bretschneider, J., Reduzierte Stillstandszeiten, *Motion World*, 2008 (3), pp. 18-19
[4] ETALON AG, Handbuch LaserTRACER, Braunschweig, September 2006
[5] ETALON AG, TRAC-CHECK Handbuch, Braunschweig, June 2008
[6] ETALON AG, TRAC-CAL Handbuch, Braunschweig, December 2008
[7] IBS Precision Engineering, MT-Check Manual, Eindhoven, January 2008

Low-frequency with passive

Conventional geophone topologies and their intrinsic physical limitations, determined by the mechanical construction, limit their velocity sensing capabilities. Therefore, Magnetic Innovations has developed a novel, patent pending topology with a passive magnetic spring, that overcomes these limitations. The compact, robust and passive design offers new improvement possibilities for semiconductor and seismic industries.

• *Johan Dams* •

In many industrial applications, especially for vibration isolation purposes, absolute velocity sensing is critical for the high level of precision and accuracy required. In lithographic and high-level inspection applications for example, absolute velocity is measured to determine disturbances of the payload caused by moving parts and external disturbances. Absolute velocity sensing is utilized in this case to accurately position and control a complex lens system. Absolute velocity measurements are also necessary in seismological research applications related to earthquake prediction or the detection of oil/gas fields; see Figure 1. A geophone, or seismometer, is a commonly used device for such measurements.

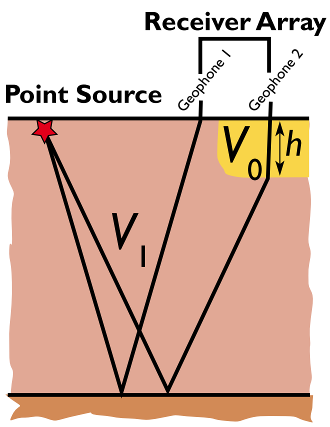

Figure 1. The principle of seismic measurement.

An important property of a geophone is the resonance frequency, which should be low to allow measurement of low-frequency signals. A large bandwidth is required as well, in order to measure high-frequency signals simultaneously. Geophones exhibiting a low resonance frequency are commercially available. However, they often have a limited bandwidth and large dimensions, or need an external power supply, which makes them too expensive for a number of applications. The main characteristic of the majority of the geophones available nowadays is the presence of mechanical springs, which limit the performance of the device.
Magnetic Innovations has developed an electromagnetic solution including a passive magnetic spring in order to resolve these limitations and to provide a very compact high-bandwidth geophone with a low resonance frequency.

Geophone principles

The elementary topology of a geophone is a mass suspended by mechanical springs, as illustrated in Figure 2.

geophone magnetic spring

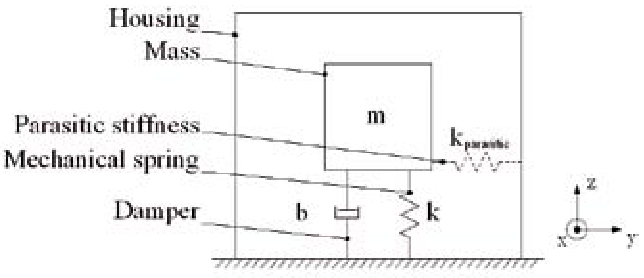

Figure 2. Mechanical geophone representation.

When a velocity, in the z-direction, is imposed on the geophone, both the suspended mass and the geophone housing start to move according to the imposed velocity for frequencies lower than the resonance frequency. For frequencies above the resonance frequency, the mass will no longer follow the movement of the housing and remain stationary. The mass *m*, depicted in Figure 2, is implemented by means of either magnets or coils. Therefore, two topologies of electromagnetic geophones can be defined, i.e., moving coil and moving magnet. Figure 3 shows a topology with a moving magnet, where the coil part is stationary, and the opposite, a moving coil topology, where the magnet is stationary.

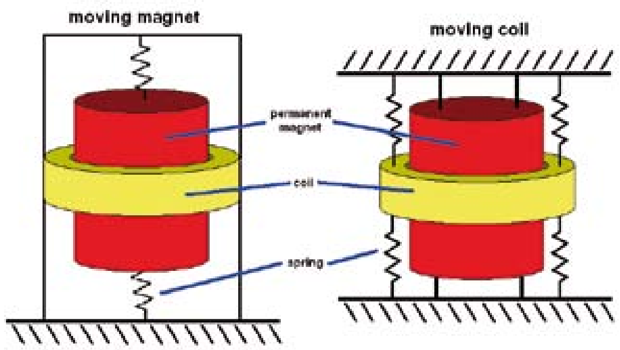

Figure 3. Geophone topologies: moving magnet (left) and moving coil.

Electromagnetic principles

Electromagnetic geophones, schematically presented in Figure 3 are based on Faraday's law. The movement of the magnetic circuit relative to the coil, or vice versa, causes a change of the magnetic flux linked by the coil, thus an emf (with an amplitude dependent on the velocity of the magnet) is induced in the coil.
Research on geophones has primarily been focused on increasing the flux rate of change, therefore the induced emf and by that the geophone sensitivity (*S*) given by

$$S(s) = \frac{U(s)}{v(s)} \qquad (1)$$

where *U* is the generated voltage by the geophone and *v* the imposed velocity. These improvements have led to geophones with a large sensitivity and improved signal-to-noise ratio. However, these developments did not solve the physical problems caused by mechanical springs if one is to obtain a low resonance frequency.

Mechanical principles

The main specifications for geophones are the bandwidth, sensitivity and phase response. For the phase response it is important that the phase shift decreases to zero, especially for motion control applications where a phase shift results in a delayed velocity signal.
Figure 4 shows a general representation of the bandwidth and the magnitude response of a geophone, where the line

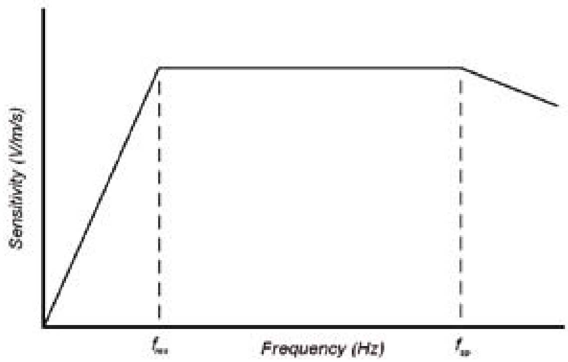

Figure 4. Response curve of a geophone.

between the resonance frequency (f_{res}) and the spurious frequency (f_{sp}) indicates a constant sensitivity.

The bandwidth of a geophone is defined as the frequency range between the resonance frequency and the spurious frequency. In this range the sensitivity, *S*, is constant. The resonance frequency is determined by

$$f_{res} = \frac{1}{2\pi}\sqrt{\frac{k}{m}} \quad (2)$$

where *k* is the spring constant and *m* is the mass, which were depicted in Figure 2. The spurious frequency is usually defined by properties of the mechanical spring, i.e. mechanical springs have instead of a spring constant in vertical direction, *z*, a parasitic constant in horizontal direction, *y*, as well. This horizontal spring constant, significantly higher than the vertical spring constant, introduces an additional resonance at a higher frequency, which is often visible in the frequency response of the sensor.

The main challenge during geophone development is to obtain a low resonance frequency and a high bandwidth by increasing the spurious frequency. Next to that, geophones with a low resonance frequency have large dimensions and need external circuitry such as a power supply, which is not desirable for passive velocity measurement. To demonstrate the main challenge, the factors that influence the resonance frequency, as given in (2), have to be analyzed.
In order to obtain a low resonance frequency, the ratio between the spring constant, *k*, and the mass, *m*, should be small. So, the mass needs to be increased in order to obtain a lower resonance frequency. By enlarging the mass, or the force *F*, the preload of the mechanical spring, *x*, indicated in Figure 5, is increasing according to Hooke's law for springs, given by

$$F = -kx \quad (3)$$

The second option to decrease the resonance frequency is to reduce the spring constant. However, this results in a larger preload of the mechanical spring as well (due to the constant mass). Lowering the resonance frequency to 0.5 Hz for example as shown in Figure 5 results in a preload of 1 m, which normally would result in mechanical failure of the spring.

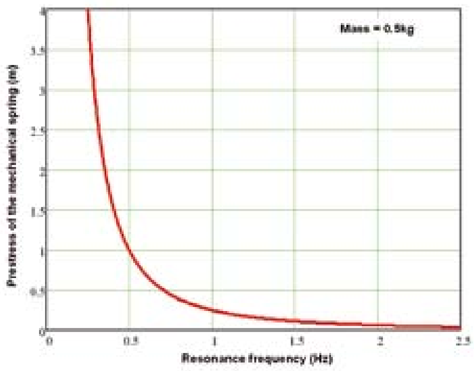

Figure 5. Preload of the spring with constant mass as function of f_{res}.

To overcome the mentioned drawbacks of existing geophones a solely permanent magnetic spring was developed by Magnetic Innovations to dramatically reduce the preload of the mechanical spring.

Sensor topology

The new geophone design is presented in Figure 6 and consists of three permanent magnet rings, a coil, and a set of mechanical leaf springs. The design incorporates moving magnets to avoid stress on the coil terminal leads during movement.

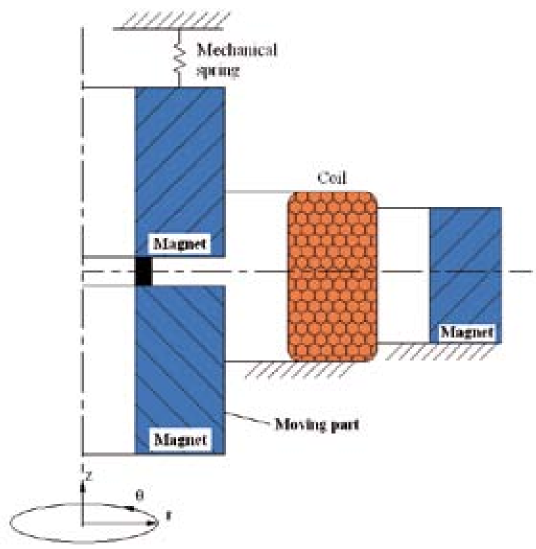

Figure 6. Geophone with passive magnetic spring.

The moving part is formed by the two inner magnets that are interconnected and suspended by mechanical springs, where the stationary part encompasses the outer magnet and the coil. All the magnets are placed in such a way that a low spring constant, which remains constant along the stroke, is obtained. The coil is positioned to obtain a constant sensitivity. Passive magnetic levitation, however, is intrinsically unstable. In the new design therefore, stability is enforced by applying cylindrical leaf springs which enable only one degree of freedom (DOF), i.e., movement along the *z*-axis.

The characteristics and magnetic behavior of the sensor were optimized by means of extensive magnetic modeling. The optimized magnetic spring constant is very low, which in combination with the mass and leaf spring results in a resonance frequency using (2), to be < 1 Hz, which is low in comparison with the majority of the passive commercially available geophones.

The geophone is represented by a second-order system, as presented in Figure 2, with a mass, *m*, spring, *k*, and a damper, *b*, which leads to the Newton equation

$$m\ddot{x} = F - b\dot{x} - kx \qquad (4)$$

where *F* is an external force and *b* is the damper constant. The constants, *m*, *b* and *k*, determine the behavior of the system.

Velocity dependency

Another important property of the sensor, as stated in (4), is the damping, *b*, which is a velocity dependent property. Damping is required to condition the signal generated by the geophone.

Equation (4) can be rewritten to a characteristic equation

$$ms^2 + bs + k = \frac{F}{x} \qquad (5)$$

This second-order system's free response, described by (5), can be characterized by the damping ratio ζ, which is defined by

$$\zeta = \frac{b}{2\sqrt{mk}} \qquad (6)$$

Three cases can be distinguished:
- critically damped,
- overdamped,
- underdamped.

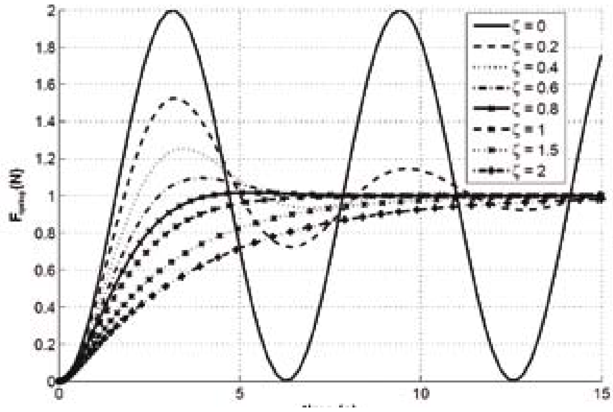

Figure 7. Step response for different values of ζ of the model.

Figure 7 shows a time response plot where ζ is varied from ζ = 0, an undamped system, to ζ = 2, an overdamped system. The value ζ = 1 represents a critically damped system.

As Figure 7 shows, overdamping results in a long settling time where underdamping results in overshoot of the signal. There are various mechanical options to implement a damper within a system. However, the damping achieved within this system has to be contactless and without any external equipment. Therefore, eddy current damping is integrated into the sensor design.

With the movement of the magnets, eddy currents are induced in an electrical conductor. These eddy currents circulate in the electrical conductor and generate a magnetic field opposing the applied magnetic field. The interaction of the two magnetic fields causes a velocity dependent repelling force. By using eddy current damping within the sensor, no external circuitry is required to provide damping, in contrast with competitor geophones. Sensor signal integrity is therefore less compromised and remains at its original sensitivity.

Results

For practical performance verification purposes the sensor, with an attached reference sensor, was mounted on a platform which was connected to a shaker. This shaker was controlled by a spectrum analyzer that had the signals from both the reference sensor and the new sensor as inputs. By using a reference sensor the exact characteristics of the shaker were not needed, only exact specifications of the reference sensor. By means of the reference sensor data the frequency response of the measured sensor can be determined.

Figure 8 shows calculated response data and measured data, indicating a resonance frequency of 0.9 Hz and a sensitivity of 36.6 Vs/m.

Vibration isolation results

In collaboration with MI-Partners, three sensors in combination with three moving magnet actuators were

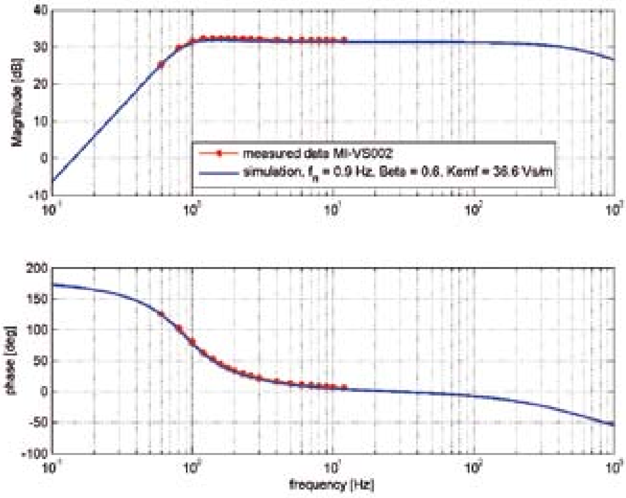

Figure 8. Frequency response of the sensor.

applied in a vibration isolation platform (Figure 9), resulting in 3 DOF (Z, Rx and Ry) vibration cancellation. Passive platform resonance frequency was tuned at 2.5 Hz utilizing springs. During closed-loop operation the applied velocity sensors were used to suppress all measured movement, to which of course the 2.5 Hz resonance frequency of the platform is a dominant contributor.

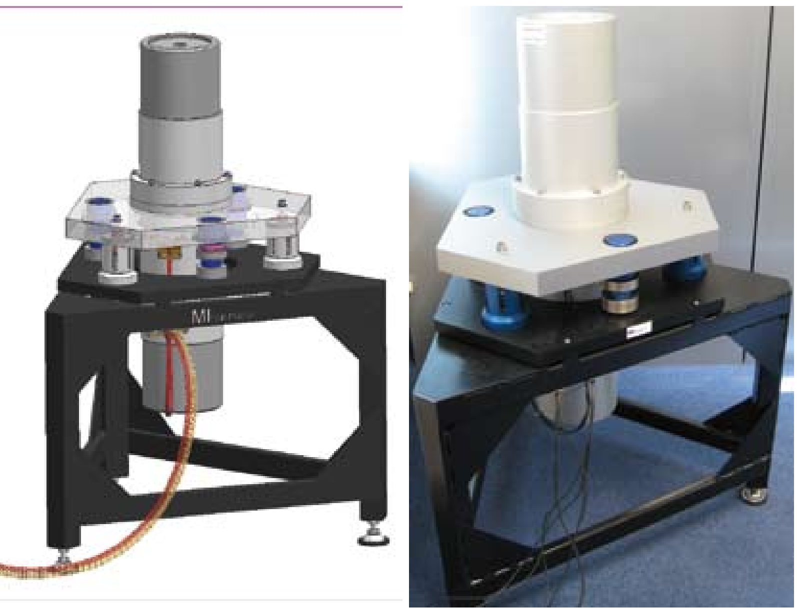

Figure 9. Vibration isolation platform (drawing on the left, actual construction on the right) with three velocity sensors.

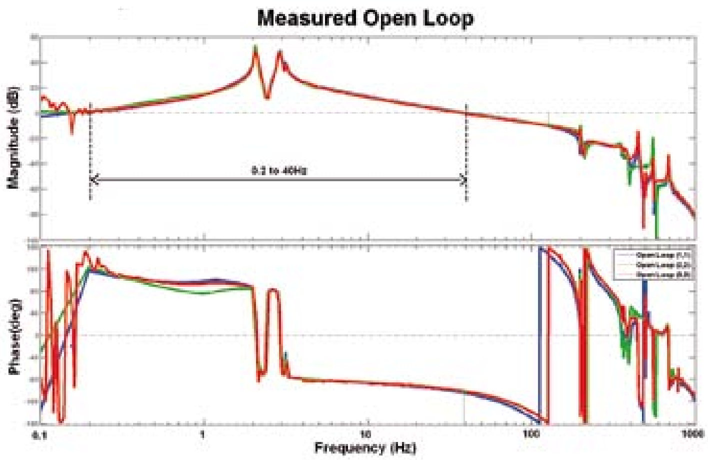

Figure 10. Measured open-loop system transfer functions with three sensors.

The measured open-loop system transfer functions listed in Figure 10 are according to simulations and indicate active vibration suppression between 0.2 and 40 Hz. All listed resonance frequencies in Figure 10 are platform related and no sensor spurious frequency was detected.

Application-oriented versions

Because the size, resonance frequency, spring constant, mass and damping coefficient can be easily varied in the design, application specific sensors can be developed with optimum characteristics for different market areas.

Author's note

After many years of designing electromechanical actuators for lithography machines, resulting in several patented applications, Johan Dams co-founded Magnetic Innovations in 2007 in Veldhoven, the Netherlands. Magnetic Innovations specializes in the design of PMSM motors, linear motors, generators, passive magnet systems, sensors and actuators.
During experimental verification of the sensor design, the Electromechanics and Power Electronics department at Eindhoven University of Technology, under supervision of Professor Dr. E.A. Lomonova, developed an analytical model of the sensor. This work will be published in 'Actuators and Sensors' (author A.J.J.A. Oome).

Information

www.magneticinnovations.com
johan.dams@magneticinnovations.com
w3.ele.tue.nl/en/epe

Innovations in

Every day, new products appear on the market. In order to meet the high quality standards that are expected nowadays by customers, reliable measurements with good accuracy are essential. This fuels a continuous demand for innovations in the field of dimensional metrology, the measurement of shape, size and position. Improvements have been made on various fronts : reliability, speed, range and accuracy. Partly, these innovations are realized by the improvement of existing techniques. But we also see the emergence of completely new measurement principles. To provide an overview of the most recent developments, a one-day symposium was organized on 5 February 2009 under the title "Innovations in Dimensional Metrology". What better location to hold such a symposium than at the Dutch national metrology institute VSL in Delft, the Netherlands?

• *Marijn van Veghel* •

The symposium was jointly organized by Mikrocentrum and VSL. There was a good turn-out, with a mixed audience from the Netherlands and Belgium. Apart from oral presentations, there was also an exhibition with suppliers showing their latest products. Prof. Piet Schellekens, well-known for his work in the area of dimensional metrology at the Eindhoven University of Technology, acted as chairman of the day.

Innovation in standards

After the opening statement of the chairman, the director of VSL, Albert Dalhuijsen, delivered the first lecture. He gave background information on VSL and its role as the national metrology institute. VSL (formerly NMi Van Swinden Laboratorium) is responsible for maintaining the Dutch primary standards (such as the meter and the kilogram) and providing traceability to these standards. The concept of traceability means that companies, institutes, government agencies, etc. can trace their measuring instruments back to the primary standards via an unbroken chain of calibration steps. VSL performs the last step or steps in such a traceability chain, which have to be done with the best possible uncertainty. Traceability is important, because it ensures that measurements are reliable and comparable.

It may seem that there is little room or need for innovation in this activity. This however is certainly not true. Over the years a lot of effort has been put into decreasing the uncertainty with which the standards of the SI system of units can be realized, and with which calibrations can be performed against these standards. More recently, the attention of the research at VSL has shifted to the development of new standards, which specifically target technological developments in society: biofuels, electrical power loss in the transportation grid, LEDs, breath analysis and structures on micro- and nanometer scale. Companies active in these areas can call upon the expertise of VSL in the form of calibrations, consultancy or custom R&D.

Task-specific uncertainty for CMMs

An example of innovations at VSL was given by the author of this article, in a talk dealing with realistic uncertainty estimations using virtual instruments. When doing a measurement, it is important to know the uncertainty, a parameter which indicates the possible difference between the measurement result and the true value. This forms a quantitative measure for the reliability of the measurement. The uncertainty should include all systematic and random effects. Whereas the latter are determined relatively easy from a statistical analysis of repeated measurements, the former are more difficult to ascertain. Still, it is important to have as realistic a value for the measurement uncertainty as possible. Underestimation will give unjustified confidence in the measurement result. Overestimation on the other hand is economically undesirable, as unnecessary efforts will be made to reduce the uncertainty to the required level.

There exists a well-accepted recipe for uncertainty estimation in the form of the ISO Guide to the expression of Uncertainty in Measurement (GUM). For some types of measurements, this approach however is inapplicable. A notable example are dimensional measurements based on 3D co-ordinate measurements, e.g. the measurement of the diameter of a cylinder on a co-ordinate measuring machine (CMM). The measurement result is calculated from many points, which contain correlated effects, such as the guidance errors of the machine. Furthermore, the calculation method is some numerical fit, which does not lend itself to the GUM recipe.

For these types of measurements a different approach is needed. At VSL, so-called Monte-Carlo methods have been developed for a variety of co-ordinate based measuring instruments. These Monte-Carlo methods are described theoretically in a newly released supplement to the GUM (2008). They use a software model of the measuring device, called a virtual instrument; see Figure 1. Uncertainty distributions are assigned to the measurement data and the model parameters. New measurement data and model parameters are generated, by randomly picking values from these uncertainty distributions. A measurement result (say, a diameter) is then calculated for the randomly generated data. By repeating this many times, a distribution of measurement results is obtained, from which the uncertainty can be determined.

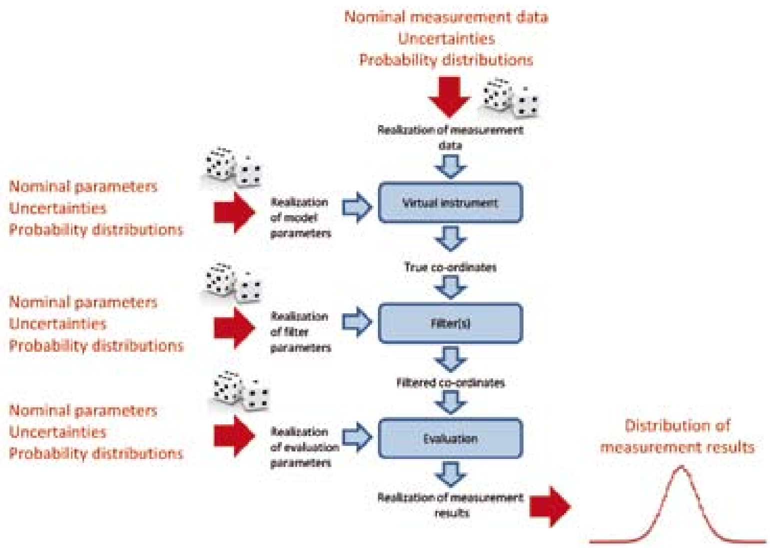

Figure 1. Schematic representation of a Monte-Carlo uncertainty calculation. (Courtesy of VSL)

Applications of this method to various instruments were shown: a stylus profiler, a scanning probe microscope (SPM) and a micro-CMM. The micro-CMM in question is the F25 developed in a collaboration between Eindhoven University of Technology, Carl Zeiss and VSL. The model parameters and their uncertainties in this case are directly linked to the results of the complete laser-interferometer-based calibration performed on the instrument by VSL. The virtual micro-CMM was tested using independently calibrated reference spheres, and the predicted uncertainty agreed well with the observed deviation in sphere diameter.

It is expected that the virtual instrument approach will be applied more and more in the future, and will also be increasingly incorporated into commercial instruments. This will enable users to obtain realistic task-specific uncertainties, instead of machine tolerances which apply to a single point only.

The topic of uncertainties of CMMs in specific measurement tasks was continued by Nick van Gestel of the K.U.Leuven. He addressed a number of influences that determine CMM uncertainty. A well-known source of uncertainties in dimensional measurements is thermal expansion. An accurate measurement of the workpiece temperature is needed to compensate for this. What is perhaps not always realized, is that temperature gradients can be more disturbing than a uniform deviation in temperature. This is especially true in large machines such as CMMs, which may deform as a result of temperature differences between two sides of the instrument. Deformations may also arise because of uniform temperature changes in materials with different expansion coefficients (aluminium, steel or granite). In planning a measurement it is good practice to keep in mind that the temperature will slowly change during the measurement, and hence measure the most critical dimensions as closely after each other as possible.

A question of great practical importance is how to distribute the measurement points over the artifact. Sampling exactly on the peaks or the valleys of the form error of the artifact will give an over- or underestimation of, say, a cylinder diameter. Van Gestel showed that for a cylinder having a 120° symmetric form error, a number of equidistant sampling points which is a multiple of three gives a large error in the diameter, but a relatively small error in the position.

Ultra-precision CMM

On the front of CMM hardware, there have also been developments, of course. One of the long-standing goals has been to reduce the measurement uncertainty. This has been realized in so-called micro-CMMs, such as the F25. These instruments realize uncertainties of down to about a hundred nanometer in a measuring volume of up to a hundred millimeter. The company IBS Precision Engineering is now developing a new ultra-precision CMM, which should realize a 3D measurement uncertainty of 100 nm within a measuring volume of no less than 400 × 400 × 100 mm³. The name of the design, which was presented by Rilpho Donker, is Isara 400; see Figure 2. The name Isara refers to a Mesopotamian goddess. It was first used for IBS's previous ultra-precision CMM, which had a measuring volume of 100 × 100 × 40 mm³.

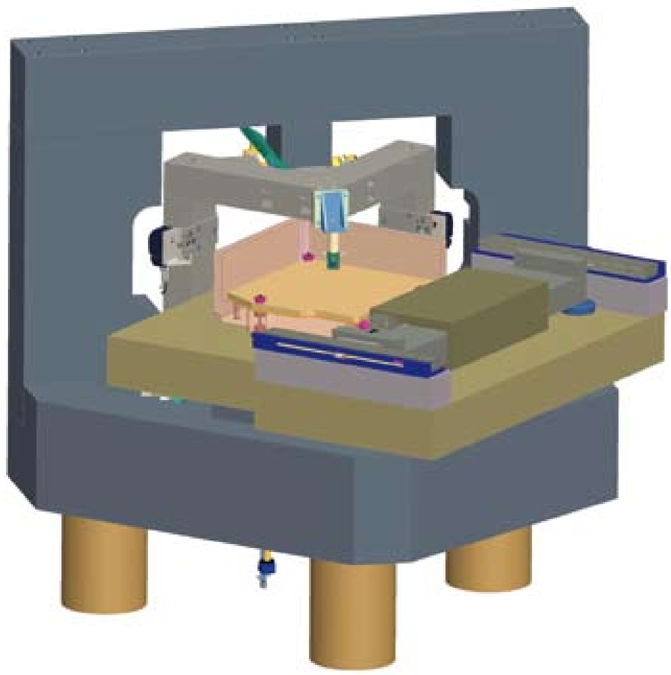

Figure 2. The new Isara 400 ultra-precision CMM being developed by IBS. (Courtesy of IBS Precision Engineering)

What the new Isara has in common with its predecessor is the 3D Abbe concept. In this concept, the x, y and z co-ordinate measurements are done with plane mirror laser interferometers. The laser interferometers are stationary with respect to the probing system and aligned in such a way that they intersect in the center of the probe sphere. The object to be measured is placed on a monolithic three-sided mirror block, with can be translated with respect to the probe. The main benefit of this construction is that the measurement always satisfies the Abbe principle, since there is no offset between the measurement axis and the probing point. Because of this, there is to first order no effect from parasitic rotations.

In the practical realization of the instrument, there are some noteworthy differences. In the original Isara, the mirror stage was translated in three dimensions, while the probe remained stationary. The new Isara uses a 2D translation of the mirror block over a stationary granite table for the x and y motion. Translations in z direction are accomplished by moving the whole metrology frame, including the laser interferometers and the probe, in vertical direction. The metrology frame, which has to be at the same time light, stiff and thermally stable, is constructed from SiC. All guides are equipped with air bearings, instead of the roller bearings in the original Isara. The cylindrical air bearings for the z drive moving the metrology frame double as a weight compensation mechanism, to minimize the power needed to hold the metrology frame in place.

The Isara 400 is intended to be a multi-probe machine. One of the probes it will use is an ultra-precision touch probe designed by IBS; see Figure 3. This probe consists of a 0.5 mm ball attached to a very thin, yet stiff stylus. The stylus is mounted onto a leaf spring design, so that it can rotate around the x and y axis and translate in z direction. The probe deflections are measured using capacitive sensors. Measurement errors in 3D for this probe were shown to less than 20 nm.

Figure 3. The IBS ultra-precision touch probe which will be used on the new Isara 400. (Courtesy of IBS Precision Engineering)

Laser scanning

Nowadays, 3D measurements are not restricted to tactile instruments. Contactless measurements make it possible to acquire a lot of data points in a short time without making physical contact with the object to be measured. Philip Bleys from the Belgian technological center Sirris presented the latest developments in laser scanning. In laser scanning based on triangulation, the workpiece is illuminated with a laser beam; see Figure 4. Reflections from the workpiece surface are captured by an imaging lens which is positioned somewhat to the side of the laser aperture in the sensor head. The lens projects the reflected light onto a digital sensor (CCD or CMOS camera). The position of the imaging lens is fixed, so that the illuminated position on the sensor is dependent on the angular direction of the light falling on the imaging lens. This in turn is directly related to the distance between the sensor and the workpiece. To improve the data acquisition rate, a line of laser light can be used instead of a single spot. This line can be generated by projecting a laser beam onto a resonating mirror or by special optics. The latter method generates a more homogeneous line.

One of the developments in the field of laser scanners is the integration of multiple scanners in a single sensor head. In a so-called cross scanner, three line scanners placed under angles of 120° are combined. This will increase the point density, but also provide a more uniform coverage of features such as circular holes. These are now covered by scan lines in three different directions, so that there is always a scan line intersecting the edge of the feature.

Other important improvements are in the digital camera and the illumination. The acquisition rate of the digital camera increases, allowing a higher point collection rate. Dynamic laser power control is a technology which actively controls the laser intensity dependent on the amount of reflected light from the surface. This is especially helpful on difficult surfaces : shiny materials, surfaces with multiple colours or with sharp reflection angles.

In terms of uncertainty, laser scanners are still inferior to tactile sensors. One of the main uncertainty sources is the heat generated in the sensor head, which is unavoidable given the presence of a light source. Various measures are taken to increase the thermal stability, such as separation of heat generating components, cooling fans and software compensation. This considerably reduces the warm-up time that should be observed before the sensor can be considered stabilized.

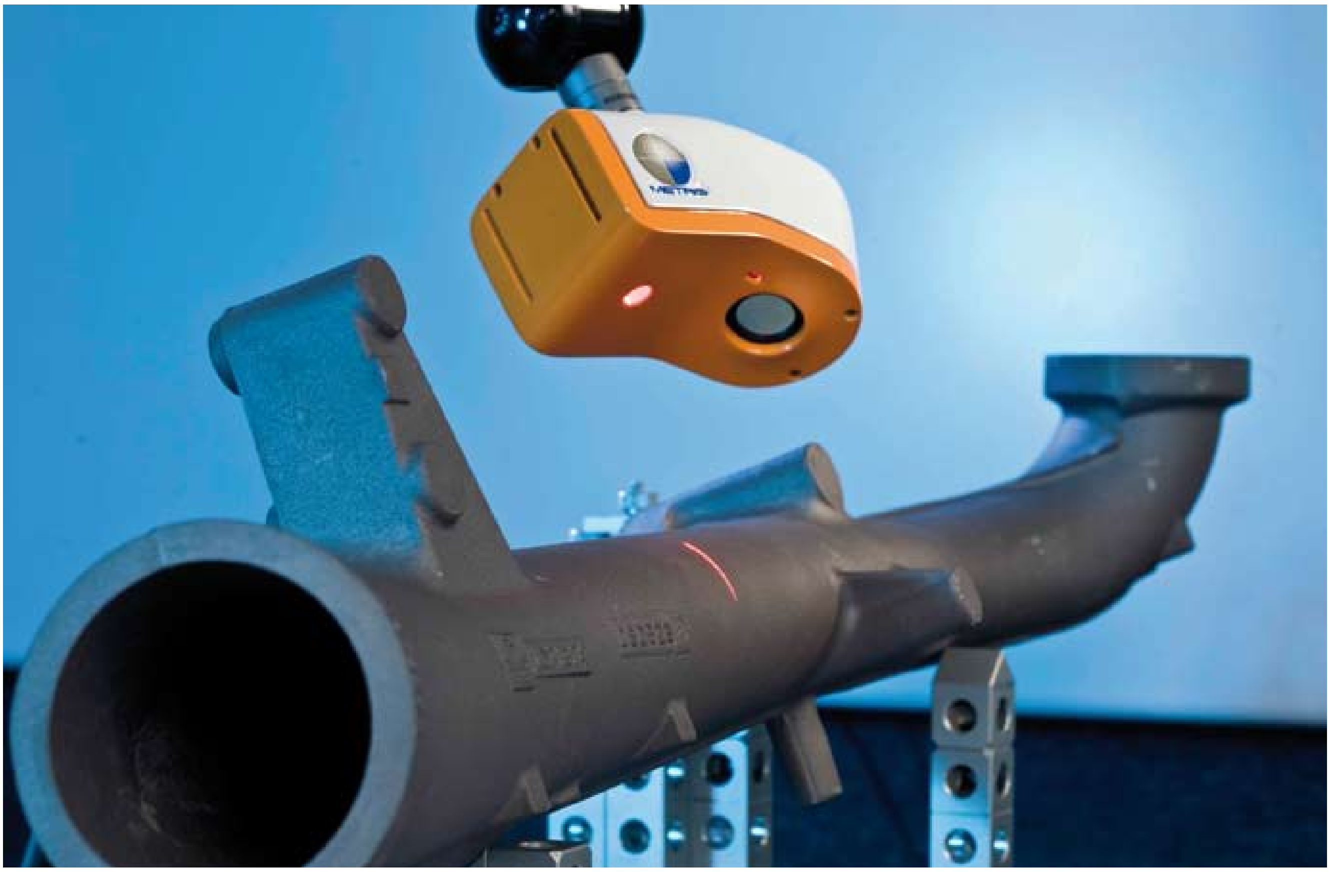

Figure 4. Laser scanner scanning a workpiece. The laser projecting the line is situated in the left part of the scanner, the lens and camera are in the right part. (Courtesy of Sirris)

X-ray tomography

The third measurement principle discussed was X-ray computerized tomography (CT). Pieter-Jan Corthouts from Metris gave his talk the title "Where tactile probes cannot reach and optical laser scanners cannot see", to emphasize the main advantage of X-ray tomography, namely the ability to measure internal features of objects. CT started as an imaging technique, to making 3D images of internal structures, e.g. for medical applications. In the last few years, CT has made the transition from an imaging tool to a metrology tool, where accurate dimensional measurements can be taken from the data.

A CT system has three main components: the X-ray source, the object table holding the workpiece to be measured and a 2D X-ray detector. In a medical system, source and detector rotate around the patient, but in a metrological CT system, the object table is rotated. At each angular position of the object, a 2D X-ray image is taken. The different shades of gray in this image correspond to different amounts of X-ray absorption along a particular line from source to detector. A computer then constructs a 3D map of the absoption from the set of 2D images. Because the absorption coefficient is material dependent, it is possible to differentiate between regions of different material composition in 3D.

Using CT for metrology purposes puts special demands on the X-ray source. A typical medical X-ray source has a size of approximately 1 mm, leading to a blurred image, which has insufficient resolution to take useful measurements. In order to get an image which is sufficiently sharp for dimensional measurements, a so-called micro-focus source with a source size of 5 μm or less is necessary. Also, the

X-ray beam has to be ‘hardened’ by filtering out low-energy X-rays, which have a low penetration depth. Otherwise there will be too much gradient in the beam intensity, leading to a deformed image.

By showing a wide range of examples, ranging from diesel injectors, hydraulic manifolds to dental parts and even fossils, Corthouts demonstrated the versatility of this technique, which will undoubtedly gain importance in years to come.

Metrological AFM

The day was concluded with a presentation on 3D measurements on the smallest possible scale. Chris Werner from the Control Systems Technology group at Eindhoven University of Technology presented his PhD-project on the design of a metrological Atomic Force Microscope (AFM); see Figure 5. This AFM is being developed in a joint project with VSL and will serve as VSL’s next generation AFM.

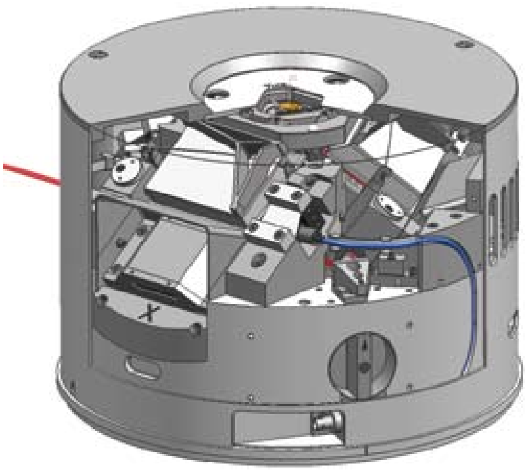

Figure 5. The new metrological AFM being developed at Eindhoven University of Technology. (Courtesy of TU/e)

An AFM measures small structures by scanning a tactile tip over a surface. The instrument Werner is developing has a target uncertainty of 1 nm over a 1 × 1 × 1 mm^3 measuring volume. For an AFM, this is exceptionally large. Unlike most commercial AFMs, the tip in this instrument is stationary and the sample is scanned underneath it. The position measurements are done with three interferometers which have their virtual measurement axes aligned on the tip, so that they are always in Abbe. The interferometers are differential interferometers, which are insensitive to drift in the position of the interferometer optics. The optics are custom-made, with a beam delivery system integrated in the instrument.

A special feature of the AFM is the rotated measurement co-ordinate frame. Instead of having the x and y axes in the horizontal plane and the z axis vertical, the measurement axes are aligned on the edges of a cube with its body diagonal in the vertical direction. This means that all three axes can be constructed identically, giving a large amount of symmetry in the system. The straight guides are constructed as elastic parallel guides, having a high eigenfrequency of 1.4 kHz. They are actuated by powerful Lorentz-type actuators delivering 57 N/A. In order to minimize power dissipation, stiffness and weight compensation mechanisms are present.

One of the nice features of the design is that by a careful layout of the components, Werner has managed to contain everything within a compact table-top instrument of 250 mm diameter. The metal components are manufactured from a single piece of aluminium, a material chosen for its good thermal conductivity and diffusivity. The expansion coefficient of this aluminium has been especially calibrated by VSL. This has been used to optimize the thermal loop, so that the instrument is insensitive to a uniform temperature rise.

Author’s note

Marijn van Veghel works as a technical consultant in the Customized Applied Metrology department of the Dutch Metrology Institute VSL in Delft.

Information

www.vsl.nl
www.mikrocentrum.nl
www.ibspe.com
www.kuleuven.be
www.sirris.be
www.metris.com
www.dct.tue.nl

Avoiding

Epidural anesthesia is a commonly used technique to anaesthetize lower regions of the body. However, the anaesthetizing procedure is risky. To obtain a better insight, a research project was conducted within the Department of Biomedical Engineering of Delft University of Technology, which specifically addressed the design of an epidural needle insertion simulator, psychophysical experiments and clinical results. This article highlights the design considerations of the simulator as well as the experimental results.

• *Luke van Adrichem* •

Besides being used as an anaesthetizing technique during operational procedures within the lower body, epidural anesthesia is also used as a welcome pain relieving mechanism for women who give birth and chronically ill patients. Although numerous applications exist, the anaesthetizing procedure is risky, because delicate tissue is approached with the epidural needle that is used in the process; see Figure 1. Furthermore, the consequence of a failed epidural needle insertion can be severe, such as prolonged headaches and even paralysis. Simplifying the epidural procedure is considered necessary, due to the fact that the demanding technique is difficult to learn and error prone. To obtain better insights into the delicate procedure and reduce the number of failed insertions, intriguing questions need to be answered. Is it possible to identify the procedure in quantifiable parameters to thereafter find improvements of the technique and subsequently increase safety and ease of application?

Introduction

Successful epidural needle insertion is a complex procedure requiring penetration of several spinal tissue layers. What makes the task even more daunting is the fact

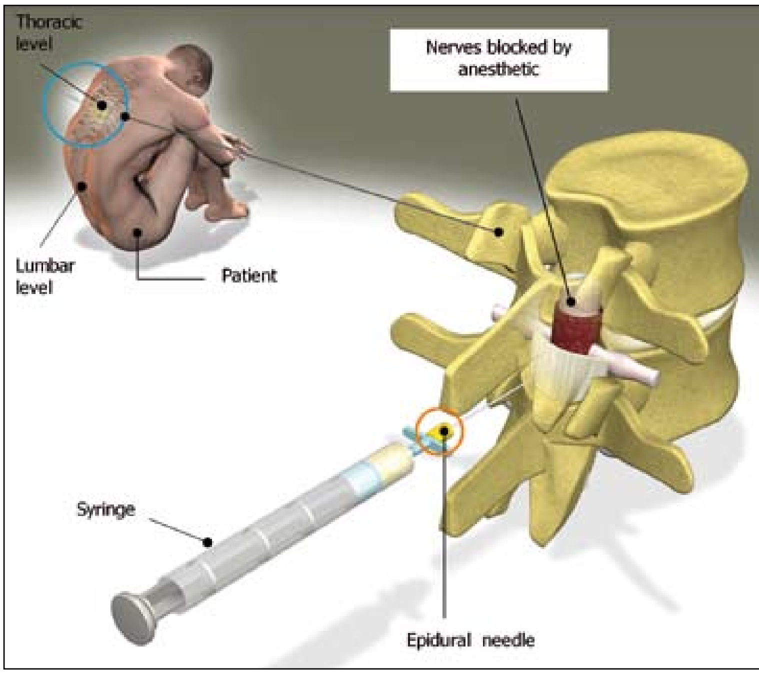

Figure 1. Human spinal anatomy with an epidural needle approaching the epidural space. (Source: Verdult, Kennis in Beeld)

overshoot

that the needle insertion needs to be stopped as soon as the needle tip reaches the space around the spinal cord, also known as epidural space. The distance the needle tip goes into the epidural space is often indicated as 'overshoot'.

The distance from skin to the epidural space in the lumbar region varies from approximately 10 ± 3 mm for small children to 50 ± 12 mm for adults [1] [2]. The depth of the epidural space (distance from start epidural space to spinal cord) depends on the spinal level. For the lumbar and thoracic region variations from 2 to 8 mm have been found [3].

When the epidural needle enters the epidural space, part of the tissue resistive forces disappear abruptly, resulting in a needle overshoot. A large overshoot might damage delicate underlying structures, such as the spinal cord or other neural tissue. The success rate of the insertion is highly dependent on the strategy of application. Part of the problem however is that it is unknown which strategy will yield the best performance. To identify this, it is necessary to fully understand the insertion technique. Understanding the process fully will make it possible to apply novel techniques, such as haptic technology, to improve the needle insertion method.

The haptic feedback during needle insertion depends on needle parameters (e.g. material friction coefficient, diameter, shape), tissue parameters (stiffness, damping, structure), and human factors such as hand position, insertion velocity, and co-contraction in the wrist. Co-contraction is the way people can make a joint 'stiff' by contracting opposite muscle groups. Influence of these parameters on the success rate of the insertion procedure requires investigation. This was achieved by identifying the effect of the parameters on the overshoot of the penetrating needle. These results could thereafter be used as input for improved man-machine interface design and/or improved training.

Haptic epidural simulator

Repeatability and accuracy of measurement are key factors for a psychophysical experiment. Real punctures on porcine specimen or cadavers have relative high haptic resemblance (fidelity) for needle insertion, but are unfavourable for their poor repeatability and accuracy of measurement. Simulators offer both these characteristics, but in general at the cost of fidelity. A simulator should display a typical resistive force pattern of a needle going through the spinal tissue layers, as shown in Figure 2, [4].

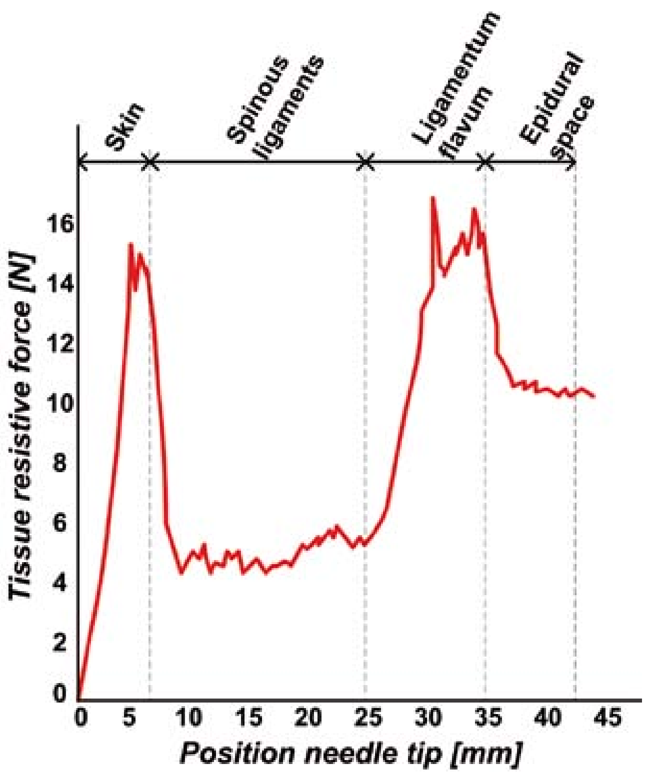

Figure 2: A typical force pattern of a needle penetrating spinal tissue layers as obtained from measurements on porcine specimen. (derived from Brett et al.)

The required accuracy of the resistive force representation is determined by the human haptic abilities. For example, a human is able to perceive only a certain force and position resolution (expressed in Just Noticeable Difference, around 7% in the hands), and force frequency bandwidth – going beyond these thresholds is a waste of effort.

A list of requirements is obtained in order to design a haptic interface with realistic, kinematic, ergonomic and haptic specifications for epidural needle insertion

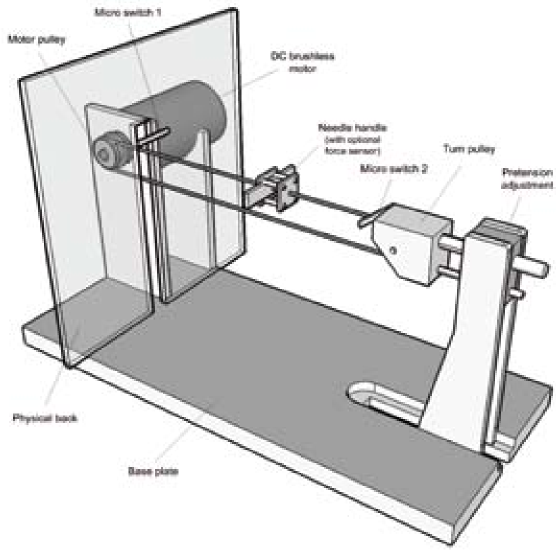

Figure 3. The epidural needle insertion simulator design.

Figure 4. The epidural needle insertion simulator as used for the experiments. (Photo: Manon Eekhout)

experiments; see Table 1. The task is typified as a gradually rising force in one translational degree of freedom, with a sudden force drop resulting in an acceleration (approx. 30 m/s^2). The simulated virtual environment will contain transitions from 'free air' movement towards relatively higher stiffness (approx. 1 N/mm). No hard contacts (e.g. bone contact) have to be simulated. Therefore, the simulator should be optimized more for transmission of high accelerations, rather than for high force or high stiffness. Accordingly, the perceived mass of the needle interface should be in the range of an epidural needle with a fluid filled syringe (approximately 30 grams).
The inherent stiffness of the set-up hardware should be as high as possible in the translational direction. An interface with high stiffness results in a high eigenfrequency, enabling transfer of high-frequency force information.

Table 1. Design requirements.

Requirement	Value	Unit
No. degrees of freedom (DOF)	1	[-]
Range of motion (ROM)	80	[mm]
Force range	0-20	[N]
Stiffness range	0-1,500	[N/m]
Total friction (max)	1	[N]
Perceived mass (max)	50	[g]
Force resolution (min)	0.5	[N]
Position resolution (min)	0.1	[mm]

A realistic needle interface and a physical back for lifelike hand support during needle insertion are qualitative requirements to fulfil. The choice was to make an impedance-controlled system; position-velocity input from the anesthesiologist results in a resistive force output. As a consequence, no force measurements are needed in the control loop, meaning the set-up should be backdriveable and have low friction.

Design

The final design is a simple cable mechanism with two pulleys; see Figures 3 and 4. The brushless dc motor drives one pulley directly without further transmission, avoiding extra friction and play.

The cable is attached to the pulley with soldered steel balls; see Figure 5. By this means the need for high pretension in order to avoid cable slip, is eliminated. The principle of inertial match was used to find the adequate pulley radius for maximal acceleration for the chosen motor.

The implemented Maxon EC40 can withstand a big radial load on the shaft (70 N, 5 mm from the flange), so no extra shaft support (extra bearing, etc.) is needed. A Scancon 2RMHF high resolution encoder (30,000 pulse/rev after quadrature) on the motor shaft is implemented to have high-precision position information and an accurately derived velocity signal. A position accuracy smaller than 0.05 mm was identified.

Figure 5. The motor pulley with the cable attached by means of steel soldered balls.

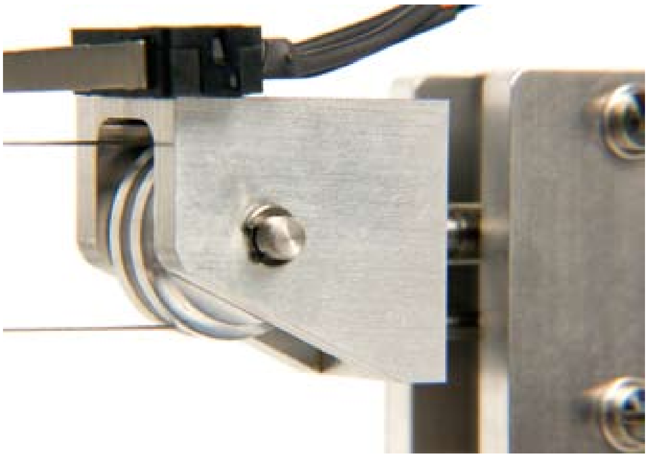

Figure 6: The turn pulley with set screw for application of pretension.

The second pulley is mounted on a slider with a low-pitch set screw for applying pretension (20 N) in the cable; see Figure 6. The two bearings in the second pulley are unshielded and dry (all oil is removed) to minimize friction.

Software

Experiments should ideally be performed under identical conditions. Therefore, secondary computations should not interfere with the controller during the experiments. To this end the simulator works as a stand-alone device in a Matlab® (R2007a) xPC Target (ver.3.2) application. A controller for a virtual haptic environment is modelled in Matlab Simulink and built on the external target pc. A Humusoft MF 624 data acquisition card is built in the external pc. Adaptive windowing is used in the Simulink model for velocity estimation [5]. Adaptive windowing has noise-filtering properties but preserves the velocity transients. The more commonly used filtered derivative for velocity estimation always faces fundamental trade-offs between time lag, phase distortion, attenuation, and cut-off precision. An adaptive window technique selects the window size depending on the signal itself, thereby optimizing for reliability (with high velocity) or precision (with low velocity).

Before conducting the experiments, the system properties were identified according to the guidelines of Hayward et al., and the set-up was calibrated [6]. The Z-width (impedance width) of the virtual environment was determined. The Z-width is a metric indicating the virtual damping and stiffness range a haptic set-up can display in a stable manner [7].

Psychophysics

The experiment was done with the task instruction to perform an optimal epidural needle insertion following a specific strategy as requested, by minimizing the needle overshoot. A group of six anesthesiologists, five residents, and five novices were subjected to these experiments and had to perform multiple needle insertions with nine different strategies. These nine strategies are combinations of three insertion velocities (free, high, low) and three levels of co-contraction (free, high, low). The 'free' velocity or co-contraction implies a speed or co-contraction level assumed by the subject to be optimal for minimal overshoot.

Measurements and results

Position-time data was analyzed and the overshoot determined for all strategy combinations. A typical combined position-time plot for high and low co-contraction is displayed in Figure 7.

From this characteristic the following features can be derived. First, the total overshoot with low co-contraction is significantly bigger than for high co-contraction strategy (average 4.9 ± 0.7 and 1.6 ± 0.6 mm, respectively). A second observation is the relative short period in which the overshoot develops. The percentage of total overshoot reached after 40 ms is 92 and 82 for high and low co-contraction respectively. The first 40 ms after the moment of entering the epidural space (MEES) is considered as passive; human active response is not expected due to physiological delays. This passivity, of the test subject's muscles or hands can be represented as a simple mass-damper-spring (MBK) model with inherent stiffness and damping. This is partly due to the co-contraction of the wrist. Fitting the MBK on the obtained position data of the first 40 ms after MEES, results in a relation between inherent stiffness and overshoot, as shown in Figure 8. It is clear that an increase of inherent stiffness will reduce the needle overshoot.

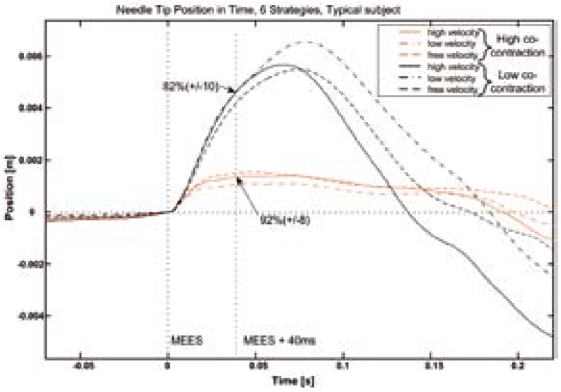

Figure 7. The position of the needle tip penetrating the virtual tissue plotted in time for a typical subject. MEES stands for: moment of entering the epidural space.

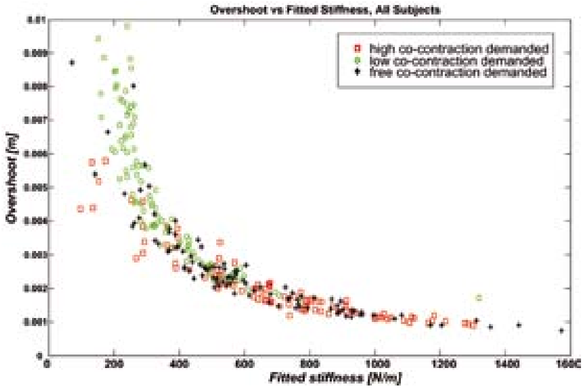

Figure 8. The overshoot as a function of the fitted inherent stiffness. The symbols indicate the co-contraction strategies used.

Conclusions

The performance of an epidural needle insertion is largely determined by the passive response of the human operator as shown in Figure 7. This research showed that increasing the inherent stiffness will result in substantial reduction of overshoot. The increase of impedance can be established by means of higher co-contraction in the wrist. Another way to increase the inherent stiffness is, for instance, the anesthesiologist's hand position/posture on the patient's back. The posture of the fingers determines how the motion can be guided and stopped by restricting the displacement physically. Closely related to the hand posture parameter is the needle length. An anesthesiologist should adjust the length of the needle depending on his estimation on the spinal anatomy out of the patient's physical appearance. An accurate needle length supports correct hand posture.

These findings are currently investigated for their implications on equipment and training, in order to make the epidural needle insertion safer and easier for every patient.
The design process of the epidural needle insertion simulator resulted in a device meeting the requirements as stated in Table 1. The simulator is currently used for further experimentation on other needle parameters and human factors of interest.

Author's note

In April 2008, Luke van Adrichem graduated with honors within the Department of Biomechanical Engineering, Faculty 3mE, Delft University of Technology, the Netherlands. The department's research focus lies in the field of man-machine interface. It participates in the Delft Haptics Laboratory, which explores the role sense of force plays in the man-machine interaction for a number of applications, such as medical, micro-assembly and automotive. This article presents a summary of the author's thesis. The work was conducted within the PhD project of Ruben Lee and was supervised by Prof. Peter Wieringa (Delft University of Technology) and Prof. Dr. André van Zundert (Catharina Hospital, Eindhoven).
Currently, Luke van Adrichem is employed by Temporary Works Design, a small Dutch engineering company that develops installations and structures for the civil and offshore markets. Besides, he is involved in running an agricultural innovation company, TinT.

References

[1] Bevacqua, B.K., Haas, T. & Brand, F. A clinical measure of the posterior epidural space depth. *Reg Anesth* **21**, 456-60 (1996).
[2] Hasan, M.A., Howard, R.F. & Lloyd-Thomas, A.R. Depth of epidural space in children. *Anaesthesia* **49**, 1085-7 (1994).
[3] Hogan, Q.H. Lumbar epidural anatomy. A new look by cryomicrotome section. *Anesthesiology* **75**, 767-75 (1991).
[4] Brett, P.N., Parker, T.J., Harrison, A.J., Thomas, T.A. & Carr, A. Simulation of resistance forces acting on surgical needles. *Proc Inst Mech Eng [H]* **211**, 335-47 (1997).
[5] Hayward, V., Janabi-Sharifi, F. & Chen, C.J. Discrete-Time Adaptive Windowing for Velocity Estimation. *IEEE Transactions on Control Systems Technology* **8**, 1003-1010 (2000).
[6] Hayward, V. & Astley, O.R. Performance Measures for Haptic Interfaces. *Robotics Research: the 7th Int. Symposium*, 195-207 (1996).
[7] Colgate, J.E. & Brown, J.M. Factors Affecting the Z-width of a Haptic Display. In *1994 International Conference on Robotics and Automation*, 3205-10 (San Diego, CA, 1994).

Information

www.bmeche.tudelft.nl

Integrating piezo components in system solutions

The number and variety of piezo applications is growing in all industries, such as semicon, medical, aerospace, consumer and industrial. HEINMADE, based at the High Tech Campus in Eindhoven, the Netherlands, deals with the integration of piezo components into system solutions. After an introduction on piezo technology various examples will be discussed.

• *Hein Schellens and Maikel Heeren* •

The company HEINMADE was founded in 2005 by Hein Schellens as HEIN MAnagement and DEvelopment, underlining that succesfull integration should be properly managed right from the start of development. As a distributor of leading piezo components suppliers (Nanomotion, Noliac and Piezomechanik), HEINMADE is supported by a solid base of piezo knowledge and know-how, and can deliver any type of piezo solution. With its residence at the High Tech Campus in Eindhoven, virtually every analytical technology and scientist is at hand to assist during development. The testing and qualification is performed in a well-equipped lab and, if needed, in a class 1000 cleanroom.

PZT

The word piezo is derived from the Greek piezo or piezein, which means to press. In response to pressure the piezo material (PZT, i.e. lead zirconate titanate) generates an electrical field over the poling direction; see Figure 1. The reverse effect is seen when under an electric field a strain is produced. The maximum strain is about 0.15% at an electric field of 3 V per µm thickness (i.e. 3 kV/mm).

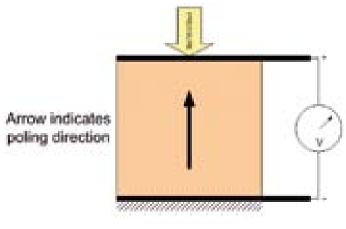

Figure 1. In response to pressure piezo material generates an electrical field.

High precision and high stiffness

The dominant use of piezo in nanotechnology is demonstrated by an example. The elongation of a single bulk element is calculated as the material constant d_{33} (piezo electric charge constant, ~ $500 \cdot 10^{-12}$) times the voltage. At a voltage of 1 V, the elongation becomes 0.5 nm. Thus at 1 mV, the elongation is 0.5 pm (= $0.5 \cdot 10^{-12}$ m), bringing subnanometer positioning 'easily' within reach; see Figure 2.

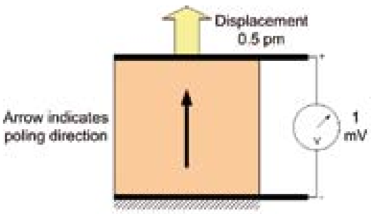

Figure 2. Piezo technology enables subnanometer positioning.

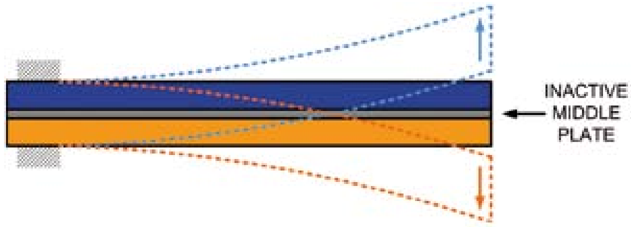

Figure 5. Bending mode of a piezo actuator.

The force required to push the actuated piezo element back to its nominal position is called the blocking force (~ 40 N per mm^2 at 0.15% strain). The relatively small strain in combination with this high blocking force, results in an extremely high stiffness. For example a 10x10 mm^2 element with a thickness of 4 mm gives a strain of 6 µm and a blocking force of 4000 N. The subsequent stiffness is $6{,}7 \cdot 10^8$ N/m, making high resonance frequencies on system level possible. Figure 3 shows the working area of a piezo actuator.

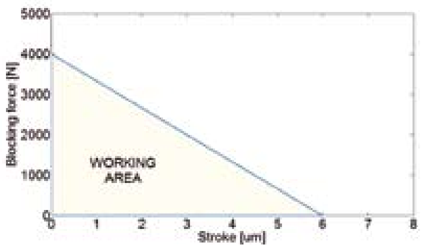

Figure 3. Working area of a piezo actuator.

Multi-layer to lower the voltage

The 4 mm height of the piezo crystal in the example would indicate a required voltage of 12 kV. Because of electrical breakdown risk such high voltages best be avoided. Alternatively, a piezo crystal can be built up from thin layers. At a layer thickness of 66 µm, the maximum voltage is reduced to 200 V for obtaining the maximum stroke. Figure 4 shows the configuration of a multi-layer component. The layer thickness can be freely chosen down to a thickness of 10-15 micron, reducing the voltage further to 30-45 V.

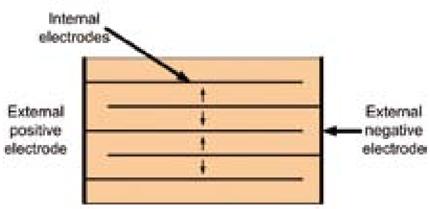

Figure 4. A multi-layer piezo component.

Increase of stroke

The limited displacement of a piezo component can be increased in three different ways: bending mode, cantilever multiplication and by means of a piezo motor. The term piezo actuator is used for the first two and links the applied voltage directly to a certain position. The term piezo motor is used in those cases where the stroke is in principle unlimited and where position is maintained at power shut down. The latter is one of the major advantages of a piezo motor compared to an electromagnetic motor. Maintaining position at standstill without power consumption does not generate any heat, and hence no additional position corrections are needed.

Bender

A well-known option for increasing the stroke is the bending mode. Two separate piezo elements are bonded, in some cases with an inactive middle plate. The bending is caused by a difference in shrinkage of the two piezo elements in the length direction due to a difference in the piezo actuation; see Figure 5.

For a multi-layer bender the active layers are split in a lower and upper section leading to the same bending option at again lower voltages. The strokes are at millimeter level and forces are around 1 N (i.e. stiffness at $1 \cdot 10^3$ N/m).

Multi-layer ring bender

As indicated in Figure 6, there is a large shift in stiffness from a piezo actuator to a piezo bender. To overcome this shift Noliac A/S developed the ring bender. The advantages of the ring bender are its low height in combination with its relative high stroke maintaining a high blocking force. Figure 7 shows a ring bender and how it works, which resembles a cupped spring washer. The stroke ranges from 20 to 200 µm at a force of around 50 N, leading to a stiffness in the range of $1 \cdot 10^6$ N/m.

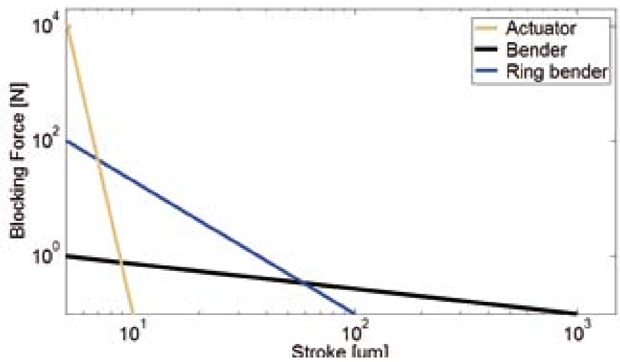

Figure 6. Comparison of blocking force vs stroke for piezo actuator, bender and ring bender.

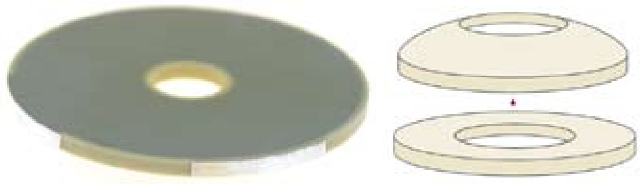

Figure 7. A ring bender and its principle of operation.

Cantilever multiplication

When placing a piezo stack in a cantilever hinge structure, the multiplication factor to increase the stroke can be chosen as needed. The multiplication factors in general range from 5 to 15. When combined with a piezo stack of 50 mm and thus 70 µm of stroke, this leads to strokes up to 1000 µm. The down side is the quadratic drop of the stiffness by a factor of 25 to 225. Figure 8 shows a solution designed and manufactured in cooperation with Brom Mechatronica using a Noliac multi-layer piezo stack.
The hinge structures are often chosen for high accuracy, absence of backlash and ease of drive.

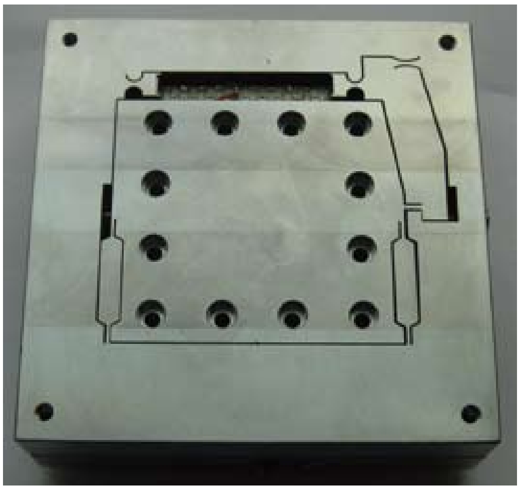

Stroke = 50-250 µm; C = ~ $5 \cdot 10^6$ N/m; F_{res} = ~ 1 kHz;
UHV compatible

Figure 8. A piezo stack in a cantilever hinge structure.

Piezo motor

Piezo motors can be diverse in shape and motion pattern. There are stepping solutions like the inch worm or the linear piezo motor by Philips. Similar solutions use a bending mode, a shear mode or saw tooth based on friction to make steps. All these versions have their own specific pros and cons, but non have reached high-volume quantities and/or can be easily designed into motion systems.

In other piezo motor solutions a tip, prestressed to a moving body, describes an ellipse at piezo resonance. The tip as such pushes the moving body in either direction, similar to Fred Flintstone driving his car by his feet. A subsequent option is to fix a piezo element to a body with tip, to bring the body in resonance and to find the optimum position for the tip. The ultrasonic motor by Nanomotion will be discussed to describe the way of working in more detail.

Nanomotion ultrasonic motor

Since the 90's Nanomotion designs and manufactures piezo motors which have proven their quality over many years of service in stringent environments. The simultaneous excitation of the longitudinal extension mode and the transverse bending mode creates a small elliptical movement of the ceramic edge, achieving the dual mode standing wave as shown in Figure 9. The principle is shown in Figure 10.
By coupling the ceramic edge to a precision stage, a resultant driving force is exerted on the stage under the spring prestress, causing stage movement. The excitation frequencies are much higher than the mechanical resonance of the stage allowing continuous smooth motion.

F = 4 N; C = $1 \cdot 10^6$ N/m; V_{min} = 1 µm/sec; V_{max} = 250 mm/sec

Figure 9. A Nanomotion ultrasonic motor exhibiting a dual mode standing wave.

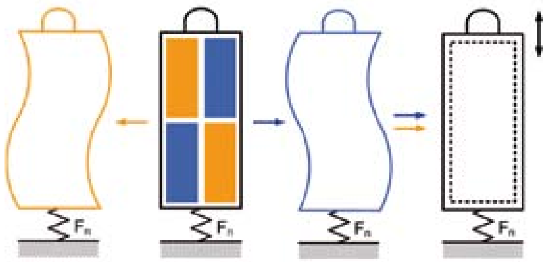

Figure 10. Principle of the dual mode standing wave.

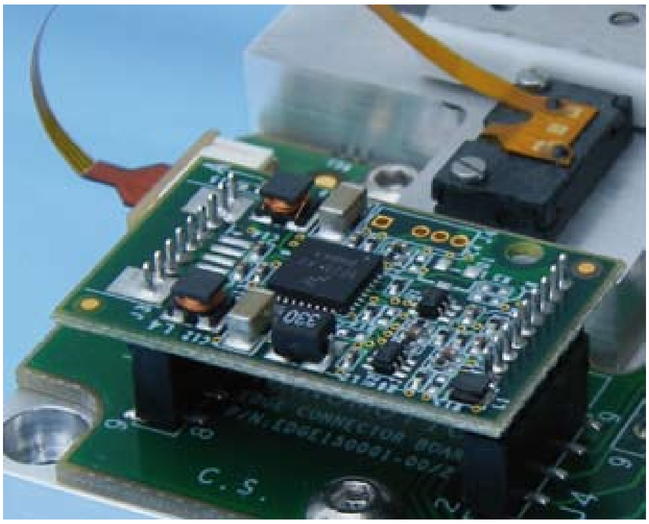

F = 0.3 N; C = 0.07·10⁶ N/m; V_{max} = 120 mm/sec; m = 0.55 gram

Figure 11. Edge motor (the black box with flex) with ASIC driver.

The size of the ellipse is determined by the height of the AC V_{pp} signal. Changing the V_{pp} level the speed can range from 1 µm/sec to 250 mm/sec. The force delivered by one Nanomotion standard HR element is 4 N. Standard motors have 1, 2, 4 or 8 elements, giving up to 32 N of force. Smaller and low-voltage versions are available. The so-called Edge motor has a size of 3.15x7.60x13.45 mm^3 and a driving force of 0.3 N at maximum driving voltages of 12 V_{rms}. Figure 11 shows the Edge motor with ASIC driver.

Three functions in one motor element

Three key characteristic functions have been incorporated in the design; see Figure 12. First, as already mentioned, the piezo element is pushed onto the stage and as such behaves like a break when power is cut off. Thus no power consumption and no heat generation. Secondly, driving the piezo at various AC V_{pp} levels the velocity can be controlled. With the wide dynamic range and velocities down to 1 µm/sec, submicron positioning is easily reached.

At standstill, the piezo can be used as a normal piezo actuator. This third key characteristic gives a stroke of +/- 0.3 µm. Although the stiffness of the HR element is limited to $1 \cdot 10^6$ N/m, the latter characteristic can be used for vibration damping. For example in diagnosis, a sample can be brought in position at a speed of 200 mm/s and submicron accuracy. In position, environmental vibrations are cancelled to allow precise diagnosis.

High-precision motion profile

To examine the limits of the Nanomotion piezo motor technology, HEINMADE built a stage with a stroke of 50 mm using the HR motors. The stage is equipped with an optical position encoder with a resolution of 5 nm. The

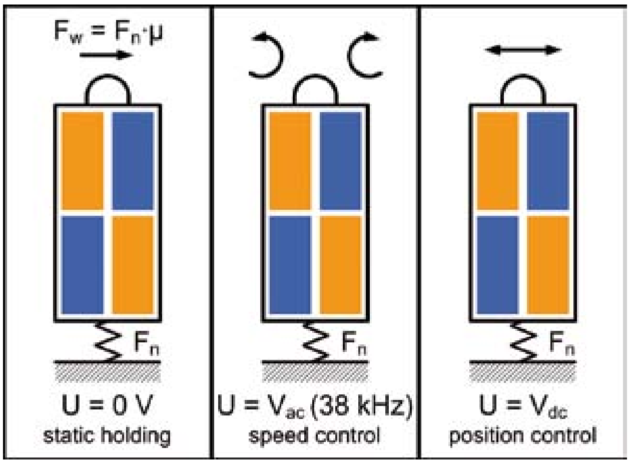

Figure 12. Three functions incorporated in one piezo motor element.

stage has a stiffness of $2 \cdot 10^7$ N/m. Figure 13 shows position profile steps of 200 nm made in both directions. Closed-loop operation is done using Nanomotion's Flex DC controller.
The position error while maintaining position is less than 2 increments, i.e. less than 10 nm. The position error peaks at acceleration and deceleration, to a maximum of 50 nm.

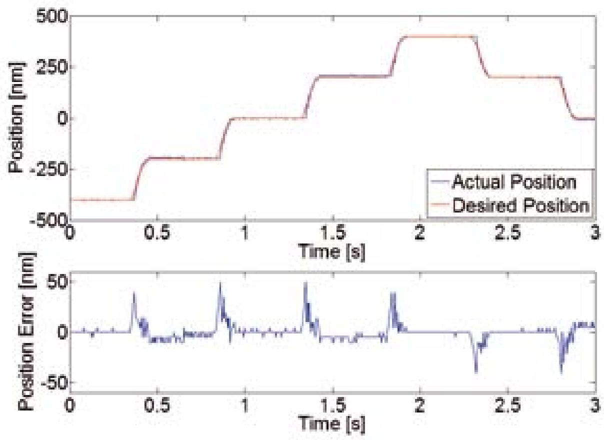

Figure 13. Position profile steps of 200 nm by a stage using Nanomotion piezo motor technology.

High-dynamic excitation

An interesting field of application for piezo is high-dynamic excitation. One example is diesel fuel injection where injection times of less than 50 µsec are required. This makes up to six injections per cylinder cycle possible, improving both the burning process (reduction of NO_x) and the performance. Further it shows that piezo meets 'under the hood' requirements: elevated temperature (> 100 °C), high accelerations (> 10.000 m/sec²) and long lifetime (> $1 \cdot 10^9$ cycles).

From top to bottom:
- Stiff frame
- Hinge to compensate for tolerances and prestress of sample
- Sample position
- Hinge structure for alignment of forces
- High-dynamic piezo actuator
- Force sensor
- Stiff frame

Figure 14. Test set-up for impact testing of structural components.

For impact testing of stiff structural components HEINMADE used these high-dynamic capabilities of piezo. Figure 14 shows the test set-up designed in collaboration with Brom Mechatronica. In this configuration forces up to 10 kN and impact durations of less than 0.1 msec are feasible. The excitation itself is in most cases limited by the electronic driver. For testing a Piezomechanik high-power amplifier was used.

Sensors for active damping

Thus far, applications of piezo in the actuation mode have been discussed. In many applications, however, the piezo is used as a sensor to detect change of forces. As mentioned above, with a change of force an electrical field is generated. The electrical signal can simply be used for on/off switching (touch panels) or power harvesting. The sensor signal itself, however, contains a lot more information, which can be used to quantify the force and frequency used in all kinds of applications.

For making small structures feasible, machines have to hold position accurately. With proper isolation of the floor, vibrations down to 1 μm are under control. To reach and maintain nanometer accuracy, piezo components are used to actively damp submicron vibrations. For this application, the submicron vibrations are sensed by the piezo sensor and the collocated piezo actuator makes the opposite

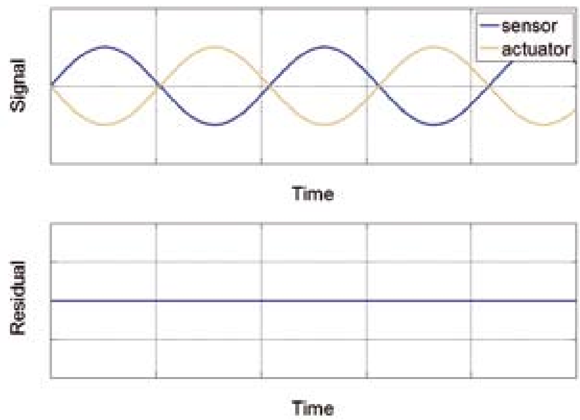

Figure 15. Active damping of (submicron) vibrations by piezo components.

movement as illustrated in Figure 15, thus damping the vibrations to subnanometer level.

In theory this seems a simple procedure, in practice several problems need to be overcome. This would cover another full article.

Summary

The above examples demonstrate the possibilities and advantages of piezo technology in precision engineering, which may be summarized as follows:
- Non-magnetic compatible
- Direct drive
- Small and powerfull
- Fast responses
- No power consumption at standstill
- Cryogenic temperatures
- Ultra-high precision
- Ultra-high vacuum compatible
- Accelerations up to 10.000 g
- Active damping
- Energy harvesting
- Ultrasonic applications
- Multi-axis stages

Authors' note

Hein Schellens is founder and owner of HEINMADE. Maikel Heeren works with High Tech Partners, a cooperation of self-employed, experienced high-tech people.

Information

www.heinmade.com

From high-tech

All MEPP (All Mechatronical Engineering Projects & Prototyping) in Eindhoven is a start-up (of November 2007) with a long history in precision engineering. When the established system supplier KMWE Precision Systems & Precision Components, also in Eindhoven, started focusing more and more on series production rather than on special engineering projects, five of its experienced engineers decided to start their own enterprise. All MEPP is an independent engineering agency that designs and constructs high-tech equipment, special machines and tooling according to the client's specifications. Now, eighteen months later, the track record is already impressive.

Of course the Eindhoven region, heart of the Dutch high-tech manufacturing industry, is a main target for All MEPP, but the engineering agency is expanding its activities throughout the Netherlands and has started exploring the Belgian and German market. All MEPP decided to stay away from the highly volatile semicon market, and to focus on stable (medical) and promising growth (solar and wind energy) markets. In the meantime, it has taken a more general approach to the machine construction market. In the automotive industry, for example, opportunities for product innovation and process automation have been identified. According to All MEPP, the key issue in automotive mechatronics is to establish progress in car systems, such as the drive train, motor management and environment control.

Engineering

All MEPP offers engineering services, from concept design to testing of first products. Its competences include mechanical and electrical engineering, software, value engineering, prototyping, assembly, feasibility analysis and project management. A fine example of value engineering (cost reduction) by All MEPP concerns FEI's tabletop electron microscope Phenom. At the moment, All MEPP employs fourteen people, and the ambition is to grow to a staff of 25. In the early days, engineers were posted at customers, but last year the company's philosophy was changed, and now all engineers but one work in-house on challenging projects.

Handling

Customers are high-tech companies in various markets, and projects thus far include the redesign of the control system of a diamond processing machine, a robot handler including fracture inspection for solar cells, a bending tool sensor, a transport case for silicon wafers, and the engineering and commissioning of a laser welding production line. A common denominator in several projects is handling (accurate transportation and positioning) in processes, both in air and in vacuum, concerning (fragile) objects such as chips, solar cells, DVDs, LED displays and liquid samples. Following work on the automation of solar

handling to pneumatic precision

cell handling, a system for measuring wafer thickness was developed; see the box.

An example of All MEPP engineering: handling system for solar cells.

High-tech and low-cost

Another example is the design of a standard, low-cost XYZ system, with a measuring range of up to 1,200 mm in all three dimensions. The system can achieve high-speed movements with high accuracy. The unique design feature of this system is the placement of the motors on the base frame, hereby strongly reducing the mass of the system. The project illustrates one of All MEPP's characteristics, the combination of high-tech and low-cost in engineering.

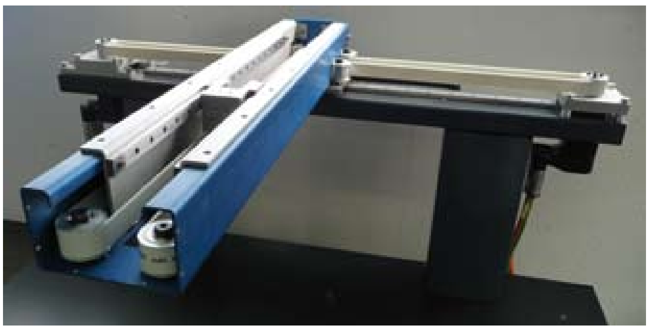

All MEPP's design of a low-cost XYZ system features a measuring range of up to 1,200 mm in all three dimensions.

Pneumatic metrology

In the course of a project on handling fragile solar cell wafers, the need for contactless measurement of their thickness came up. An accuracy of 5 μm was requested. All MEPP elaborated a pneumatic metrology that under laboratory conditions has achieved an accuracy of 0.1 μm.

Nozzles connected to air tubes are placed above and below the wafer, allowing at both sides for a small gap between nozzle and wafer surface. This gap represents a pneumatic impedance to an air flow escaping through the nozzle. At the nozzle, the air flow (laminar within the tube) will become turbulent, which makes the impedance quadratically dependent on the flow. As the pneumatic impedance also depends on the gap size, this allows – after calibration – for determination of gap size. To that end, a control loop is implemented that keeps the flow constant, hence 'measures' a variation in impedance that reflects the variation in gap size. These variations in gap size, when combining the signals from above and below the wafer, offer a measure of thickness (variations).

This principle of measurement may find other applications, for example in checking the print quality of printing machines.

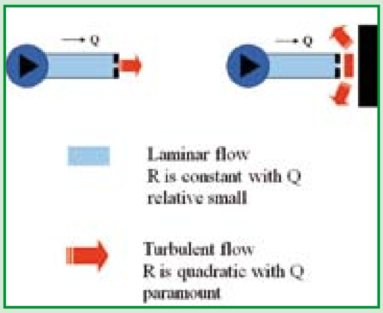

The underlying physics of All MEPP's pneumatic metrology.

Set-up for thickness measurement using the pneumatic metrology.

Information

www.allmepp.nl

Advanced improves

A multi-disciplinary team of Philips Applied Technologies has developed technology with which medical devices can be remotely controlled while actually feeling the force that is applied on the human body by the device. With this technology the team built an ultrasound scanner allowing the medic to scan in a position that is not causing strains, being able to operate another device as well and without running the risk to be exposed to radiation such as X-ray. The so-called Tele-Operated Ultrasound Probe (TOUP) is now being tested at a hospital in London and first users' reactions are very encouraging.

• *Peter Frissen, Dennis Bos, Kees-Jan Zandsteeg and Kawal Rhode* •

Minimally invasive interventions such as cardiac procedures are typically executed using X-ray imaging for feedback. In many cases, the surgeons would like to use ultrasound as well since it provides additional diagnostic feedback and is also safe for the patient and the surgeon. Some doctors hope that ultrasound could completely replace X-ray in certain procedures in the future.

The use of ultrasound however requires an additional person (termed sonographer or echoscopist) to be present near the X-ray beam. This skilled worker needs to manually manipulate the ultrasound probe during the interventional procedures, which can be time consuming. This adds costs and additional ergonomic and safety issues to the situation. Many sonographers report strain problems in neck, arms and shoulders as a consequence of their daily working routines already. The Tele-Operated Ultrasound Probe system as described in this article provides a solution that enables the use of ultrasound imaging during interventional procedures and that at the same time may be used to improve the ergonomic aspects of the diagnostic routine of sonographers; see Figure 1.

Figure 1. Manual (left) and remote control (right) of an ultrasound probe.

hospital ergonomics

The remote ultrasound probe allows sonographers to manipulate an ultrasound probe from a location some distance from a patient in an upright position, not causing strains. Philips Applied Technologies has leveraged its unique knowledge of haptic feedback and servomechanics to accurately reproduce dynamic forces between the probe and the patient's body in the system's control joystick. This enables the sonographer to feel and manipulates the tissue of the patient very naturally, allowing him to optimize image quality. At the same time, the natural feeling is used to maintain a safe operation. Next to that, the sonographer is out of reach of X-ray beams. Philips Applied Technologies has developed a first sample for clinical studies.

Haptic tele-operation

Tele-operation is defined as the indirect manipulation of an object by a human using two manipulators connected to each other via a controller. A tele-operation system contains in general five parts. In the general nomenclature, the user of the system is the 'Operator'. The operator gives force or position commands to the leading device, the 'Master'. The master is virtually connected via the 'Controller' to the 'Slave' device. The slave interacts with the 'Environment'. A general haptic tele-operation network is shown in Figure 2.

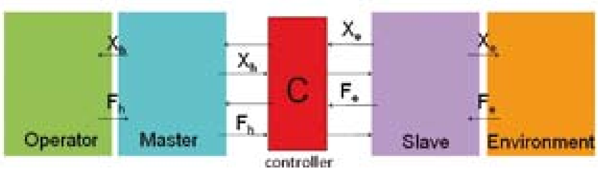

Figure 2. Structure of haptic control.

The interaction between the various elements of the systems will be described shortly. The sonographer operates the system via the haptic master. The actual position of the master in five degrees of freedom (DOFs) is sent to the slave as a setpoint. The slave follows the setpoint while interaction forces with the environment of the three translational degrees are fed back via the master to the operator. In this way, it is possible to locate e.g. ribs of a patient, as illustrated in Figure 3. Forces related to the rotations are very small. Consequently haptic torque feedback is not necessary in this TOUP application.

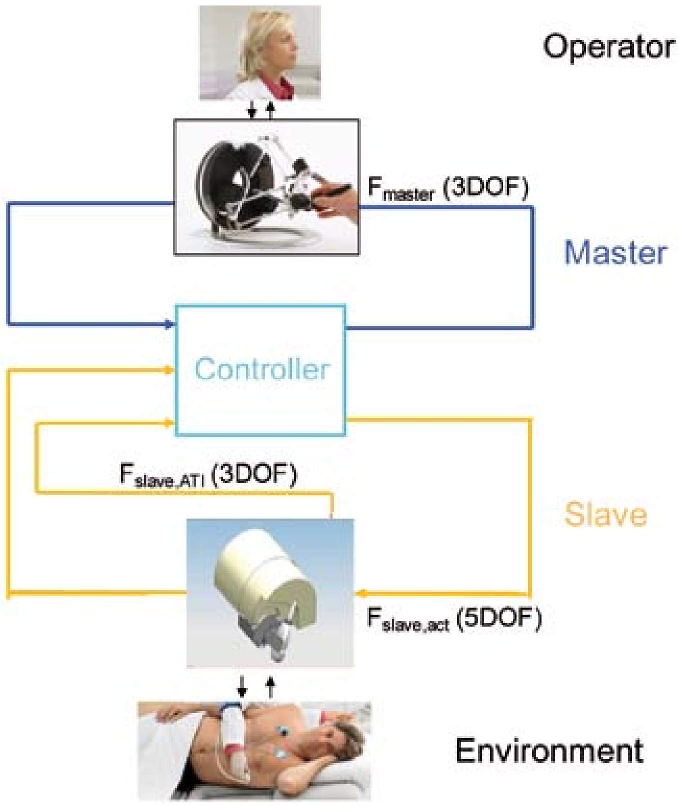

Figure 3. The TOUP system.

Figure 4 shows the master and slave robots of the TOUP system. The master is the Force Dimension Omega.6 and is commercially available. It has six DOFs, three translations and three rotations. The translations are created via the so-called delta structure, with a closed kinematic structure. The delta structure contains three arms which are identical. All arms share the same base and end-plate and consist of a link with a parallellogram. Each arm has internally seven joints. The rotations are mounted on the delta platform with

a rather flexible construction having an eigenfrequency of 20 Hz. Only the translations are actuated.
The slave robot is a proprietary designed and built manipulator optimized for clinical use and safety. It has five DOFs, all of which are actuated and sensed. This slave robot is based on serial kinematics.

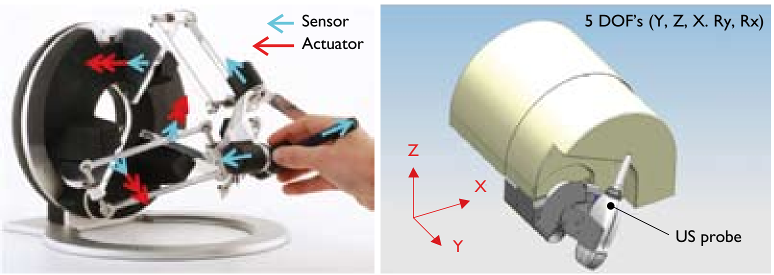

Master robot: Force Dimensions Omega.6

Slave robot: Homemade manipulator

Figure 4. Master and slave.

Controller design

A challenging aspect of the overall system design is the controller. Its design is done by modeling the physics of the system and comparing different controller structures and their effect on the performance. Driven by the different types of tissue encounter in humans, e.g. muscle, fat and bones, the tissue characteristics are taken into account. First, the theory of the haptic feedback system is explained. As illustrated in Figure 3, four systems interact with each other. The master has direct interaction with the human operator and the slave has direct interaction with the environment (see Figure 2). Four channels with information communicate via a controller to the other half of the system. Namely, the force applied by the operator, the position of the operator, the force applied at the environment, and the position of the environment.

The most common notation for the analysis of haptic tele-operation systems is the hybrid parameter matrix. This matrix describes both the position on the environmental side and the force at the operator side as a function of the force (F) and position (X) of the environment and operator, respectively:

$$\begin{bmatrix} F_h(s) \\ -X_e(s) \end{bmatrix} = \begin{bmatrix} h_{11}(s) & h_{12}(s) \\ h_{21}(s) & h_{22}(s) \end{bmatrix} \begin{bmatrix} X_h(s) \\ F_e(s) \end{bmatrix}$$

The above notation is the so-called two-port notation. Each of the parameters in the matrix can be interpreted physically. The first term h_{11} is the impedance of the system in free movement. Term h_{21} represents the position tracking in free motion, term h_{12} the force tracking in contact and h_{22} the contact admittance. The parameters can be visualized as indicated in Figure 5.

$h_{11}(s) = F_h/X_h$, felt impedance in free motion:

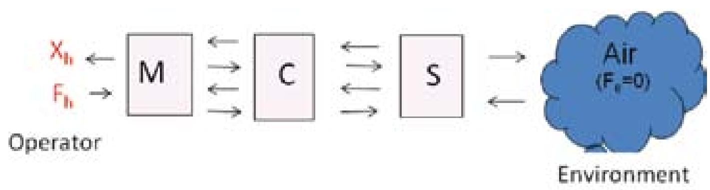

$h_{12}(s) = F_e/F_h$, force tracking with fixed master:

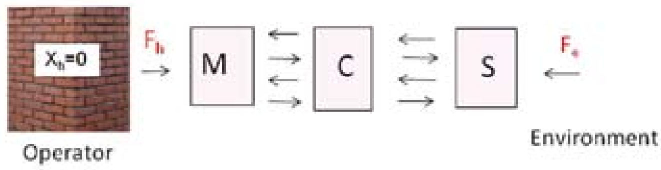

$h_{21}(s) = X_e/X_h$, position tracking in free motion:

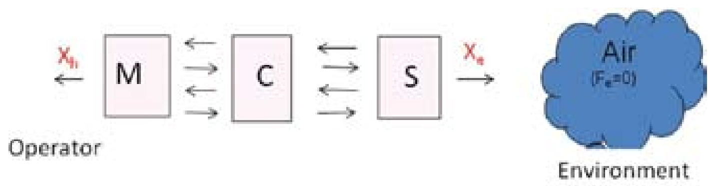

$h_{22}(s) = X_e/F_e$, output admittance at slave with fixed master:

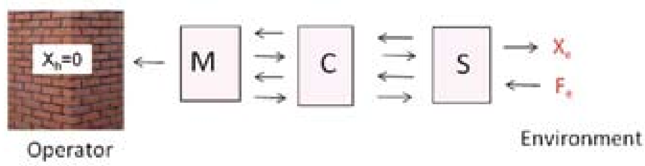

Figure 5. Explanation of the four elements of the hybrid matrix.

Transparency is defined as the ratio of impedances felt by the operator and the environment. The impedance felt by the operator is defined as:

$$Z_{to} = \frac{F_h}{X_h} = \frac{h_{11} + (h_{11}h_{22} - h_{12}h_{21})Z_e}{1 + h_{22}\,Z_e}$$

In case of ideal transparency, the ratio between the impedance felt by the operator and the environment is given by:

$$H_{ideal}(s) = \begin{bmatrix} 0 & 1 \\ -1 & 0 \end{bmatrix}$$

In the ideal case, this matrix must be valid for all frequencies. Notice that in the ideal case $Z_{to} = Z_e$. For the TOUP, the so-called kinesthetic sensing is applicable. Kinesthetic sensing goes up to 10 Hz and is mainly used to discriminate shape, size and mechanical properties (of e.g. ribs and tissues).

Experimental results

As mentioned earlier, the performance of the designed haptic tele-operation controller is investigated both by modeling and simulations as well as by means of measurements. The transparency is determined for three different environments, ribcage, muscles and fat. Figure 6 shows the results in z-direction for the slave. It can be seen that the highest bandwidth is achieved for the stiffest environment. The error in transparency for softer environments, muscle and fat, is caused by the inertia of the haptic tele-operation system components. The average bandwidth is about 3 Hz. This is sufficient for the first TOUP clinical tests. Notice also the good correspondence between model and measurement.

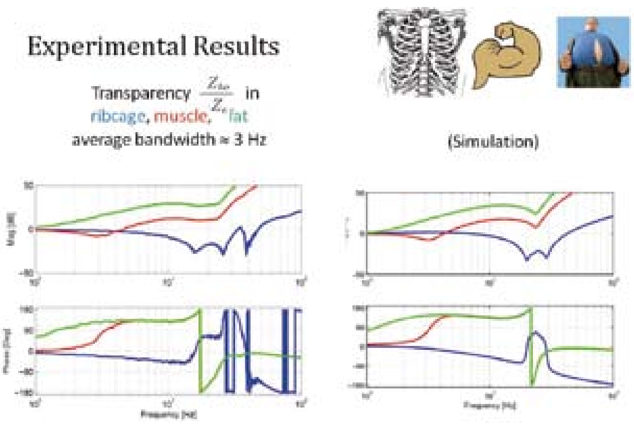

Figure 6. Transparancy of the haptic tele-operation system in Z-direction for ribcage (blue), muscle (red) and fat (green).

Beside transparency, also stability robustness for all frequencies and environments is important. A lot of successful investigation has been done to improve the control design by implementing other control architectures, e.g. by compensating the master and slave dynamics.
A reproducibility for displacement and rotations of 0.1 mm, respectively 1 mrad at the tip of the ultrasound probe is obtained.

Clinical studies

The practical implications of the TOUP system are evaluated during a clinical study; see Figure 7. A patient undergoes a pacing study prior to pacemaker implantation for heart failure; see Figure 8. This study aims to find the best lead position on the hart tissue using ultrasound imaging. More specifically, simultaneously to the TOUP, data is collected of the position of the pacing leads using sequential X-ray images, the intra-cardiac electrical measurements and the left ventricular pressure. The collected data from X-ray and ultrasound are fused. This 'data fusion' provides very rich data to evaluate the outcome of the pacing modes.
An unexpected advantage of the TOUP system is discovered: the position of the ultrasound probe in 3D space is normally gained by an external optical tracking system. This position is required for adequate image fusion. However, the TOUP system knows the position of the probe since it is directly related to the positions of the robot's internal degrees of freedom. This information is tracked during the procedures and used in the data fusion process.

Figure 7: Clinical case of the hybrid system ultrasound (TOUP) and X-ray.

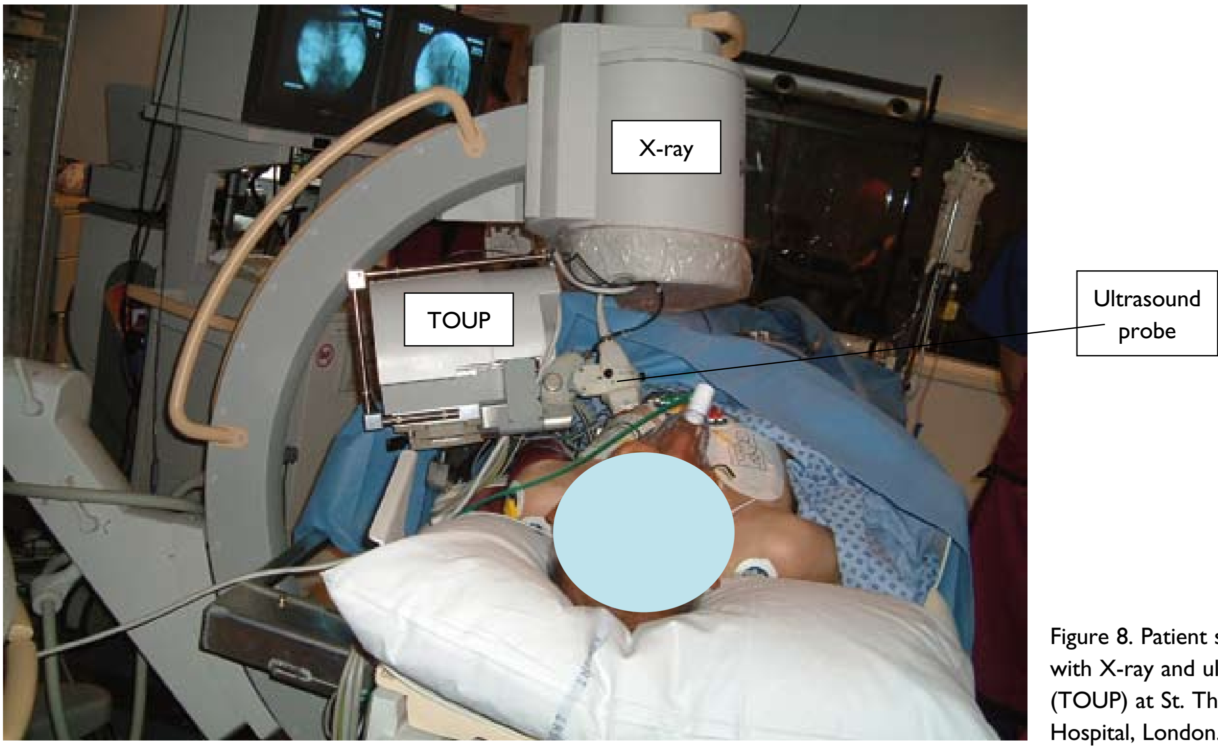

Figure 8. Patient study with X-ray and ultrasound (TOUP) at St. Thomas' Hospital, London.

As an example of the data registration, a part of the left ventricle (blue object) and electrical measurement catheter (pink object) is segmented and overlaid onto one of the 2D X-ray images; see Figure 9. By a visual inspection, the registration is well within the clinical accuracy requirement of 5 mm for these types of procedure.

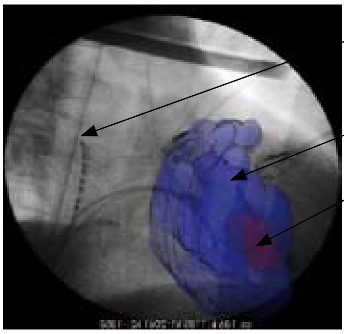

Figure 9. Data fusion of X-ray and ultrasound.

Conclusion

A challenging aspect of the overall system design is the controller. Its design results in a successful performance with measurements executed on different tissues. Ultrasound is a completely safe and well-established imaging modality that provides high quality heart images. There is much recent interest in exploring the use of ultrasound for guiding cardiac catherisation procedures. By developing the TOUP, an elegant solution is made available for the safe and robust use of ultrasound within the catheter laboratory. Recently, the research team at King's College London and St. Thomas' hospital explored the use of the TOUP during several different types of catherisation procedures. Furthermore, the ultrasound probe can be manipulated precisely in a comfortable position, which leads to considerable reduction of physical stress for medics.

Acknowledgment

The project is executed by Philips Applied Technologies in cooperation with:

- Eindhoven University of Technology, Faculty of Mechanical Engineering, Department of Dynamics and Control Technology (Eindhoven, the Netherlands);
- King's College London, Department of Clinical Science and Imaging (London, UK);
- Philips Healthcare (Best, the Netherlands).

Authors' note

Drs. Peter Frissen is senior project leader working in the department of Mechatronics at Philips Applied Technologies located at the High Tech Campus in Eindhoven. Ir. Dennis Bos is senior system architect and works at the same department. Ir. Kees-Jan Zandsteeg works at Eindhoven University of Technology. Dr. Kawal Rhode, Ph.D., is lecturer at Image Processing of the Clinical Science Imaging department of Kings's College London and St. Thomas' Hospital.

Information

www.apptech.philips.com/techtubes
p.c.m.frissen@philips.com

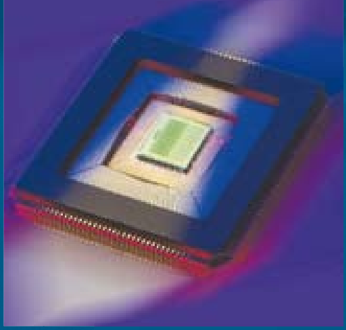

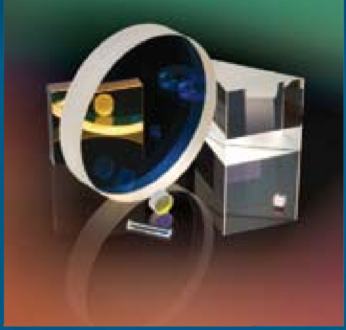

Elastic elements generating a

In mechatronic machines with a high positioning accuracy (i.e. submicron positioning), it is often necessary to have a stiff connection between the machine components. It can be deduced from the mechatronic model of a machine of this type that a certain connection between components has to be stiff (but not necessarily strong). A defined pretension force between the components is needed to optimise connections for (contact) stiffness. The design principle of a harmonica bush offers an elegant solution.

• Paul Brom •

It is not always possible to realise a connection by simply bolting one component to another. Optical components, for example, can be fragile or susceptible to induced (elastic or even plastic) deformations. These unwanted deformations are typically the result of the moments and forces that are generated when fixing the bolts using tools such as wrenches or screwdrivers. The mounting torque that is needed to generate the pretension force has to be eliminated from the design. This can be done by using an extra element between the bolt head and the component that will generate the pretension force without using torque. By using elastic elements, the pretension force can be generated and applied to the components in a controllable and defined fashion.

Harmonica bush

A good alternative for an elastic element would be a stack of disc springs. Disc springs are cheap and compact but have the disadvantage that the force level depends on tolerances of the discs in the stack and is hence less controllable. In one particular case, the requirement for a controllable pretension was included in the design at a later stage, which meant that there was only a limited volume left in which to create a solution. There is a good example of an elastic element that is used for generating pretension force, namely a harmonica bush ([1], page 130); see Figure 1. This principle was used in the design. Graphs from [1] can be used to determine the optimal dimensions of a harmonica bush; see Figure 2.

Definitions

I = moment of inertia [m^4]
I_p = polar moment of inertia [m^4]
C_z = axial stiffness [N/m]
M_w = torsion moment [Nm]
M_b = bending moment [Nm]
E = modulus of elasticity [N/m^2] (Young's Modulus)
G = shear modulus [N/m^2]
F = force [N]
r = radius [m]

for pretension force

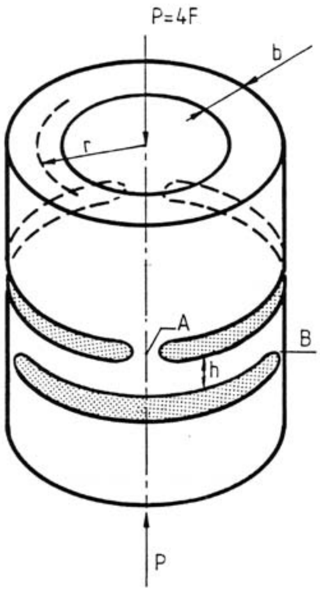

Figure 1. The harmonica bush design principle [1].

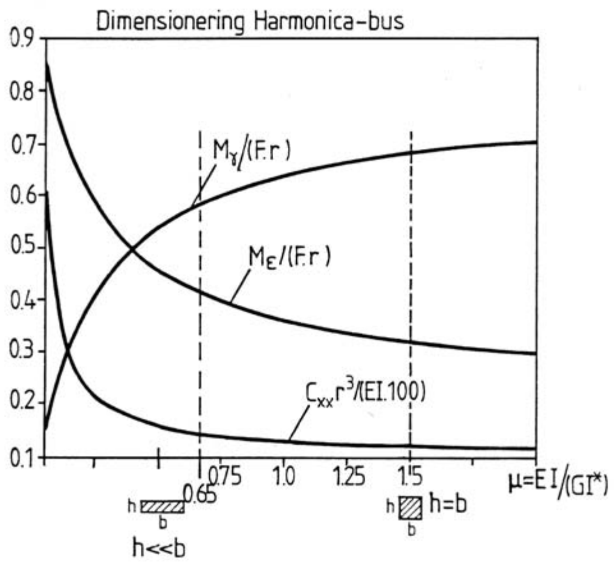

Figure 2. Dimensioning graphs for a harmonica bush, [1].

Formulas

It proved impractical to check these graphs for every iteration in the parameter set (height, width, radius, number of windings). The exact formulas for these graphs were not available, so approximations were generated for use in optimizing the design. By using fit-software on data points taken from the graphs, it was possible to convert the graphs into formulas.

The graph depicting the axial stiffness C_z is of shape:

$y_{'}^2 = a + (b/\sqrt{x_{'}})$;
with a = 0.0032976225 and b = 0.013599364.

Also valid is: $y_{'} = (C_z * r^3)/(E*I*100)$; $x_{'} = (E * I)/(G * I_p)$.

Using these formulas, an expression for C_z can be found and pasted in a spreadsheet.

The graph depicting the bending moment M_b is of shape:

$y_{''} = c + d * e^x + f/x_{''}$;
with c = 0.66689208; d = 0.0099309907 and
f = 0.078606373.

Also valid is: $y_{''} = M_b /(F* r)$; $x_{''} = (E * I)/(G * I_p)$

Thus an expression for M_b can be found.

The graph depicting the torsion moment M_w is of shape:

$y_{'''} = g + j *(\ln x_{'''})^2 + k * \ln x_{'''}$;
with g = 0.3512396; j = 0.027846045 and k = 0.11052021.

Also valid is: $y_{'''} = M_w /(F* r))$; $x_{'''} = (E * I)/(G * I_p)$

Using these formulas, the expression for M_w can be found.

Each of the four elastic elements of one winding is actually a curved leafspring.
The I (bending) and the I_p (torsion) of a leafspring can be determined using Roark's Formulas for Stress & Strain ([2], Table 10.7, page 401).

If *w is* width and *h* is height of the leafspring and also $w = 2*m$ and $h = 2*n$ are calculated, then the expressions for I and I_p are:

$$I = 1/12 * (w * h^3);$$

$$I_p = (m*n^3) * (16/3 - 3{,}36 * \frac{n}{m} * (1 - \frac{n^4}{12 * m^4})).$$

Using these formulas, expressions for I and I_p can be found and pasted in the spreadsheet.

Pretension

The pretension level of the completely squeezed bush can be calculated. The dimensions of the slots in the harmonica bush are such that if the bush is squeezed completely, the desired pretension level is reached. The accuracy of the slots (made by wire eroding) is a direct measure for the accuracy of the pretension level. The maximum stress in the bush can be calculated using the bending and torsion moments. Next, all the parameters and formulas were pasted in a spreadsheet. Using the spreadsheet makes it possible to rapidly iterate the design of the harmonica bush to an optimum for the given volume and requirements. The design was verified with finite-element analysis (FEA) at a later stage. (Note: the iterating process for achieving the optimum design with the spreadsheet is quicker than with FEA).

Final design

A final design is shown in Figure 3. As an added feature, there are four holes that are partially threaded at the bottom. Using four small screws, the harmonica bush can be squeezed and locked prior to mounting in the machine; see Figure 4. When mounting the bush in the machine, the central bolt must be mounted hand tight (low distortion) on the counterpart and the bush. Then the four small screws are loosened and the pretension that was locked in the bush is subsequently transferred to the counterparts. It is possible that loosening the four small screws can also introduce unwanted moments and forces into the construction. But these will be much smaller as the central bolt will only be stretched in a defined manner. Even these final small disturbances can be removed if an anti-torque leafspring is used underneath the four screws.

Author's note

Paul Brom is a mechanical designer.

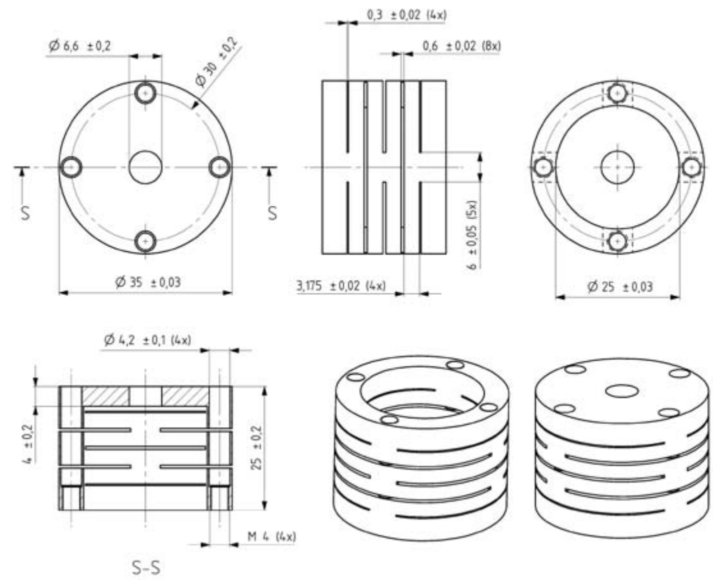

Figure 3. A final design of the harmonica bush.

Figure 4. The harmonica bush, on the right in its 'locked state' with the four screws that are used for controlling the pretension.

References

[1] Koster, M.P., Constructieprincipes (Mechanical Design Principles, in Dutch), third edition, Twente University Press, 2000.

[2] Young, W.C., Budynas, R.G., Roark's Formulas for Stress & Strain, seventh edition, McGraw-Hill, 2002.

Special times demand a special(ist) approach

The current economic downturn affects the majority of high-tech companies, but it does have at least one advantage. It offers companies the opportunity to self-evaluate and ask themselves what markets they serve, who their competitors are, how they can stand out and prepare for the future and for the economic upturn.

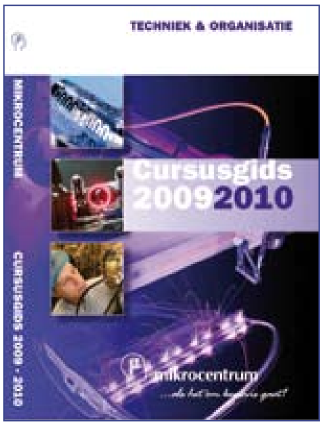

The Mikrocentrum 2009 course guide.

Mikrocentrum can be of help (see also the box), offering some 200 courses on technological and organisational improvement, provided by a team of specialists. The new course guide gives a complete overview. Now is the time to invest in employees' knowledge development, Mikrocentrum says.
If financial means are lacking, Mikrocentrum can help find practical funding solutions.

Phone 0031 40 - 296 99 33 or email opleidingen@mikrocentrum.nl for more information.

Mikrocentrum

Eindhoven-based Mikrocentrum is an independent competence centre with a history of over 40 years in supporting companies and institutes. The main objectives are to improve know-how and stimulate intercompany networking and co-operation. Mikrocentrum's network extends into government and government-related organisations, as well as into scientific and educational institutes, and its High Tech Platform comprises nearly 500 high-tech industrial companies.

Each year, over 20,000 people participate in events organised by Mikrocentrum, which include 30 to 40 special interest sessions on topics ranging from technology, product development and manufacturing to quality and management. Mikrocentrum also offers a comprehensive array of short, concise practical courses and workshops in technology and management at all educational levels, with an approach ranging from the hands-on technical to the academic. Mikrocentrum also organises a dozen trade fairs a year in fields such as precision technology, vision and robotics, and health and technology.

www.mikrocentrum.nl

Precision Fair 2009

The *Precisiebeurs* (Precision Fair) has grown to become the most important precision technology event in the Netherlands and has gained an international reputation. The objectives of the Precision Fair include creating an awareness of the available knowledge and expertise, facilitating knowledge exchange, matching supply and demand and promoting and improving co-operation and networking within the European region around Eindhoven, aimed at new product and market development.

At the two-day fair, over 200 exhibitors will be presenting their precision solutions, which range from micro to nano. General overviews of the field of precision technology and specific cases will be given during the lecture programme. In the Technology Hotspot, universities and knowledge institutes will display their expertise and research projects.

The 9th edition of the Precision Fair is to be held on 2 and 3 December 2009 at the NH Conference Centre Koningshof in Veldhoven (near Eindhoven), the Netherlands. About 3,000 visitors are expected.

seminar@mikrocentrum.nl www.precisiebeurs.nl

Environment, power and size

On 8 April 2009, the FHI trade association for industrial electronics, in collaboration with the Dutch Technology Foundation STW, organized Sense of Contact 11. The goal was to show the potential of sensors to solve current issues and challenges. This eleventh edition of the sensor technology workshop, in Zeist in the centre of the Netherlands, focussed on three issues: environment, power and size. Dutch universities, institutes and industry presented their recent sensor (and actuator) research and development results pertaining to these three challenges.

• *Joris Gonggrijp and Hans van Eerden* •

As an 'appetizer', Frank Linde of Nikhef (the Dutch National Institute for Subatomic Physics) gave a presentation on the world's largest 'scientific istrument' equipped with giant sensors, the Large Hadron Collider at CERN (Geneva). Later this year, experiments will start to register head-on collisions of protons with energies up to 7,000,000,000,000 eV. At these unprecedented energies physicists hope to observe new phenomena, like: the Higgs particle (assumed to be responsible for the concept of mass in our universe); supersymmetric particles (the lightest of which could explain the nature of dark matter in our universe); and mini black holes (pointing at the existence of extra spatial dimensions in our universe). Any of these will revolutionize our view of the world we live in.

Micro

The rest of the day was filled with parallell sesions, and closed in a plenary session by Han Gardeniers from the University of Twente, on microfluidic sensors. State-of-the-art microfluidic technology allows precise handling of nanolitre to microlitre fluid volumes, in microsystems with integrated sensing elements. This enables in-situ studies of biological and chemical processes with minimal sample consumption and high spatial resolution. The presentation demonstrated the need for microsensors, and thus underlined size as an issue in sensor technology.

One of LHC's 'sensors', the giant CMS detector. (Photo: CERN)

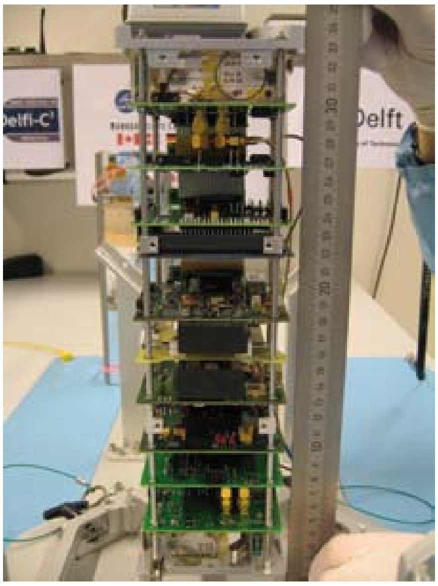

The interior of the Delfi C³ satellite, which was launched last year in India.

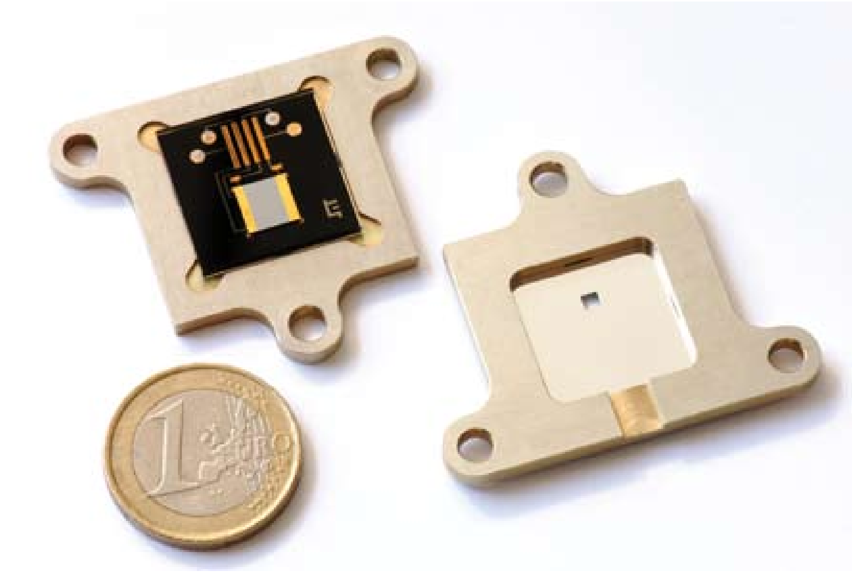

Both sides of a sun sensor designed by TNO Science & Industry. (Photo: TNO/Fred Kamphues)

Related contributions came from University of Twente spin-offs Micronit and Kryoz Technologies, on microreactors used in research and industrial production, and micro cryogenic cooling systems, respectively.

Space

Sensor size is also an issue in space, where the mass (and therefore the size) of the payload of satellites and spacecrafts has to be reduced as much as possible, to minimize energy/fuel consumption and extend operational lifetime. Chris Verhoeven from Delft University of Technology presented the case of so-called CubeSats, of which the recently launched Delfi-C³ satellite is a good example. This 2.2 kg CubeSat, constructed by Delft students and staff, carries a payload including thin-film solar cells (Dutch Space) and an autonomous wireless sun sensor (TNO). According to Verhoeven, CubeSats may be the heralds of a new way of space mission design. Exploiting modern microelectronics and microsystems, colonies of small spacecraft seem to become a challenging but feasible option.

Environment

More extensively, sun sensors were discussed by Johan Leijtens of TNO Science and Industry, focussing on their design and qualification for space travel. Here, the environment (during the launch and in space) is a prime design determinant. In reducing the sensor size, power supply, data handling, manufacturability and integrated packaging have to be considered. Sun sensors may find various applications in space (satellite altitude control, solar power generation) as well as down on earth, for example in domotics (home automation) and airconditioning control in cars.

Sensor networks may be used, for example, to monitor the environment, to gain insight in complex phenomena such as global warming. Environment-related sensor applications are also found in (sustainable) energy. The Dutch energy research institute ECN, for example, conducts sensor research for fuell cell technology and smart gas meters.

Power

Another current issue in sensor technology is power. Energy harvesting is an option for powering autonomous (wireless) sensor systems that can serve many domains for an ambient intelligent future (e.g. body area networks for medical applications, 'smart buildings', automotive, predictive maintenance). True autonomy can only be achieved using energy harvesting, i.e. taking up (e.g. photovoltaic, vibration, thermal or radio-frequency) energy from the environment. Ruud Vullers of the Eindhoven-based Holst Centre discussed principles of energy harvesting, recent results and challenges, and gave an outlook. Micromachining, he concluded, will be the key to mass application of energy harvesters.

Authors' note

Joris Gonggrijp is former director of LiS (Leiden instrument makers School) and former DSPE board member. Hans van Eerden is editor of Mikroniek.

Information

www.fhi.nl/senseofcontact

Balancing low mass

To increase the accuracy as well the production speed of industrial machines, dynamic balance is becoming a key issue. Instead of applying complicated control strategies to reduce machine vibrations, and damping systems to suppress vibrations, in dynamic balancing the mechanism parts are considered and designed such that the machine does not vibrate at all. Surprisingly however, dynamic balancing techniques are not yet widely applied. This is probably due to the lack of knowledge of dynamic balancing and the fact that in general relatively a lot of mass and inertia is added to obtain a dynamically balanced mechanism. This study focuses on the reduction of the additional mass and the additional inertia with dynamic balancing. For that purpose common balancing principles are analyzed and compared, guidelines for low mass and low inertia dynamic balancing are formulated, and new balanced mechanisms that have a low mass and low inertia are synthesized.

• *Volkert van der Wijk* •

Due to motion of mechanism parts, reaction forces (shaking forces) and reaction moments (shaking moments) are exerted to the base of a mechanism (i.e. machine, robot). This is a major source of vibrations, inducing noise, wear and fatigue problems, and discomfort. Common solutions to reduce the influence of vibrations on the performance of the mechanism are the application of damping and including waiting times in the motion cycle to wait until vibrations have died out. With dynamic balancing however, the mechanism is designed such that all vibrations are eliminated. As a result, balanced mechanisms can have both shorter cycle times and higher accuracy.

Generally, a mechanism is (shaking) force-balanced if the linear momentum of all the mechanism parts is constant and a mechanism is (shaking) moment-balanced if the angular momentum of all mechanism parts is constant. A constant linear momentum implies that the center-of-mass (COM) of a mechanism must be stationary or move with constant velocity. A drawback of dynamic balancing is that (counter-)mass and (counter-)inertia needs to be added, which can lead to a higher power consumption.

Balancing principles

In literature, three generally applicable dynamic balancing principles can be found [1]. In Figures 1-3 these balancing principles are shown as being applied to balance a link. The link is modeled as a lumped mass m with inertia I at a distance l from the center of rotation. Figure 1 shows the balancing principle with Separate Counter-Rotations (SCRs). For the force balance, a countermass (CM) m^* is added to the link such that the COM of the link is at pivot

and low inertia addition

O. For the moment balance of the (force-balanced) link a separate counter-rotating element is mounted somewhere at the base and connected to the link with a pair of gears.

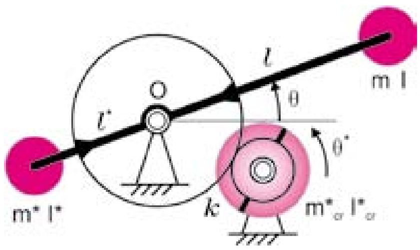

Figure 1. Balancing principle with a Separate Counter-Rotation (SCR).

The inertia of the CM, however, can also be used for balancing the moment of the force-balanced link, omitting the addition of a SCR. This solution of using Counter-Rotary Counter-Masses (CRCMs) is shown in Figure 2. To have the CRCM rotate in opposite direction of the link, a pair of gears can be used and can be applied in three different ways. In Figure 2a a chain (or belt) is used with one gear (or pulley) being mounted to the CRCM and another being mounted to the base, coinciding with the pivot. In Figure 2b an additional external gear is used and Figure 2c shows a solution with internal gears.

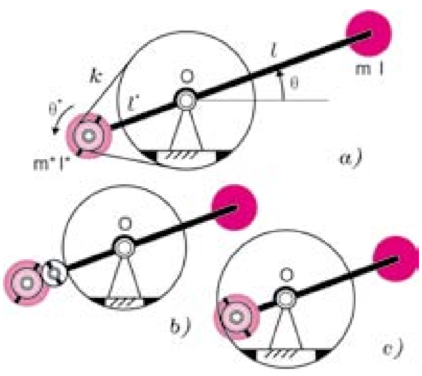

Figure 2. Balancing principle with a Counter-Rotary Counter-Mass (CRCM) configuration with: (a) gears and chain, (b) external gear, (c) internal gear.

A third way to achieve dynamic balance is by applying axial and mirror duplicates of the initial mechanism that move synchronically, as shown in Figure 3. Because a mirror duplicate mechanism produces equal but opposite reaction forces and moments, the horizontal mirror duplicate balances the horizontal force and the moment of the link, and vertical mirror duplicates are used to balance the vertical force.

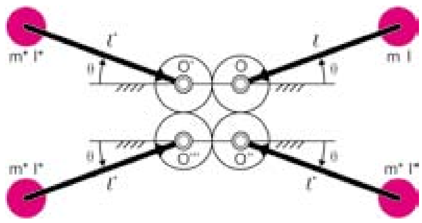

Figure 3. Balancing principle with axial mirror duplicates of the initial mechanism (DM).

Analysis and comparison

Two comparative studies of the balancing principles were done and both showed that using CRCMs instead of SCRs, is favorable for low mass and low inertia [1] [2]. One study compared the balancing principles applied to a rotatable link, which are the configurations in Figures 1-3. The second study compared the balancing principles applied to a double pendulum (or dyad).
The double pendulum is found suitable for a fair comparison, representing a large category of mechanisms. This is because many mechanisms can be synthesized from double pendulums, the balancing performance of an open-loop mechanism does not change by constraining its motion to obtain a closed-loop mechanism (i.e. the mechanism is balanced for any motion), and in practice mechanisms are balanced link by link. A rotatable link is most suitable for the detailed study of the balancing parameters.

The relation between the reduced inertia of the rotatable link (the inertia that an actuator feels when driving the mechanism) and the total mass for each principle are obtained theoretically and illustrated by a numerical example in Figure 4. All masses were modeled as discs with thickness 0.01 m made of steel (ρ = 7800 kgm^{-3}) and the parameter values were chosen as m = 0.3 kg, l = 0.25 m, and I = 184 kgmm^2. The curve for the CRCM principle remains below the curves of the SCR principle. However, the DM principle, which has a single value, is even lower. This implies that improving on the DM principle result is not easy to achieve.
Another interesting observation is the necessary trade-off between the addition of mass and the addition of inertia. Clearly it is not possible to balance a link by having both a low mass and a low inertia. The results of the comparative study with the balancing principles applied to a double pendulum are similar.

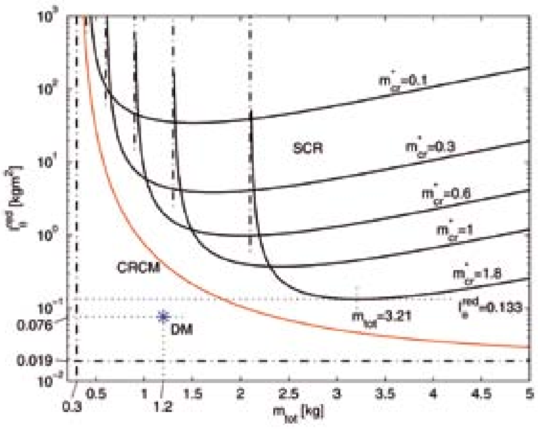

Figure 4. Comparison of balancing principles; relation between inertia and total mass.

Synthesis

A double pendulum is a useful ‘building element’ in the synthesis of a wide variety of mechanisms. Equivalently, a dynamically balanced double pendulum is a useful ‘building element’ in the synthesis of dynamically balanced mechanisms. In fact, combining independently balanced mechanisms results in mechanisms that are also balanced. There are various ways to balance a double pendulum, for instance by applying the DM principle for the lowest mass and lowest inertia addition. However the balanced mechanism then becomes rather large and complex. The DM principle is advantageous if in practice four of the same mechanisms are needed and they can be placed such that they balance each other.

Figure 5 shows a double pendulum that is balanced with two CRCMs and is characterized by having a low inertia, since the transmission of gears is designed such that the rotation of I^*_2 is not influenced by link 1 [3]. Figure 6 shows how a double pendulum can be fully dynamically balanced with a single CRCM, of which the counter-

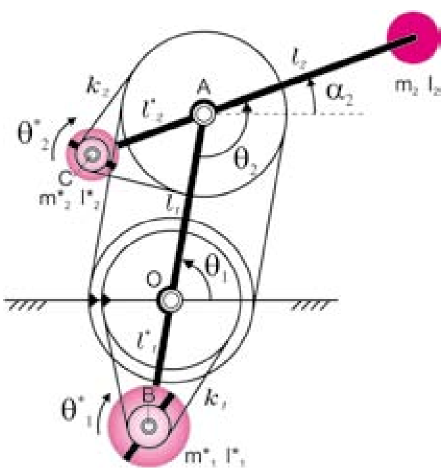

Figure 5. CRCM-balanced double pendulum with low inertia.

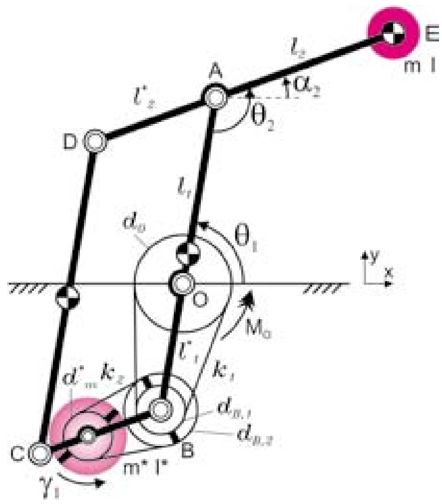

Figure 6. Actively CRCM-balanced double pendulum with a single CRCM for complete dynamic balance.

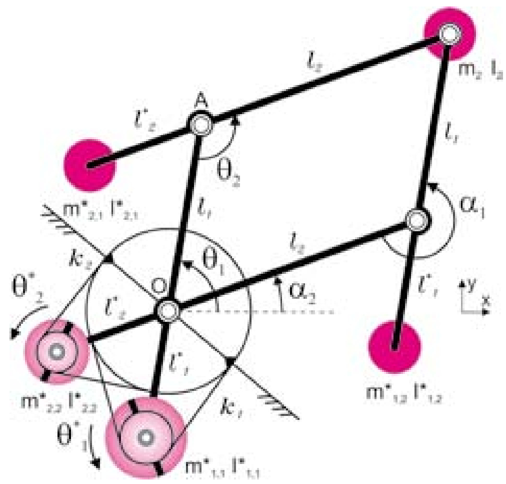

Figure 7. 2RRR five-bar mechanism balanced with two CMs and two CRCMs [6].

rotation is actively controlled with an additional actuator at the base [5]. In this case, fixed gears cannot be used, since the inertia tensor of the mechanism about the base pivot is not constant for any motion.

By combining two CRCM-balanced double pendulums, the balanced 2RRR five-bar mechanism of Figure 7 is obtained. $m^*_{1,2}$ and $m^*_{2,1}$ could be CRCMs (as in Figure 5), but if the links are such that the mechanism is a parallelogram (parallel links have equal angular velocity), these can be fixed CMs and only two CRCMs are needed for the moment balance of the complete mechanism.

In Figure 8, a balanced crank-slider mechanism is shown, which was derived from Figure 7 by guiding the endpoint along a line and changing the dimensions of one side. Because of the parallelogram, one of the CMs can be taken

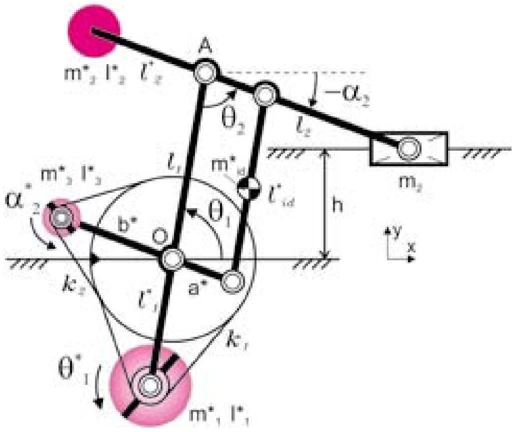

Figure 8. CRCM-balanced crank-slider mechanism deduced from Figure 7.

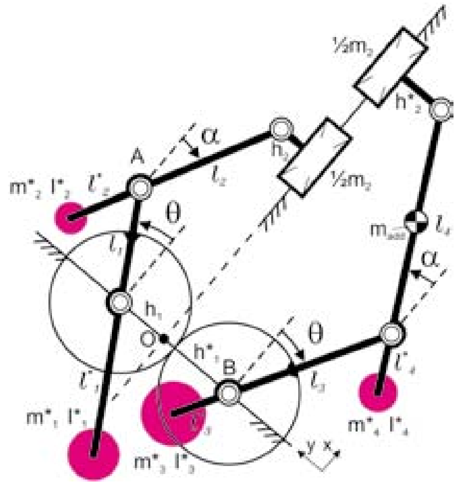

Figure 10. Balanced crank-slider by specifically designed counter-mechanism.

out (this can also be done in Figure 7). By using CRCM-balanced (single and) double pendulums, an unlimited number of multi-DOF, planar and spatial balanced mechanisms can be created. Just start puzzling!

Innovative solutions

For crank-slider mechanisms it is often difficult to attach gears and other elements to the coupler link (link 2), for instance if the mechanism is large or if additional elements interfere with the workspace. Figure 9 shows a crank-slider mechanism that is dynamically balanced with a CM on the coupler and a single CRCM at the crank. This CRCM balances the moment of both crank and coupler. This is achieved by a specific transmission, mounted on a third link (link 3) which runs parallel with the coupler. In fact this transmission is a mechanic ‘summator’, adding the angular velocities of both links and changing its sign to have a counter-rotation. The advantage is that this balancing system can be scaled to a small size and is situated away from the workspace.

The DM principle showed to be advantageous for low mass and low inertia. This is mainly because links are used for balancing the moment. These counter-rotating links have a

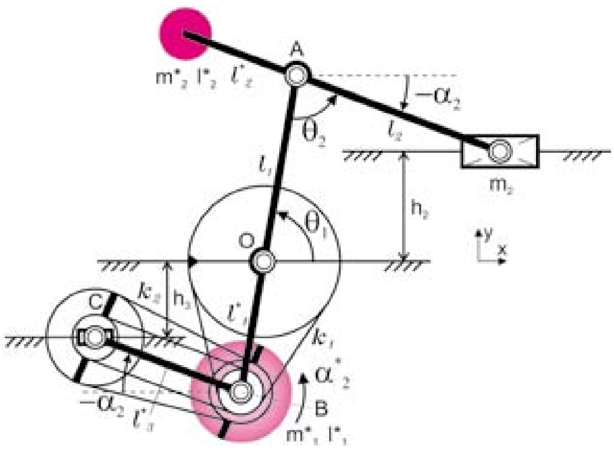

Figure 9. Balanced crank-slider mechanism with balancing elements away from the workspace.

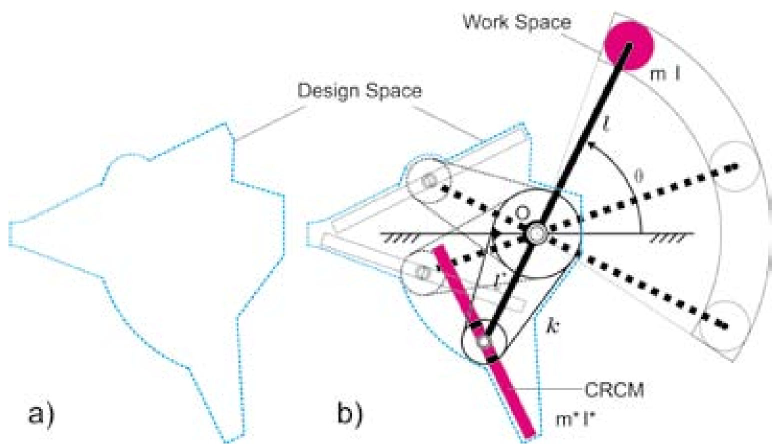

Figure 11. Counter-rotating links for balancing within a small space.

relatively low mass and high inertia, by which the (counter) rotational velocities are low and therefore the reduced inertia of the mechanism is low as well. Instead of adding three mirror duplicates, Figure 10 shows how a specifically designed counter-mechanism can be used for balancing. A crank-slider mechanism (l_1-l_2) is balanced with a counter-mechanism (l_3-l_4) which is also a crank-slider. Both mechanisms are force-balanced individually and move synchronically and opposite of each other by gears. The moment balance is obtained if the inertia of link 2 and 4 are equal and the inertia of link 1 and 3 are equal.

Design space

For the designer it is always challenging to design all machine parts within a small area, and it even becomes more challenging when also the balancing parts have to be included. Counter-rotating links that do not have full revolutions appear to be advantageous for balancing within a small space. As an example, the configuration of Figure 2a, but with the CRCM designed as a link and driven with a transmission ratio of -1, is shown in Figure 11. In this way the counter-rotating link can move in between the other machine parts.

Guidelines

From this study, general guidelines for low mass and low inertia dynamic balancing have been obtained [4]. The use of CRCMs is advantageous especially if the CRCM is designed with low mass and high inertia (e.g. as a link). For a low mass addition, counter-masses have to be placed far from the center of rotation, while for a low inertia addition they have to be placed close to the center of rotation. For low inertia addition, counter rotations should be rotating slowly, which is also achieved by balancing with duplicate mechanisms and counter-mechanisms. For a low mass, it should be omitted to balance CMs with other CMs.

Acknowledgements

The author thanks Prof. Just Herder, Delft University of Technology, Department of Interactive Mechanisms Research, and Bram Demeulenaere, PhD, K.U.Leuven, research group of Prof. J. de Schutter, (currently working at Atlas Copco Airpower, Antwerp) for their advice and supervision of this study.
Recent work includes the development of an actively dynamically balanced xy-robot (in cooperation with Stamhuis Lineairtechniek, Ternet, and Control Techniques) and a dynamically balanced Delta Robot (in cooperation with Blueprint Automation).

Author's note

Volkert van der Wijk is a PhD student in the Department of Biomechanical Engineering of Delft University of Technology. He is the recipient of the Wim van der Hoek Award 2008.

References

[1] Van der Wijk, V., Herder, J.L., Demeulenaere, B., 2009. "Comparison of various dynamic balancing principles regarding additional mass and additional inertia". *Journal of Mechanisms and Robotics (in print)*.

[2] Van der Wijk, V., Herder, J.L., Demeulenaere, B., Gosselin, C.M., 2009. "Comparative analysis and optimization for low-mass and low-inertia dynamic balancing of a rotatable link balanced by a counter-rotary counter-mass". *Journal of Mechanisms and Robotics (accepted)*.

[3] Van der Wijk, V., and Herder, J.L., 2009. "Synthesis of dynamically balanced mechanisms by using counter-rotary counter-mass balanced double pendula". *Journal of Mechanical Design (in print)*.

[4] Van der Wijk, V., Herder, J.L., 2009. "Guidelines for low mass and low inertia dynamic balancing of mechanisms and robotics". *German Workshop on Robotics, Braunschweig*.

[5] Van der Wijk, V., Herder, J.L., 2008. "Dynamic balancing of mechanisms by using an actively driven counter-rotary counter-mass for low mass and low inertia". *Proceedings of the Second International Workshop on Fundamental Issues and Future Research Directions for Parallel Mechanisms and Manipulators, Montpellier*, pp. 241-251.

[6] Menschaar, H.F., Ariens, A.B., Herder, J.L., Bakker, B.M., 2006. "Five-bar mechanism with dynamic balancing means and method for dynamically balancing a five-bar mechanism", *Patent number WO 2006/080846*.

Information

www.imr.bmeche.tudelft.nl

'Mechatronics moves you!'

On 16 April, Mechatronics Valley Twente Foundation (MVT) held its sixth TValley conference. The well-attended event comprising a conference and exhibition on innovation and business for the high-tech manufacturing industry had the theme 'Mechatronics moves you!' The conference was held on the campus of the University of Twente and particularly focused on robotics and mechatronics as an attractive choice for study and work. TValley 2009 also marked the start of the Robotics Centre Twente.

• *Hans van Eerden* •

Motion – highly accurate and/or superfast – forms the heart of high-tech machine and equipment manufacturing in the Netherlands. Despite the current recession, the development of high-tech motion solutions is continuing unabated behind the scenes, for which the growth of young talent is indispensable. Now that technical study programmes are no longer the most popular, it is important to highlight that mechatronics is an attractive choice for both study and work. And the subject of robotics can help. After all, robots appeal to many peoples' imagination and are often examples of 'high-tech motion' – industrial robots as well as new generation robots for medical, household or other 'social' applications. All these perspectives were covered during TValley 2009.

Social themes

The conference was opened by the vice-chancellor of the University of Twente, which has become something of a tradition in recent years. Prof. Ed Brinksma, who took office at the beginning of this year, outlined a future for mechatronics and robotics as technologies in search of broader social themes. According to the vice-chancellor, the University of Twente has the disciplines to undertake this search. Technical medicine, for example, is a relatively new discipline in the up-and-coming field of medical robotics and the social scientists in Twente can provide input in answering social-ethical questions regarding the use of robots in our society.

Robotics from the perspective of space

Chairman for the day, Herman Soemers, who works for Philips Applied Technologies and is professor at the University of Twente holding the MVT-financed chair in Mechatronic Design, then introduced keynote speaker Prof. Gerd Hirzinger. Hirzinger is director of the DLR Institute of Robotics and Mechatronics, which is one of the world's largest and most renowned institutes in this field, and part of DLR, the Deutsches Zentrum für Luft- und Raumfahrt (German Aerospace Centre). In the 1990s, Hirzinger was a driving force behind the first experiments in remote-controlled robots for the Space Shuttle and the ISS. This experience of space has been translated by Hirzinger's institute into diverse robot applications here on earth, which he discussed under the title "Robotics and

Ed Brinksma, the vice-chancellor of the University of Twente opens TValley 2009. (Photo: University of Twente)

Mechatronics – From Space to Surgery and the Virtual World”.

However, there are still significant challenges in the field of robotics in space in 2009. Hirzinger outlined the problem of space debris that is growing as a result of collisions between satellites, for instance. High-tech robot arms should be used to repair satellites that have become non-operational and to pluck those posing a risk of collision out of space. Hirzinger said that there would be an important (political) conference dedicated to this issue in Berlin in mid-May.

He went on to speak about the great success of the DLR MiroSurge, a robot for endoscopic surgery. Medical applications for robotics have long been overlooked by the medical community, but have recently been on the up and up. Hirzinger saw a key role cut out for mechatronics here as well as in artificial organs and prostheses. Finally, he showed impressive 3D images of cathedrals and other cultural heritage made with high-tech cameras, developed by his institute and suspended from robot helicopters that can record from every angle.

ProBot

Bart Deen from MVT member IMS, which specialises in the construction of assembly lines for microsystems, spoke about the development and application of ProBot. This new module for IMS’ existing generic assembly system is

The DLR MiroSurge surgical robot. (Illustration: DLR)

intended for the flexible supply, orientation, assembly and testing of small and medium-sized products. The products are localised and controlled using camera (vision) technology, picked up by free programmable units (e.g. robots with special grippers) and placed (or directly assembled). In comparison with other modules, the ProBot supply systems are less product-specific, so that changes can be made to the products to be handled more easier and quickly.

The new, flexible assembly platform of IMS, ProBot.

New lithography

Rather than robotics, Guido de Boer from Mapper Lithography offered high-tech mechatronics instead. The 2001 spin-off from TU Delft is developing a maskless lithography machine for semiconductor production; see the article in this issue. Mapper’s breakthrough technology, based on more than ten thousand electron beams that are controlled by microstructures through ultrafast optical data transport, promises reductions in production costs. As a result, the machines are significantly cheaper and have a much smaller footprint than ‘conventional’ lithography machines, as well as eradicating the need for expensive masks. However, it should be noted that the productivity of the Mapper systems is significantly lower; the next generation must be ten times more productive than is currently achievable, De Boer said. The first machines will be delivered to customers in August and Mapper hopes to increase staffing levels this year to more than 200.

De Boer went into the system design of the Mapper machine and mentioned the input of Twente-based companies (MVT members) in the design and production of components such as the wafer stage, their primary task being to make stages (relatively) cheap and reliable. The biggest challenge facing the Mapper concept was mainly in the metrology.

Compact Coriolis flow meter

Marcel Katenberg from Bronkhorst Cori-Tech, a sister company of MVT member and developer and manufacturer of mass flow meters, Bronkhorst High-Tech, discussed the compact Coriolis flow meter. The meter was developed in collaboration with the University of Twente, TNO and MVT member and mechatronic design company DEMCON. Using the well-known Coriolis measuring principle, a mass flow is measured without being influenced by other properties of the medium. A curved thin tube is excited into rotational vibration. The liquid or gaseous medium flowing through the tube generates Coriolis forces, which influence the vibrational motion. Measuring this immediately allows a determination of the mass flow. Katenberg discussed several innovations in the design, including the tube’s suspension, excitation of the vibrations, measurement and signal processing.

Solar

A promising growth market for the Dutch high-tech machine manufacturing industry is solar energy. A significant player in this market, Eindhoven-based OTB Solar, designs, manufactures and sells production equipment and complete production lines for solar cell manufacturing. Marcel Grooten outlined the development and technological complexity of a production line with the relevant processes. He also mentioned the crucial input of Twente-based companies such as MVT members Tecnotion (linear motors) and Bronkhorst High-Tech, and machine manufacturer Masévon Technology.

Bronkhorst’s compact Coriolis mass flow meter/ controller, the mini CORI-FLOW.

A unique application of solar cells was highlighted in the presentation by Anne Leenstra of the Solar Team Twente, which will take part for the third time in the World Solar Challenge, a bi-annual solar car race through Australia. Leenstra spoke about the innovations in solar cars in Twente such as the tilt wing and an optical system, both used to maximise the absorption of light. Based on this, he went into various aspects of the energy management for a solar car, such as the efficiency of the solar cells and other (electrical and mechanical) components, the aerodynamics and the rolling resistance of the wheels. The Solar Team Twente, which comprises students from the University of Twente and the Saxion University of Professional Education, is sponsored and given technical support by countless institutions and companies, including several MVT members. In October, the team will once again await their baptism of fire in Australia, this time with a new car design.

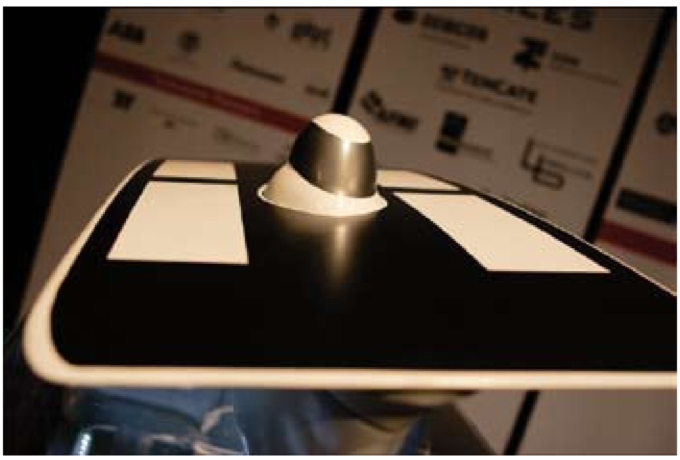

The new design for a Twente solar car. (Illustration: Solar Team Twente)

Presentation of the MVT Mechatronics Award, with left to right jury chairman Herman Soemers and prize winners Jan Bennik, Bob Reilink and Ludo Visser. (Photo: University of Twente)

Twente Humanoid

Yet more edifying work by (former) students of the University of Twente was presented by Jan Bennik, Rob Reilink and Ludo Visser. They displayed their design for a head and neck for the Twente Humanoid robot, which was mentioned by UT vice-chancellor Brinksma in his opening as a motivator for the younger generation. The trio's mechatronic tour de force was rewarded with the MVT Mechatronics Award, which was presented for the third time by a jury lead by Herman Soemers.

The Twente Humanoid is intended as a platform for research into human-robot interaction. The design for the head assumes seven degrees of freedom, which enables the head to not only follow humans and objects, but also to show expression. To increase the 'human character' further, the head had to be able to move with a speed comparable to that of a human. Crucial aspects of the design were the vision-based image processing for determining a target to be followed and the control for the degrees of freedom.

The Twente Humanoid is intended as a platform for research into human-robot interaction.

Robotics Centre Twente

The Twente Humanoid formed a perfect prelude to the opening of the Robotics Centre Twente. Stefano Stramigioli, professor of Advanced Robotics at the UT, held a dazzling presentation, which mixed impressions of the Twente exploratory Humanoids & Home Robotics mission to Japan with images of Twente-based projects in the field of non-industrial robotics. The mission took place late last year under the auspices of the Romech Foundation (Advanced Robotics & Mechatronics), established by the University of Twente and MVT companies.

Stramigioli outlined the future for the robotics outside the industry – in the health care sector, public space and the household – and the potential in that field in Twente: the knowledge, the existing research collaborations between different disciplines and the ambition to develop the new, as yet virtual Robotics Centre Twente, into a world player. The centre is to design 'personal assistive, intelligent service and medical robots' and develop socially useful applications for them.

By way of an official opening, Stramigioli presented the first copy of 'The Future of Robotics' to Prof. Hirzinger. This report describes the developments in the field of robotics – from car manufacture to society – and the plans in Twente, and contains an extensive account of the

Prof. Gerd Hirzinger (left) accepts the first copy of 'The Future of Robotics' from Prof. Stefano Stramigioli. (Photo: University of Twente)

mission to Japan. This marked the end of a successful TValley 2009.

Author's note

Hans van Eerden is a freelance text writer in Winterswijk, the Netherlands, and editor of Mikroniek.

Information

www.tvalley.nl
www.romech.nl

Co-Nanomet (Co-ordination in Nanometrology)

The European Society for Precision Engineering and Nanotechnology (euspen) and partners are currently leading a two-year European 7th Framework Programme funded project in the field of nanometrology. Co-Nanomet (Co-ordination in Nanometrology), which started in January 2009, is addressing the need within Europe to develop the required measurement frame to successfully support the development and economic exploitation of nanotechnology.

Nanotechnology offers a huge potential of applications and economic benefits, which may contribute to the European economy. A worldwide race for progress in this field is underway, driving out enormous technological advances and Europe currently holds a promising position in the field. Scientifically and economically, nanometrology is an indispensable part for nanotechnology, and must develop hand in hand with nanoscience and -technology.

Suitable measurement framework

A range of activities have been and are taking place across Europe to define the potential industrial development of nanotechnology from which associated nanometrology needs may be derived. These include national foresight studies for nanotechnology, European Commission Reviews as well as roadmapping activities for nanometrology such as that undertaken in the European Nanostrand project. A pan-European coordinated response to these defined needs is required from the National Metrology Institutes to provide a suitable measurement framework for the effective commercial development of nanotechnology. To address this requirement a European Strategy for Nanometrology will be delivered in consultation with key stakeholders.

Action groups

Five European Action Groups in Nanometrology are being implemented addressing the following fields: Engineered Nanoparticles; Nanobiotechnology; Thin Films and Structured Surfaces; Critical Dimension and Scanning Probe Techniques, and Modeling and Simulation. These groups address the need to put in place a process chain for the dissemination of metrology techniques as well as traceability to national standards and internationally harmonised standard methods specific to the particular nanotechnology area addressed.

Training needs

To bring nanotechnology through to successful business, calls for access to not only the relevant metrology tools but also suitably skilled human resources able to implement such tools at the appropriate level. Educational programmes addressing nanometrology across Europe are being reviewed, a future training needs analysis completed and recommendations for training curricula made. Training will be provided in basic nano metrology concepts as well as standardisation.

Capabilities review

Future nanometrology capacity development in Europe must build out from a clear and common understanding of current capabilities and competence as well as emerging future needs. To address this, a European capabilities review is underway. Exisiting and future requirements for large infrastructures as well as capability gaps are being assessed. Traceability and metrology in industry will also be addressed.

Partners

Co-Nanomet will take input from a range of stakeholders including industry, research institutes, National Metrology Institutes, regulatory and standards bodies as well as the EC. The project is being delivered by a consortium representing a unique body of leading experts in the fields of nanometrology, nanotechnology, technology transfer and specialised training.

Co-Nanomet is funded under the European 7[th] Framework Programme.

Further information

Dr Theresa Burke
Tel +44 (0)1234 754064
theresa-burke@euspen.eu
www.euspen.eu
www.co-nanomet.eu

European Nanometrology Workshop 2009

From 8-9 September 2009 a workshop will be held to review and discuss European strengths and future needs in the field of nanometrology. The venue will be the Federal Institute for Materials Research and Testing, Berlin. Users and developers of nanometrology services from industry and research will come together with National Metrology Institutes as well as relevant standards and regulatory bodies. Focussed discussion groups will be held for the Action Groups detailed above.

www.co-nanomet.eu/europeanworkshop09

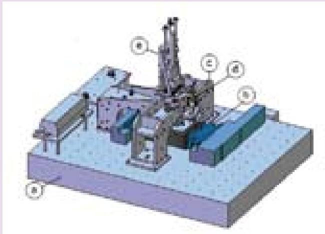

NPL Areal Instrument – enabling traceable three-dimensional measurements of surface texture at nm level. (Image courtesy of Prof. Richard Leach, NPL, UK)

Henny Spaan appointed president of euspen

At the eu**spen** 9th International Conference & 11th Annual General Meeting, 2-5 June 2009 in San Sebastian (Spain), Henny Spaan, founder and director of IBS Precision Engineering in Eindhoven, the Netherlands, was appointed president of eu**spen**. Spaan succeeded Hendrik van Brussel, professor at the University of Leuven, who served as president for two years. The new president will strive to achieve a greater involvement of the industry with eu**spen**, as it offers them a valuable knowledge platform.

Hendrik van Brussel (right) congratulates his successor as eu**spen** president, Henny Spaan.

Improved vibration isolators

Newport Corporation, a worldwide leader in laser and photonic solutions, has introduced the new S-2000 Stabilizer™ Series of pneumatic vibration isolators. It incorporates Newport's patented self-centering pendulum design, laminar-flow damping system, and precision auto-leveling valves to deliver high vibration isolation performance. Additionally, the new S-2000 design incorporates extra features including enhanced leveling indicators, recessed lifting channels, and a significantly lower magnetic permeability design. These new features, according to a Newport press release, greatly improve the ease of use, and functionality.

The S-2000 is a solution for isolating optical tables, large inspection equipment, heavy machinery, and large area sub-floors. Its performance delivers a 1 Hz vertical resonant frequency and a vertical isolation efficiency of 98 percent at 10 Hz. Horizontal isolation begins at 2.5 Hz and reaches 95 percent efficiency at 10 Hz.

www.newport.com/s-2000

It's official: DSPE

At the general meeting of NVPT last 14 May in Delft, the Netherlands, it was officially decided. Formerly known as NVPT, the Dutch Society for Precision Engineering will live on as DSPE. The new name reflects the international orientation and collaboration the DSPE board is pursuing. One of the manifestations of this internationalization ambition is Mikroniek, which, starting from 2009, will appear three times a year as an English-language magazine, having additional distribution among the eu**spen** membership.

www.dspe.nl

Analysis of micro- and nano-fibers

FEI, a leading provider of electron imaging and analysis systems, has introduced the Fibermetric™ system powered by the Phenom™ personal electron microscope. The Fibermetric system is designed to discover and quantify the properties of woven and nonwoven fiber samples in minutes, making direct observation and measurement of micro- and nano-fibers faster, more accurate and easier. Magnifications up to 24,000 times produce accurate information on fibers as small as 100 nm in diameter. The system accurately images and measures almost any fiber sample with its 4.9 nm/pixel resolution and a Gaussian fit function, which automatically finds and measures fibers and pores. Nano-fibers with diameters of 100 nm are routinely measured with greater than 97 percent accuracy.

www.phenom-world.com/fiber.

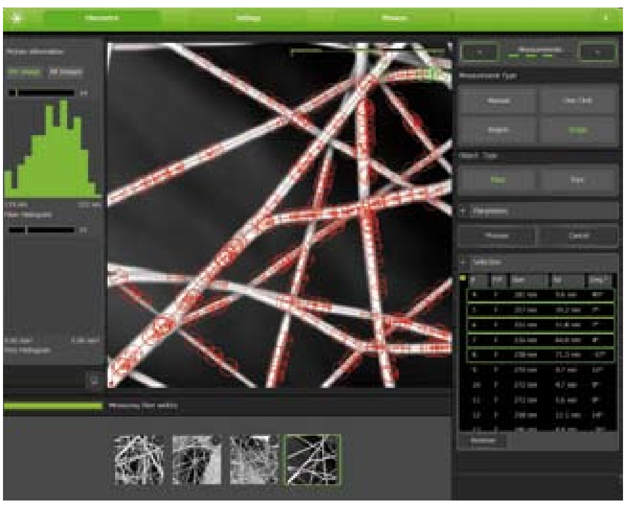

A screen shot showing an example of the Fibermetric system's automated measurements of fiber diameters.

Van Hoorn Carbide for top quality tools

Van Hoorn Carbide is geared towards shaping innovation and that is where its strength lies. With this in mind, Van Hoorn develops high-speed endmills. It has proven to the mould and die industry, to toolmakers and other professionals in the metal cutting industry that it contributes added value.

Van Hoorn Carbide in Weert, the Netherlands, has ultramodern equipment for developing and producing high-speed endmills at its disposal. Production takes place using highly advanced CNC grinding machines, and CAD/CAM is used in work preparation. Further facilities include product simulation, an extensive metrological department and quality control. Before delivery, all tools are subjected to a comprehensive inspection, which is carried out in a fully climate-controlled production facility and contributes significantly to the development and production of top quality tools.

Company philosophy

Product quality and accuracy standards are rising every day. By using the most advanced production and automation technologies available, Van Hoorn Carbide can deliver tools of the highest standards within microns. Its unique company philosophy enables Van Hoorn Carbide to meet every customer's needs. Established in 1990, the family company upholds strong values. Its clean office policy is implemented throughout the company and exemplifies this philosophy. Not only does the office look good, it works well, too.

Knowledge

Due to years of experience in grinding carbide and in the application of cutting tools, Van Hoorn Carbide is able to offer the best tools available in the market and to make complex cutting challenges work efficiently. Tools have been developed for use in High Speed Milling (HSM) applications. HSM is a huge success in the metal cutting industry. More and more manufacturers are recognising the advantages of this technology. Van Hoorn's highly skilled and experienced application engineers can provide further detailed information about HSM technology and the strategies employed.

Information

www.hoorn-carbide.com

ADVERTISERS INDEX


ALT
Tailored down to the nanometre
Having the right tie with the right suit means everything fits like a glove and conveys the image you want. As if it had been made for you. Wouldn't it be nice to have that in your work, too? Unfortunately, in your search for a product that fits, all you find is ready-to-wear.
ALT is different. ALT delivers customised piezo solutions for micron and sub-micron positioning projects. Together with our manufacturer, we sit down with you to gain detailed insight into precisely what it is you are looking for. Then, working according to a set series of steps, we generate a design that answers your specific project needs. The result is a uniquely tailored product that we can subsequently put into batch and volume production.
ALT PUTS YOU IN POSITION
www.alt.nl


HEIDENHAIN
How precise must semiconductor manufacturing be in the future?
Nobody really knows what the world of tomorrow will look like. All we know for sure is that the structures produced during semiconductor manufacturing are constantly shrinking. And that the demands placed on linear and angular metrology equipment will therefore continue to increase. Continuous improvements in accuracy and reproducibility are expected. Our grid interferometers with structure widths of 256 nanometers over measuring lengths of 320 mm make measuring steps in the subnanometer range possible, with interpolation errors on the order of picometers. This means that we already fulfill many of these demands today, while we continue to work on the technology for tomorrow. Enjoy the advantages of our competence, and join us to master the challenges of the future. HEIDENHAIN NEDERLAND B.V., p.o. box 92, 6710 BB Ede, phone: (0318) 581800, fax: (0318) 581870, http://www.heidenhain.nl, E-Mail: verkoop@heidenhain.nl
angle encoders + linear encoders + contouring controls + digital readouts + length gauges + rotary encoders